80p

GEMP-190e
(INFORMAL)

FACILITY FORM 602
N64-29788 (ACCESSION NUMBER)
80 (PAGES)
CR-52952 (NASA CR OR TMX OR AD NUMBER)
1 (THRU)
23 (CODE)
(CATEGORY)

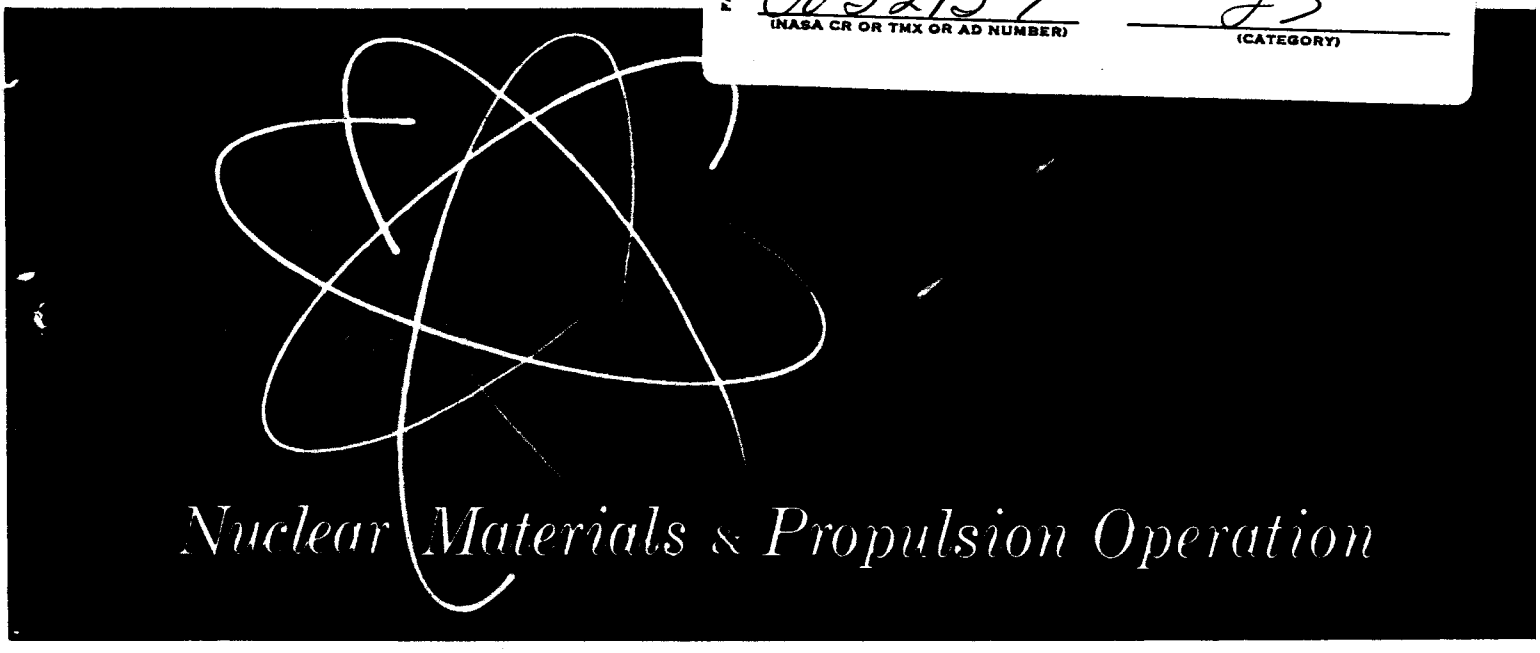

INTRODUCTION TO NUCLEAR PROPULSION

Lectures 7 and 8 - REACTOR SYSTEM DESIGN

Russell E. Motsinger

OTS PRICE

XEROX $ 2.60ph

MICROFILM $ _____

FLIGHT PROPULSION LABORATORY DEPARTMENT

GENERAL ELECTRIC

SOT-10563a

GEMP-190e
(INFORMAL)

INTRODUCTION TO NUCLEAR PROPULSION

Lectures 7 and 8 - REACTOR SYSTEM DESIGN

Russell E. Motsinger

March 19, 20 and 21, 1963

Prepared for the George C. Marshall
Space Flight Center of the National
Aeronautics and Space Administration

Contract No. NAS8-5215

PREFACE

The topic of these two lectures is concerned primarily with the factors involved in the reactor design, particularly, how one approaches the problem of designing a reactor system for a new application, without limiting the discussion to the rocket application. The basis for this lecture is the experience gained during the aircraft nuclear propulsion effort, which in many respects required a degree of design sophistication the same as the nuclear rocket. A subsequent lecture, number 20, will be devoted to the particular facets introduced by the rocket.

In Lecture No. 1 the technical differences between chemical and nuclear systems were discussed. Significant factors differentiating nuclear from chemical systems are, briefly:

1. Operational - Flight procedures should be essentially identical, but afterheat removal may require significant fractions of the propellant for aftercooling. Ground handling and maintenance will require protection of personnel from nuclear radiation.
2. Weight - The need to protect the propellant from nuclear radiation heating, primarily gammas, or to protect a crew in a manned vehicle introduces the need for a maximum shield thickness. This emphasizes the need to restrict the reactor diameter, hence shield diameter, so as to restrict the shield weight. Minimum rocket weight tends to be determined by the shield weight requirement, depending upon the fraction of payload weight which can be devoted to shielding. In space, natural radiation levels tend to reduce the differences between nuclear and chemical systems in terms of shield weight required.
3. Propellant - The gain in specific impulse allowed by nuclear heating stems primarily from the elimination of the need for an oxidizer; hence, the low molecular weight of hydrogen can be used to fullest advantage. The low density of hydrogen requires relatively large weight fractions for the tank.
4. Temperatures and Pressure Levels - To achieve the highest specific impulse, highest possible temperature levels for the propellant should be achieved. The limit in a convective-heat-transfer rocket, as determined by allowable fuel element temperatures, is somewhat lower than in a chemical rocket. Pressure level has only secondary effect upon specific impulse but determines the size of flow passages required, hence, the [illegible] reactor and hot parts of the rocket.

These [illegible] serve as a first guide to the relative importance of the several areas discussed [illegible] ure notes.

ACKNOWLEDGEMENT

[illegible] part of this lecture is an abstract of notes originally prepared by M. E. Lapides as a [illegible] ide for engineers in a reactor systems design unit.

TABLE OF CONTENTS

REACTOR DESIGN

1 INTRODUCTION

The following quotation, from a paper* presented at the NASA-University Conference on the Science and Technology of Space Exploration, conducted in Chicago, November 1962, states the major problem confronting the designer of the nuclear rocket reactor.

"The design of a nuclear-rocket reactor that will produce maximum propellant-gas temperature for limited core-material temperature required successful integration if the mechanical, thermal, and nuclear aspects of a complex problem. The strong interaction of the three-dimensional heat generation with heat transfer to the propellant requires "tailoring" of reactor composition and geometry. The techniques used are zoning of uranium concentration, metering of gas flow through fuel-element cooling passages, core moderator zoning, and judicious use of reflectors.

"Control systems should encompass sufficient reactivity to start, shutdown, and restart a nuclear rocket engine without introducing severe power distortions."

This discussion presents considerations associated with the reactor design sequence and introduces the broader philosophy and nature of the reactor design art, reflected by GE-NMPO experience with gas-cooled, high-temperature reactors.

The design sequence proceeds from initial exclusion calculations, the primary purpose being to eliminate impossible designs, while retaining for consideration those that may be feasible. This step is executed with optimisitic assumptions and computations that tend to be approximate. Subsequent iterative design studies are aimed at narrowing potential working areas to realistic working areas and identifying both a final design configuration and required developmental efforts. The iterative studies include analyses and, generally, experimental efforts, such as exploratory critical experiments and empirical developments of flow configurations. Experimental activities in particular are significant in those areas in which other efforts do not permit narrowing the working area from which to select the final design.

The initial design studies include a formulation of primary design restraints that evolve from the overall power plant system. Thermal design considerations include power distribution effects and design control of power distribution; design control of coolant flow and assessment of sensitivity of reactor temperatures to flow non-uniformities; and the selection and sizing of fuel element heat-removal surfaces. Nuclear design considerations include those generally associated with reactors, including heterogeneity and gas void effects. Because of the high heat-transfer surface temperatures and increased temperature sensitivity associated with the use of compressible fluids, gas-cooled high-temperature reactors place a significant premium on the development of an ability to provide for careful design control of power distribution throughout the operating life of the reactor.

*"Nuclear Physics of Solid-Core Gas-Cooled Rocket Propulsion Reactors," D. Bogart and E. Louty, NASA SP-20, Nuclear Rocket Propulsion, p. 17.

Completion of the preliminary design phase results in a narrowed working area for the final design phase and an identification of required experimental and developmental activities. These activities are started during preliminary design and continue on an expanded basis into the final design phase. The preliminary design activity is aimed at an identification of the essential features of the reactor, whereas the final design becomes an activity aimed at producing complete specifications required for fabrication. The final design phase includes extensive endurance testing of reactor components under simulated reactor operating conditions. Although complete duplication of reactor conditions cannot always be obtained, component proof tests performed under such conditions contribute significantly to the predictability of the reactor operating endurance.

Much of the final reactor design analysis is based on experimental data obtained from mockup assemblies. These data include nuclear data, such as power distribution and secondary heating, data depicting the flow characteristics of the coolant in the system, and mechanical data such as the relationship of fabrication tolerances to assembled tolerances.

One restraint that usually becomes more restrictive in the final design phase than in the preliminary design phase is that of schedule. Sensible final design schedules will overlap fabrication schedules, particularly those of materials procurement and the design of fabrication tooling. Considerations such as these have a significant influence on the sequence of design decisions. After establishing a final design schedule, many other activities or functions become closely allied to the final design activity; e.g., component test operations and preparation of facilities for the reactor test. The wide involvement and integration of other functions with the final design activity becomes a restraint on freedom of design choice. As the design is determined in detail, proposed modifications must be carefully assessed in relation to the total program and possible increases in cost and elapsed time. Generally, proposed design changes can logically be accepted only if they are needed to meet performance goals or to assure safety of operation.

2. GENERAL PHILOSOPHY OF REACTOR DESIGN IN THE INITIAL DESIGN SEQUENCE

2.1 PHILOSOPHY OF THE INITIAL DESIGN SEQUENCE

Because of the number and types of variables in reactor design, it is not possible to establish a general design technique. It is possible, however, to indicate a systematic design approach.

Figures 1 and 2, which characterize reactor design work, are useful for establishing definitions. Ultimately, the design must reflect considerations in the following categories: (1) thermal, (2) nuclear, (3) mechanical, (4) materials, and (5) economics. However, initial design assessments must often be based on assumptions and incomplete recognition of problems in these areas. Thus, many design iterations may be required

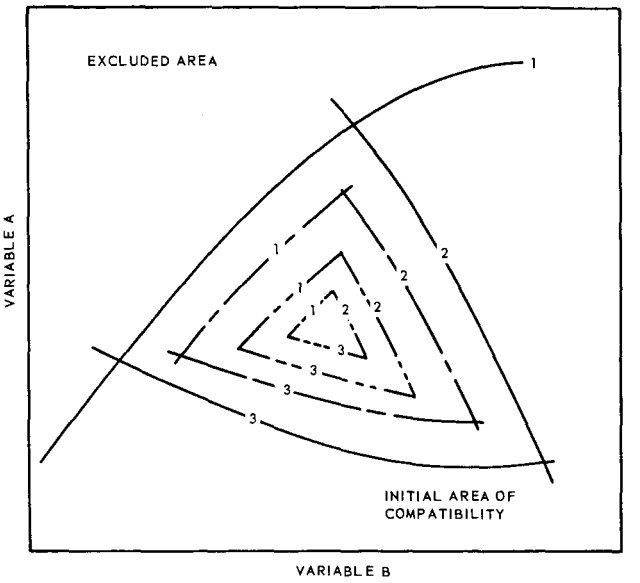

Notes:
Schematic design approach for a system defined by restraints 1, 2, and 3, expressed in terms of variables A and B.

1. Initial calculations (solid line) represent most optimistic representation of restraints 1, 2, and 3, which establishes maximum initial area of compatibility.
2. Subsequent calculations represent refined estimates of area of compatibility based on F_R, a correction to the preceding estimate accounting for limiting interrelations among restraints.

Fig. 1 – Exclusion calculation concept

before a suitably qualified design can be established. Figure 1, a representation of this iterative sequence, shows the technique of establishing areas of compatibility for several design restraints in terms of a set of variables common to these restraints. This is done first with a series of optimistic assumptions with the intent of establishing impossible rather than possible combinations. Then, as the working area is narrowed, more definitive evaluations are made. Figure 2 illustrates a typical relation between the adequacy of design representation and the degree of system specification, as well as an auxiliary relation that indicates the remaining number of design combinations that satisfy design restraints. Many of the design considerations cannot be taken properly into account at the design initiation because of the following: (1) there are a large number of interrelated variables, and (2) the design is generally paralleled by a development effort, the results of which must be used prematurely in the design.

The following outline is sometimes used in design scoping:

1. Formulation of primary design restraints (system specifications which remain invariant throughout the study)
2. Exclusion calculations (determination of maximum area of compatibility dictated solely by primary design restraints)
3. Determination of a base point design in the remaining area of compatibility, and its use to discover limitations that are not obvious in the primary design restraints
4. Design iterations as required
5. Final design selection

The aim of exclusion calculations is to eliminate the impossible design parameter combinations. Hence, the initial calculations are based on those items which are known with the greatest accuracy or can be expressed most conveniently. For example, the specifi-

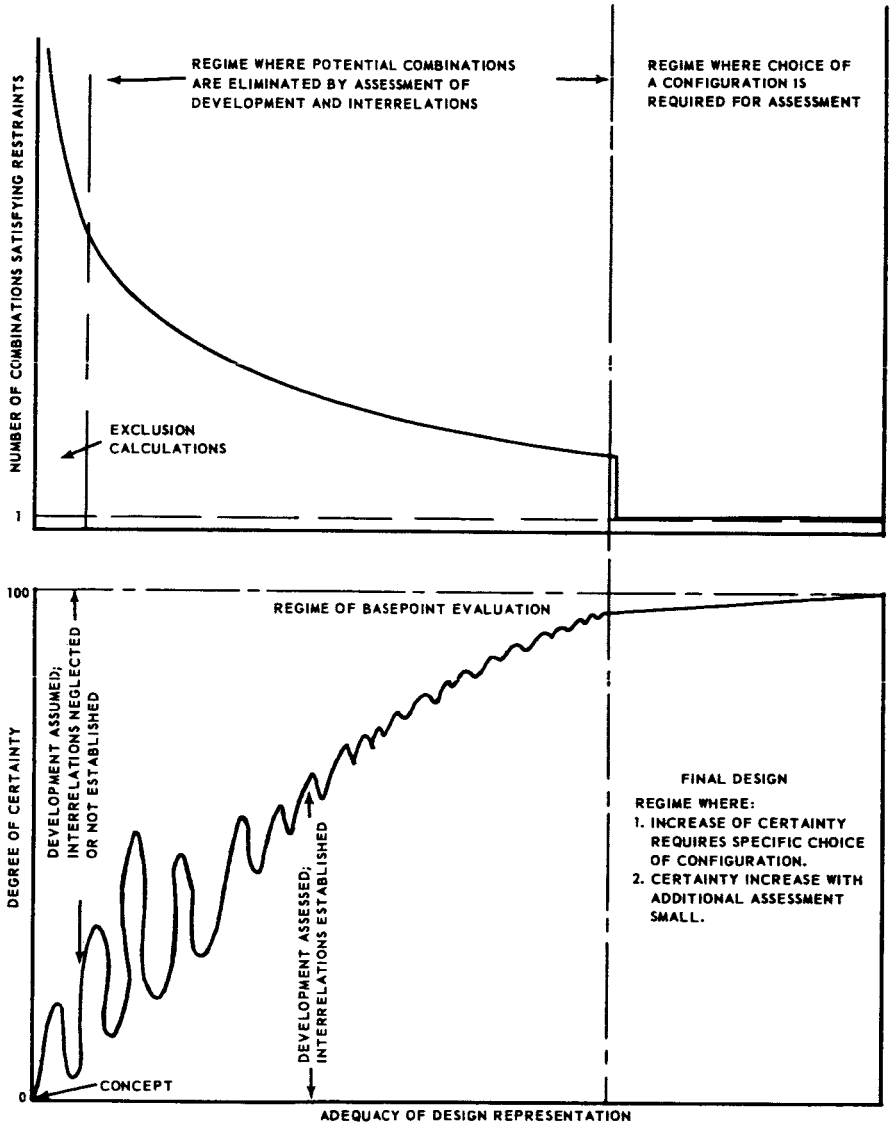

Fig. 2 – Design sequence

cation of natural fuel as a primary design restraint implies a fairly limited range of reactor sizes, fuel element geometries, and materials consistent with known or easily identifiable nuclear considerations. Thus, the initial calculations of natural fuel systems are predominantly nuclear in nature. In contrast, the use of enriched fuel permits considerable nuclear design flexibility; the usual point of departure in enriched fuel studies is a thermal design study.

In order to illustrate various problems and approaches, consider the design of an enriched fuel power reactor. The primary design restraints for the system are as follows:

1. Power to coolant ($\dot{Q}_m$)
2. Coolant (single phase)
3. Flow rate ($\dot{W}$)
4. Heat capacity (C_p)
5. Inlet temperature (T_i)

6. Outlet temperature (T_o)
7. Inlet pressure (P_i)
8. Fuel (enriched)
9. Core configuration (cylindrical)
10. Pumping work (expressed as allowable coolant pressure loss) (ΔP or $P_i - P_o$)
11. Maximum surface temperature of fuel element material ($T_{s_{max}}$)

The objective is to establish a reactor size and fuel element geometry consistent with these design restraints.

For any fuel element it is possible to establish relationships based on established heat transfer coefficients and friction factor relations (for a single-phase fluid) such as:

$$\frac{h(A_H)}{V_f} = \Psi\left[(T)\ ,\ \left(\frac{W}{A_f}\right)\ ,\ \left(\frac{1}{FECD}\right)\ \right] \tag{1}$$

$$\frac{\Delta P}{L} = \Psi\ \left[(T)\ ,\ (P)\ ,\ \left(\frac{W}{A_f}\right)\ ,\ \left(\frac{1}{FECD}\right)\ \right] \tag{2}$$

where

h = heat transfer coefficient
A_H = fuel element surface area
V_f = volume of fuel element channel = $A_f L$
A_f = fuel channel frontal area
L = fuel element length
W = coolant flow rate
T = fluid temperature
P = fluid pressure
P_t = power
FECD = fuel element characteristic dimensions
Ψ = designates function of

These equations are equivalent to conventional heat exchanger sizing relationships, except that they are expressed in a form convenient for nuclear work.

Appendix A includes generally applicable data, explicitly showing the functional relationships given in Equations (1) and (2); a discussion is also given there of the concepts of the convective heat transfer coefficient and friction factor. The sequence of design is as follows:

1. Establish required value of $(hA_H)/V_f$ by solution of an equation analogous to the usual convective heat transfer relation, which, in terms of previous nomenclature is:

$$\frac{P_t}{V_f} = \frac{(hA_H)}{V_f}\ (\Delta T_D)\ K_D \tag{3}$$

where

ΔT_D = fuel element surface-to-fluid temperature difference at location of $T_{s_{max}}$
K_D = a distribution function which corrects the average power density (P_t/V_f) to the value extant at the maximum temperature locale

2. For known or assumed values of ΔT_D and K_D, Equations (1) and (2), plus the primary design restraints, establish individual relations among fuel element volume distributions (A_f and L) and specific characteristics of the element. Comparison of these individual relations establishes mutually compatible dimensions.

3. The potential area thus defined is examined in the light of other apparent limitations, such as minimum value of the tube diameter, minimum volume of the reactor consistent with attainment of criticality, maximum size limitations, etc., all of which serve to alter the area of compatibility. The composite results of such calculations, used to define a potential design area, can be as indicated in Figure 3.

The essential characteristics of exclusion calculations, in contrast to the more realistic calculations of subsequent iterations, can be illustrated in terms of the design sequence. For example, all items used in calculations involving the fuel element thermal design are given by the primary design restraints except the term ($K_D \Delta T_D$). The exclusion calculation would postulate an optimum value for this term, whereas subsequent iteration work would be initiated on the basis of a probable value. In this case, the optimum thermal design combination of ($K_D \Delta T_D$) would be one yielding maximum temperature everywhere within the element; hence, maximum heat transfer per unit surface area. This combination can be expressed as:

$$(K_D \Delta T_D)_{optimum} = \ln \frac{T_o - T_i}{\left(\frac{T_{smax} - T_i}{T_{smax} - T_o}\right)} \qquad (4)$$

which permits determination of a maximum area of compatibility exclusively in terms of primary design restraints with no additional qualifications being required. In a comparable manner, an exclusion calculation from a nuclear standpoint would attempt to define the least limiting relation of total reactor volume, or relations between A_f and L, by including best possible assumptions concerning the items affecting minimum critical volume.

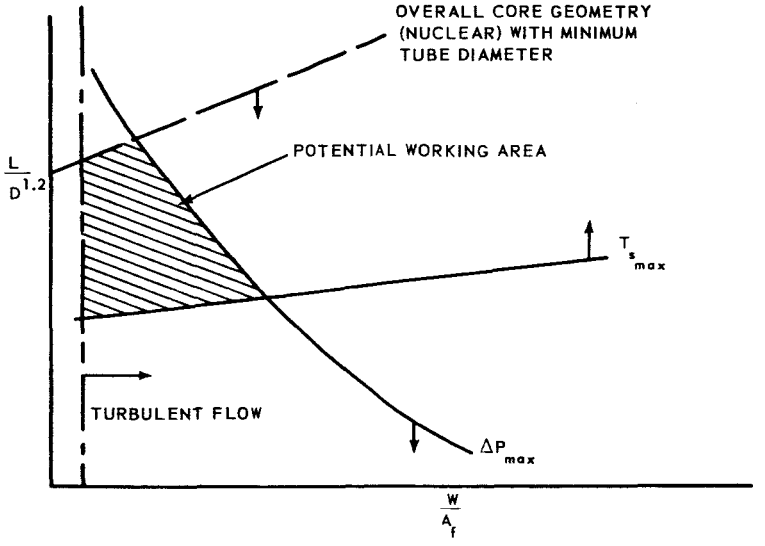

Fig. 3 – Potential design area

Under usual circumstances, exclusion calculations will be very useful in such design areas as establishing a basic incompatibility among design restraints, and choosing the fuel element type or establishing a basic index for evaluation of development work. Conversely, they will be of only limited utility in practical application to design. Nevertheless, the exclusion approach yields high dividends because it accents developmental needs or possibilities and contributes to simplification and reduction of the necessary scope of detailed analysis. While it is not possible to define probable success of design sequences, the generalizations of the following paragraphs may be of value.

Problem areas evolve from items such as changing the basic design during the course of the study, inability to define basic interrelations, and inability to analyze situations resulting from the interrelations. A good deal of insight regarding probable success in handling these problems can often be established by fairly simple artifices.

Figure 4 shows typical screening analyses for two very different systems. The results shown in Figure 4a imply that the design is not restrained by thermal stress, nuclear, or pumping loss considerations, but are dictated by heat transfer effects. This early isolation of such a single limiting factor indicates that a successful design can probably be achieved, and the system is feasible. In contrast, the small area of compatibility shown in Figure 4b suggests that intensive development is required and that subsequent, more accurate evaluations will prove nonfeasibility.

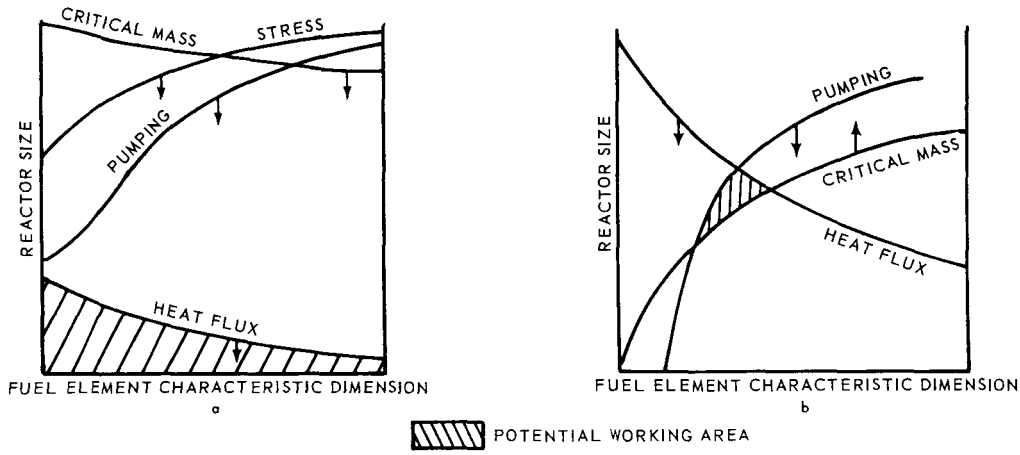

Fig. 4 – Results of screening analyses

A good scale for estimating ability to analyze situations resulting from design interrelations is given by the degree of component symmetry and system homogeneity. Generally, the closer the approach to complete symmetry and homogeneity, the more applicable are ordinary analytical tools, particularly in the nuclear area. In addition, increasing the symmetry and homogeneity may eliminate many potentially limiting relations. As an example, a homogeneous version of the sample design, which conceivably could consist of fuel-moderator plates exclusively, eliminates the necessity for designing flow passages to match both fuel and moderator and requires very limited analysis of secondary heating. Use of water as a coolant would yield similar facility, in addition to obviating fine power flattening, because of the moderating properties of the coolant.

Although the number of steps in a design sequence can often be minimized with the use of proper initial estimates, maintenance of the multistep, exclusion-type sequence is desirable for several reasons. (1) The sequence is usually concerned with assessing a development program, in addition to establishing the design itself. Hence, the more steps considered, the higher the probability both of uncovering potential developmental paths and of properly assessing them. (2) The use of exclusion calculations affords considerable calculation simplification until a reasonably good frame of reference for final design is established. For example, design sizing relationships can contain assumptions (such as Reynolds Analogy, neglect of the effect of surface temperature on heat transfer coefficients, and the neglect of second order pressure loss effects) which yield considerable calculation simplification even though the assumptions are slightly optimistic in some

circumstances. The sacrifice of accuracy for utility is of small concern so long as the design orientation is exclusion rather than inclusion. After the final design arrangment has been specified, accurate analyses that make use of appropriate computer codes with the utmost sophistication, or experimental development when sufficient sophistication is not available, are appropriate to achieve the desired design conditions with confidence.

2.2 THERMAL CONSIDERATIONS IN THE INITIAL DESIGN SEQUENCE

This section describes some of the general design considerations that must be included in the initial design sequence in order to evolve a satisfactory choice of the reactor fuel element and flow passage arrangement and configuration.

2.2.1 Power Distribution Effects

The usual relative power distributions in cylindrical systems are cosine functions longitudinally and zero order Bessel functions radially. However, both distributions are well approximated by sine or cosine functions, the use of which often affords considerable calculation simplification. Estimates of power distribution can be prepared by assuming that flux is a continuous function from a maximum value in the active core center down to zero at some point exterior to the active core as illustrated in Figure 5.

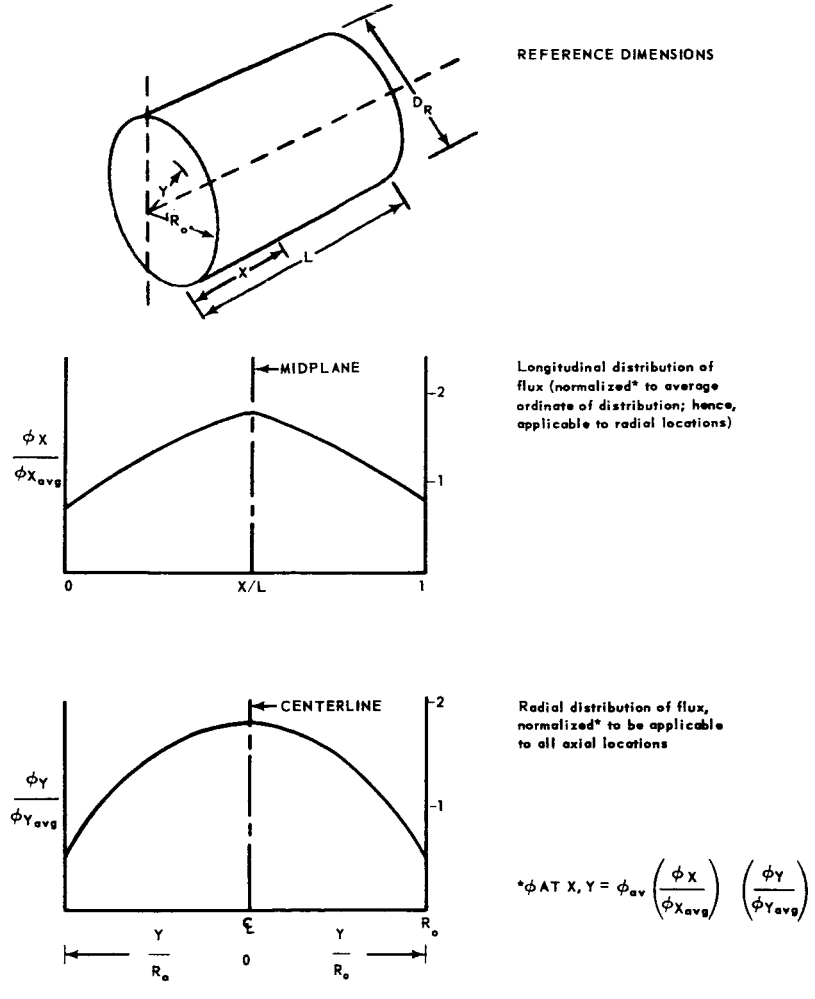

Fig. 5 – Reference flux distributions, cylindrical core

The reflector affects reactor power distribution but information pertaining to the effect of the reflector usually is not immediately available, so assumptions are required in order to initiate design. A guide to aid in these assumptions is given in the following tabulation:

TABLE 1

ASSUMPTIONS REQUIRED TO INITIATE DESIGN

Distribution In Core	Ratio Of Maximum To Average Power Density		
	Radial	Longitudinal	Overall Reactor
1. 2:1 cosine	1.35	1.21	1.63
2. 1:0 cosine	2.17	1.57	3.4
3. Optimum	1.0	(value which yields maximum temperature utilization)	

Item 3 is the best case from the standpoint of power extraction; item 2 is a good approximation of the "worst case" power distribution that a reactor is capable of yielding (bare reactor). As previously indicated, the exclusion calculation makes the tacit assumption that the optimum power distribution can be obtained. A typical basepoint calculation would be initiated on the base of something between the optimum and "worst case" situations. Item 1 is a typical compromise. It is based on the assumption that most practical reactors have appreciable reflector savings which makes the "worst case" highly improbable.

Another typical basepoint calculation is suggested by overall reactor geometry considerations. In order to limit fuel requirements, nuclear core geometries tend towards those with minimum surface-to-volume ratios so that neutron leakage is not excessive. A cylindrical system usually approximates a right circular cylinder since this is the minimum surface-to-volume geometry. In many cases, considerable variation is possible but extremes ('pancake' or 'long tubes') are generally inadmissible because of high leakage and resultant inability to attain a critical state. Generally, the exclusion calculations would make no limiting geometry assumption whereas the basepoint calculation would make use of specific geometry. Similarly, when dealing with a nonmoderating coolant, some assumption may be required concerning the allowed volume fraction of the reactor.

2.2.2 Altering Power Distribution

The various methods of altering power distributions can be illustrated in terms of the relation for nuclear heat generation:

$$Q''' = C\ N\ \sigma_F\ \phi \qquad (5)$$

where

C = Constant
N = Number of fissionable nuclei per unit volume
σ_F = Fission cross section
ϕ = Neutron flux
Q''' = Volumetric heat-generation rate

In the normal reactor, $N\ \sigma_F$ is everywhere constant; hence, volumetric power generation varies directly with the flux distribution. However, power distribution can be varied by several methods which include: (1) variation of N by means of increasing fuel concentration in the plates, and enrichment variation; and (2) variation of ϕ by means of variation of moderator and absorber concentration, fuel concentration, and variation of reflector size and location.

In addition, as previously indicated, it may be possible to compensate for a given power distribution by matching flow to power distribution by variation of the fuel channel size or by orificing fuel channels. The constant wall temperature can be achieved by altering variables in the following basic convection equation:

$$Q = hA_H\,(T_S - T) \text{ or } Q''' = \frac{hA_H}{V_f}\,(T_S - T) \qquad (6)$$

Possible methods of changing either Q''' or hA_H/V_f are illustrated in Figure 6. Possible examples of such methods are shown in Figure 7.

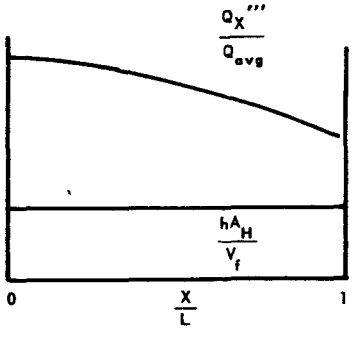

Q''' Variants

Shift power curve by concentrating fuel in forward section of reactor; by use of large front end reflector; by absorber location; or by concentration of moderator in forward section.

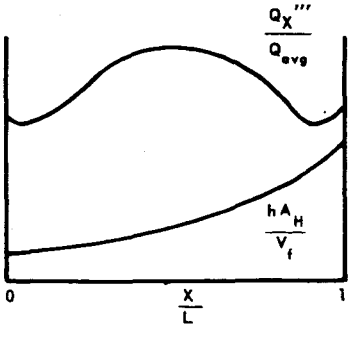

$\frac{hA_H}{V_f}$ Variants

Variation of surface area with length (design of incremental fuel elements); variation of h or $\frac{A_H}{V_f}$ by channel-size variation with length.

Fig. 6 – Control of longitudinal temperature by fuel element design

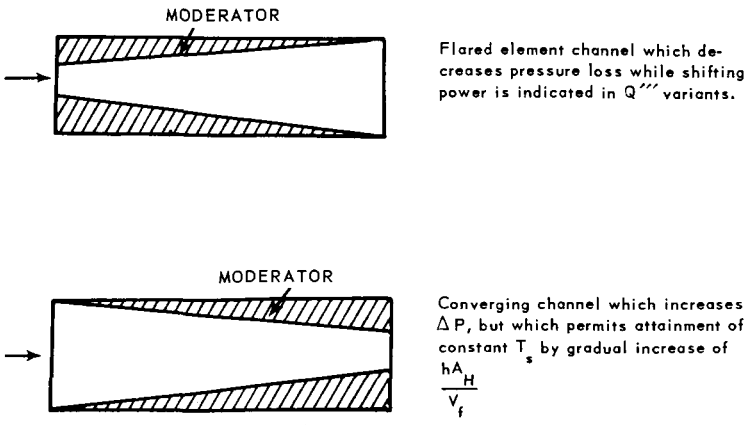

Fig. 7 – Control of longitudinal temperature by moderator and channel design

Radial power flattening can be accomplished in a variety of ways, but it is common in most reactors to accomplish at least part of the flattening with a reflector, especially since the use of a reflector leads to lower fuel inventory requirements. In a bare cylindrical reactor, the power generation in a channel on the reactor axis is about twice the average. If a reflector is used, the ratio can be reduced to the range of 1.2 to 1.4 times the average, or somewhat lower. If attempts are made to reduce the ratio to a much lower figure by means of reflector variation, the location of the maximum value of $(Q''' \text{ max}/Q''' \text{ av})_R$ may shift as illustrated in Figure 8.

As shown, adjustment of radial power to a uniform distribution is virtually impossible by reflector variation alone, therefore, some additional alternate is required. If all fuel channels are to be kept identical in structure, it is possible to power flatten radially by variation of the absorber or moderator, or to compensate by matching flow distribution to the radial power distribution, using orifices (or other flow resistances). The first approach used in GE-ANPD designs was radial variation of moderator volume fraction with uniform fuel cell sizes. Early utilization of hydrogenous solid moderators was with a radial variation of hydrogen concentration. Later designs varied both moderator-volume fraction and fuel cell size while maintaining uniform hydrogen concentration. Ceramic reactors utilizing composite bodies of fuel and moderator were radially power flattened by variation of the fuel-to-moderator ratios, or alternately were temperature flattened by radial variation of coolant-volume fraction with a uniform fuel-to-moderator ratio.

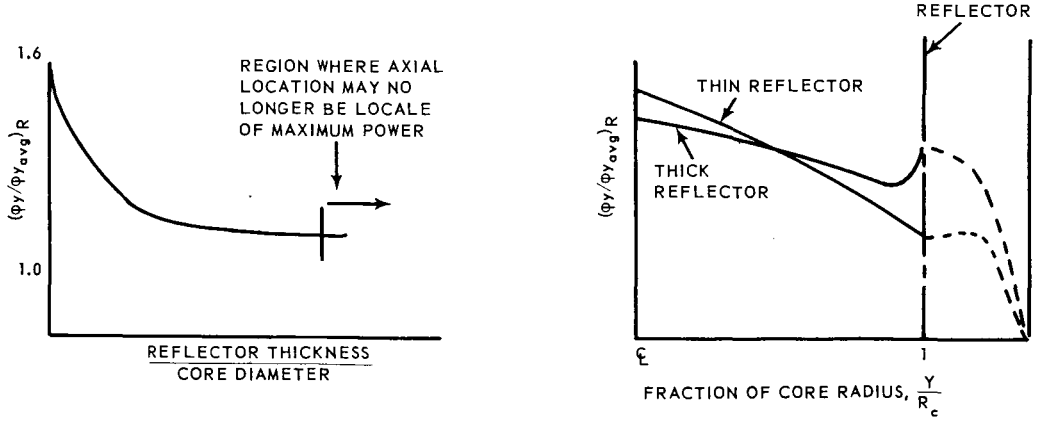

Fig. 8 – Reflector effects on radial power distribution

2.2.3 Pressure Loss Effects

The non-uniform radial power distribution calculation establishes a system pressure loss based on matching flow and power distribution to achieve a uniform coolant exit temperature. The first approximation of the pressure loss is given by the Fanning friction-factor relation:

$$\Delta P = \frac{4fG^2L}{2g_oD\rho} \qquad (7)$$

which, for constant geometry and friction factor becomes:

$$\Delta P = \frac{C(\dot{W}_\rho)^2}{\rho} \qquad (8)$$

where

ρ = Coolant density
$\dot{W}_\rho$ = Coolant flow to channel
C = Constant

If flow and power are matched (yielding constant ρ), the pressure loss in the "hot" (axial) and average channel will be in the ratio of $(1.35:1)^2$ or 1.823. However, for a series of channels connected to common headers, the flow distribution is dictated by the condition that all channels yield the same static pressure loss. Thus, in order to achieve the matching of flow and power indicated, the system must be designed to the pressure loss indicated by the highest power section. Then some additional form of flow resistance, such as an orifice, must be introduced in the remaining channels to permit attainment of the same pressure loss as the high power section, but with a lower coolant flow rate.

The preceding example suggests that the approximate design pressure loss for a non-uniform radial power system yielding constant coolant discharge temperature is $\Delta P_D \cong \left(\frac{Q'''\,max}{Q'''\,avg}\right)_R^2 \times \Delta P$ uniform

where

ΔP uniform = Pressure loss based on average conditions
$\left(\frac{Q'''\,max}{Q'''\,avg}\right)_R$ = Ratio of maximum to average radial power density

In many cases, the increased pressure loss may be prohibitive and it might be preferable to accept some degree of coolant overtemperature. Ability to accommodate this variation is, to a large degree, dependent on coolant characteristics. For example, for two channels with different heat input, the condition of constant static pressure loss yields with Equation (7).

$$\frac{W_1}{W_2} = \sqrt{\frac{\rho_1}{\rho_2} \cdot \frac{f_2}{f_1}} \qquad (9)$$

Note: Subscripts refer to channel number.

and, for ideal gas, where $\rho = p/RT$ (10)

$$\frac{W_1}{W_2} = \sqrt{\frac{p_1}{p_2}\frac{f_2}{f_1} \cdot \frac{T_2}{T_1}} \qquad (11)$$

The density of most single-phase incompressible fluids is not strongly affected by either temperature or pressure. Therefore, in this case, the ratio of coolant flow in the two channels does not change significantly with variation of heat input. For gases, however,

the situation is considerably different. If the heat input to all channels is identical, all terms on the right hand side of Equation (11) will be constant and W_1, the mass flow through channel 1, will be identical to that of channel 2. If channel 2 receives more heat than channel 1, T_2 is greater than T_1. Hence, W_1 is greater than W_2. Overaverage heating yields lower-than-average density and, hence, higher-than-average pressure loss per unit of flow. Since each channel must have the same pressure loss, the hot channel must receive less than average weight flow. Thus, the amount of overtemperature must be greater than just a simple function of the amount of overheating. (In certain systems, additional variations arise when f increases with temperature.) This problem, called "power induced flow variations" often represents a significant design limitation. The following study illustrates utilization of an approximate graphic solution for the case of gases given in Figure 9.

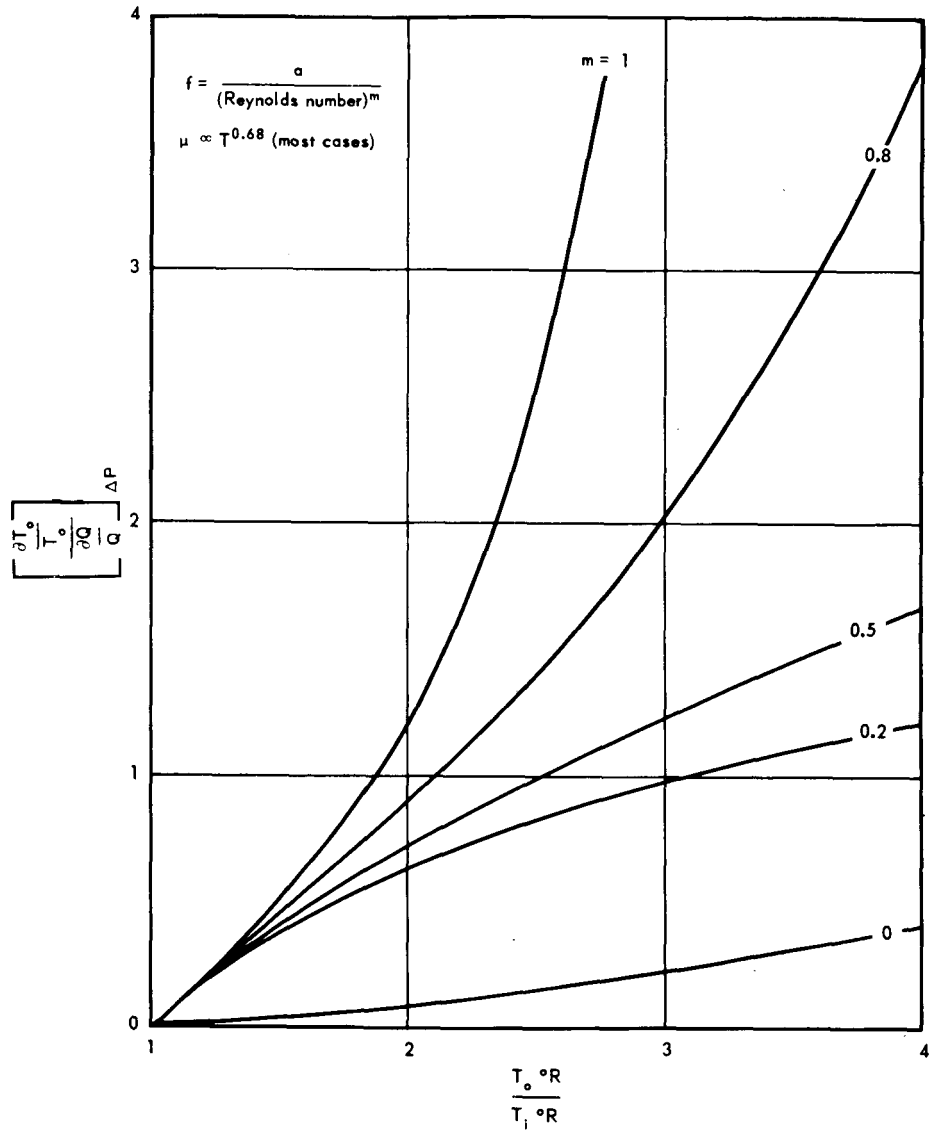

Fig. 9 – Plot of temperature sensitivity of gas flow in parallel-heated channels

Given:

$\frac{T_o}{T_i} = 2.18$

m = Friction factor exponent = 0.2

$\frac{\partial T_o}{T_o} = \frac{(T_o' - T_o)}{T_o}$

$\frac{\partial Q}{Q} = \frac{(Q' - Q)}{Q}$

T_o' = Discharge temperature from hot channel
T_o = Average outlet temperature = **1660°R**
Q' = Hot channel heating rate
Q = Average heating rate

$\left(\frac{\partial G}{G}\right)_{\Delta P}$ = Mass velocity variation at constant static pressure drop

from Figure 9:

$$\left[\frac{\frac{\partial T_o}{T_o}}{\frac{\partial Q}{Q}}\right]_{\Delta P} = \left(1 - \frac{T_i}{T_o}\right)\left[1 - \left(\frac{\frac{\partial G}{G}}{\frac{\partial Q}{Q}}\right)_{\Delta P}\right] = 0.7 \qquad (12)$$

Power-induced flow variations for several values of $\frac{Q'''\,max}{Q'''\,avg}$ are shown in Table 2.

TABLE 2

POWER-INDUCED FLOW VARIATIONS

Radial Power Distribution Factor (Q'''max/Q'''avg)

$\left(\frac{Q'''\,max}{Q'''\,avg}\right)_R$	1.1	1.2	1.345
$\frac{\partial Q}{Q}$	0.1	0.2	0.345
$\left[\frac{\partial T_o}{T_o}\right] \times T_o$	0.07 (1660) = 116	0.14 (1660) = 232	401
T_o'	1316°F	1432°F	1601°F
$\frac{\partial G}{G}$	-0.029	-0.058	**-0.101**
$\left(\frac{W}{A_f}\right)$	$0.971\left(\frac{W}{A_f}\right)_{avg}$	$0.942\left(\frac{W}{A_f}\right)_{avg}$	$\mathbf{0.899}\left(\frac{W}{A_f}\right)_{avg}$

Significant design problems and limitations may arise in the absence of power flattening with compressible fluids. The problem becomes especially acute with gases operating at high ratios of (T_o/T_i) or in laminar flow (m greater than 0.2, note m = 1 for laminar flow in tubes). The graphic data are not strictly accurate but are adequate for most reactor calculations where the Mach number is less than 0.3. For accuracy and for higher Mach numbers, pressure losses should be computed by more exact methods, such as by incremental integration of Equation **(15)**.

Once the reactor is designed in detail, more accurate appraisals are possible by means of a series of calculations of pressure loss versus heat input that lead to a precise curve of the same form.

With two-phase fluids (e.g., boiling water), the problem of power-induced flow variations can be especially acute because of the marked change in effective density associated with small changes of vapor content. In this case, the sequence of formation of a slight excess of vapor that leads to a decrease of coolant flow to the channel, or to further vapor formation, etc., may ultimately yield near-complete flow starvation in the channel (comparable to laminar flow of heated gases).

If flow starvation appears probable or if the magnitude of power-induced flow variation is high, the design may be predicated on methods of alleviating the situation. For example, if an appreciable fraction of the total channel pressure loss is taken up by an entrance orifice, the problem is largely obviated since variation of heat input will not significantly alter channel flow. (i.e., System pressure loss is not significantly affected by heat input.)

Items that influence both the plate thickness and the ability to attain uniform radial power and/or idealized power distributions are considered next.

2.2.4 Fuel Element Plate Thickness and Channel Size Effects

Required fuel element volume is a function of fuel inventory, allowable fuel concentration in element material, cladding thickness, allowable burnup, and mechanical strength requirements. For purposes of illustration, assume that the use of uranium oxide (UO_2) rather than uranium metal is necessitated by the high-temperature requirement of the system. The fuel plates could be constructed as shown in Figure 10.

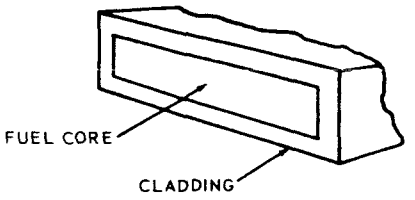

Type A: Nonintegral core and cladding
Core: fuel plus nonstructural filler
Clad: nonintegral, structural.

Type B:
Core: fuel and structure
Cladding: integral structural or nonstructural.

Fig. 10 – Cross section of typical fuel plate

For type A fuel plates, the structural or load-carrying member would also be the cladding; the core would not be a structural member. For type B plates, the cladding thickness would be the minimum required for fission product retention plus whatever additional thickness is required to protect the core against erosion, corrosion, or other clad-penetrating effects. Type A plates may permit higher core fuel concentrations at the expense of thicker cladding and possible high temperatures within the core itself because of poor conductance of the core-to-clad contact.

Type B plates are generally limited in maximum permissible fuel concentration for one or more reasons. (1) Uranium oxide is a ceramic material. If it represents more than 30 percent of the volume of the core mixture it is doubtful that uranium oxide can be combined with metal without seriously impairing core strength or preventing attainment of a uniform distribution of fuel during fabrication. (2) Uranium oxide has a low thermal conductivity, and if it is present in high concentration, significant internal temperature differences may result.

The degree of fuel burnup, with the resulting formation of fission-product gases and possible pressure buildup, may be reflected as an increase in cladding thickness or a porosity allowance in the filler of type A fuel plates. As a general rule, the cladding thickness required to stop (energy attenuation) fission products is small. The actual cladding thickness is dictated by mechanical or erosion-corrosion effects. Specific exceptions occur with ceramics which, because of their method of fabrication (hot pressing and sintering of powders), **are inherently porous. Thus, if ceramics with ceramic clads are considered, the cladding thicknesses will be relatively large. Also, because of fabrication limitations, ceramic plates cannot generally be made in small thicknesses (metallic fuel plates of 10-mil thickness may be practical compared to a ceramic plate thickness of 40 to 80 mils minimum).**

Fuel element thickness can also be determined by internal temperature effects which could yield either stress or overtemperature problems. The maximum internal-to-surface temperature difference in the fuel plate, ΔT_p, is given approximately by:

$$(\Delta T_p)_{avg} = \frac{Q_{in}}{A_H}\left[\frac{(t_{core})^2}{4k_{core}} + \frac{t_{clad}}{k_{clad}}\right] \qquad (13)$$

where t = Thickness
k = Thermal conductivity

Local or maximum values can be evaluated from local heat flux ratios and plate thickness variations. Large cladding or core thicknesses and high fuel concentrations tend to increase ΔT_p.

Before choosing the actual number of fuel channels certain assumptions must be made. Pressume a review of the problems in adjusting power distribution has been made and has indicated that; (1) both the radial and longitudinal distributions are peaked in the ratio of

2:1 maximum to minimum; (2) this must be considered as the basepoint for design; and (3) a fuel element plate thickness of 0.020 inch yields a satisfactory total volume for fuel. It is not possible to introduce all of the items of concern that would dictate the choice of channel size. Therefore, the following paragraphs cover only problem areas of a specific example for purposes of illustration. The number and size of fuel channels is affected by the following items, expressed as the advantages and the disadvantages in considering the choice of a small channel:

Advantages of Small Channel Size

Nuclear - Smaller cell size permits more effective utilization of fuel in a heterogeneous fuel-moderator system. The analysis of the system is easier in a homogeneous model.

Mechanical - Permits design for high pressure differential across channel wall with minimum wall thickness; may also permit design for higher system-pressure loss in some cases.

Thermal and Cycle Design - Provides high ratio of channel-wall-to-element-surface areas exposed to coolant. This is an advantage when the moderator is cooled by the main coolant.

Materials and Others - Permits use of dimension-limited materials (e.g., ceramics), enhances flexibility for location of penetrating control mechanisms, and possibly enhances ability to compensate for nonpower flattening by channel size variation.

Disadvantages of Small Channel Size

Nuclear - Higher ratio of nonfueled material in both element and channel wall, which promotes higher fuel inventory requirements.

Mechanical - Effect of dimensional tolerances and differential thermal expansion on nominal coolant-flow passage size becomes significant; channel structure and attachment mechanism may be size and shape limited.

Thermal and Cycle - Excessive nonfueled surface increases ΔP; high wall surface exposed to moderator may promote high direct-heat transfer losses to the moderator; small channel size may prevent compensation for self-shielding of fuel effects and yield high channel inlet and exit pressure losses.

Materials and Others - Limits ability to accommodate certain radius of curvature forms in elements. Larger number of channels required yields increased production problems; may limit volume available for moderator.

The preceding illustrates some typical limiting relations which are to be expected in further design investigation. A possible conflict exists between an ability to withstand pressure within a fuel cartridge and fuel inventory requirements. The former is abetted by a small channel size and thick channel walls, both of which serve to increase the amount of nonfission nuclear absorption. This increases the required fuel inventory; hence, some compromise, usually nonoptimum, is required for either alternative.

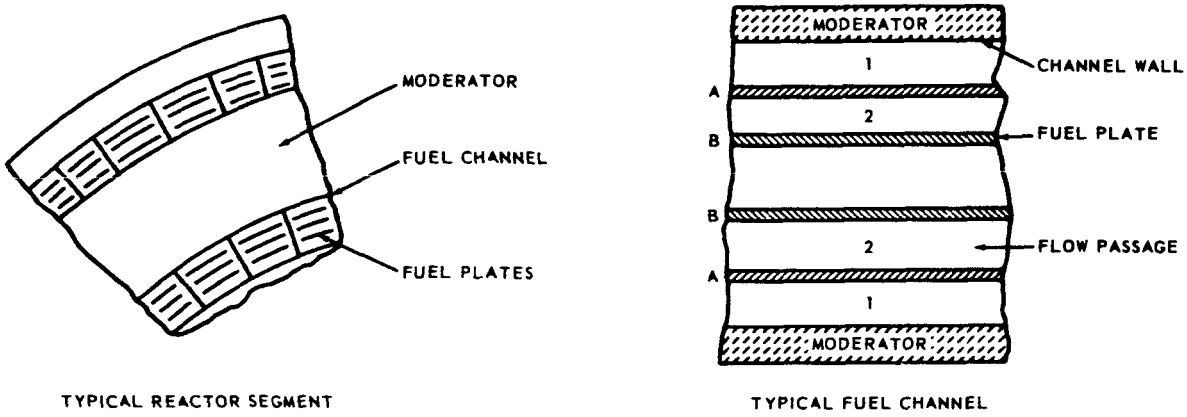

Fig. 11 – Typical reactor segment and fuel channel

The selection of a channel size in a thermal reactor is also affected if the coolant is nonmoderating in a heterogeneous fuel-moderator arrangement such as shown in Figure 11. (This factor is covered in detail in a subsequent section, so only a simplified version, aimed at identifying a particular design problem area, is considered here.) The moderator can be considered essentially as the source of all neutrons that cause fission. The plate nearest the moderator senses the complete neutron flux as it leaves the moderator. The next plate senses the complete fission flux, less that utilized or absorbed in the first plate. More formally $\phi_1 > \phi_2 > \phi_3$ down to a minimum at the centermost plate. Therefore, a significant variation of power production per plate, surface temperature, and power distribution among interplate channels can occur. These variations can yield flow maldistribution problems between individual fuel plates as well as between individual fuel element channels. Such problems also become of extreme concern if either the fuel per plate or the absorption cross section of the fuel plate material is high, since the flux depression will be accentuated in either case. In some cases, the self-shielding effect may cause such a significant flux depression that it becomes necessary to consider a smaller channel size and hence fewer shielding plates between the moderator and fuel. The methods of correcting or compensating for this effect parallel those mentioned earlier. In particular, the fuel concentration can be varied in order to achieve uniform power from plate-to-plate, noting, however, that a possible snowballing effect may occur. For example, increasing fuel in plate 2 to raise its power more nearly equal to plate 1 necessitates even further increase in fuel requirements for plate 3, etc., in some cases. This particular problem can be relieved by increasing the homogeneity of the core (i.e., a more homogeneous mixture of fuel and moderator or complete elimination of moderator). Also, if no attempt were made to flatten fine power, the possibility of flow compensation within a channel would have to be considered.

Again, for illustration, assume that the basepoint channel choice is satisfactory for additional evaluation. If some variation should be necessary, system pressure loss evaluations and methods of decreasing pressure loss should be considered. The pressure loss calculation presumed so far is an approximation, as are all integral pressure loss relations for examples of heat addition to a compressible fluid. The relation stems from the basic differential equation

$$d \ln P = \frac{-\gamma M^2}{2} \left(\frac{4 f dX}{D} + d \ln T \right) \qquad (15)$$

Assuming that M = a constant, M_{avg}, permits integration of Equation (15) to give an approximate relation

$$\ln \frac{P_2}{P_1} = -\frac{\gamma}{2} M_{avg}^2 \left(\frac{4 f \Delta L}{D} + \ln \frac{T_2}{T_1} \right) \qquad (16)$$

where P = Total pressure
M = Mach number
γ = Ratio of specific heats Cp/Cv
T = Total temperature
f = Friction factor
X = Length
ΔL = Incremental length between X_1 and X_2
D = Diameter
Subscripts 1 and 2 denote particular locations along the length of the reactor.

Under usual gas flow conditions in process and reactor work, the ratios of total-to-static pressure and temperature are close to unity (because of the low Mach number) and the values can be used interchangeably. The static and total pressure loss values, however, may vary significantly particularly if T_o/T_i or $\Delta P/P_i$ are large (e.g., T_o/T_i greater than 2, $\Delta P/P_i$ greater than 0.2). In instances where more precise evaluation of ΔP is required, Equation **(16)** must be applied incrementally, i. e., the flow passage length, L, must be represented by the sum of several incremental lengths, ΔL. Generally, M_{avg}, γ, and f will have to be evaluated for each increment. Instead of evaluation based on the pressure and temperature at the beginning of each increment, iterative computations, with evaluations based on increment average conditions, will provide greater precision. Use of short increments also provides increased precision.

With the basepoint channel size established, revisions of pressure loss estimates to account for entrance and exit losses, losses associated with the mode of fuel element support, etc., should be made. Again, the adequacy of these estimates will depend on the degree of system specification. However, a good guide to loss magnitude can usually be established by an examination of system dynamic heads. The dynamic head is defined by:

$$q = \frac{G^2}{2g_c\rho} = \frac{V^2\rho}{2g_c} \qquad (17)$$

where q = Dynamic head
V = Fluid velocity

Usually entrance losses can be held to less than one-half a dynamic head; and exit losses, to less than one dynamic head, in simple channel systems. Orificing to match flow and power must be based on total channel pressure loss.

Assessment of a suitable friction factor for the fuel element is also of concern. In particular, if the various plates as shown in Figure 11 can be made continuous and be supported only by channel sidewalls or if continuous tubes are used, the friction factor should be one for simple conduits. If, however, many internal support spacers must be included or if plates or tubes cannot be made continuous because of fabrication or structural requirements, the friction factor must be adjusted. In such instances, the friction factor would account for expansions and contractions in spaces between fuel plate stages. A suitable estimate of the friction factor can be established by an analysis similar to that shown for entrance and exit losses. If an interrupted or "staged" fuel element is considered, the friction factor is dependent upon the plate thickness because of expansion and contraction losses. As the structure becomes more and more removed from a simple continuous conduit, experimental determination of pressure losses becomes mandatory.

3. NUCLEAR CHARACTERISTICS AND CONTROL EFFECTS

A suitable basepoint for the next step in the design sequence is the nuclear requirement. Problems in this area include fuel inventory and distribution of power (to qualify the previous thermal design assumptions). A specific problem results from the dependency upon critical experiment results for design because of the limitations in analytical methods for high-performance systems. Also, it is not uncommon to find that nuclear characteristics are extremely sensitive to other design limitations, and, as a result, nuclear calculations often lag behind other design studies. Frequently, this timing problem can be the most critical nuclear design problem.

In the following paragraphs, an attempt is made to relate nuclear problem areas to associated power extraction problems, as opposed to detailing methods of nuclear physics. It is important to note that the nuclear characteristics of reactors are not basically amenable to generalization even though this is partially attempted herein.

3.1 Fuel Inventory

Nuclear design incorporates the following considerations:

1. Preliminary estimate of feasibility based on a homogeneous, bare or reflected reactor configuration, using simplified approximations to establish critical mass
2. Detailed considerations of fuel inventory as listed below:
   a. Fuel burnup
   b. Fission product poisoning during operation and after shutdown
   c. Other control effects (temperature, startup, shutdown)
   d. Basic heterogenity effects (cell correction)
   e. Heterogenity effects induced by power shaping and flattening requirements
3. Power distribution
   a. Delineation of basic gross power distributions
   b. Fine power distribution effects
   c. Variation of power distribution with time, operating conditions, and control

Nuclear design studies generally proceed according to the general format of the design sequence. It includes a series of screening calculations with successive degrees of refinement that lead to progressive exclusion of unworkable areas so as to identify the regime that meets design requirements. Figure 12 is representative of information

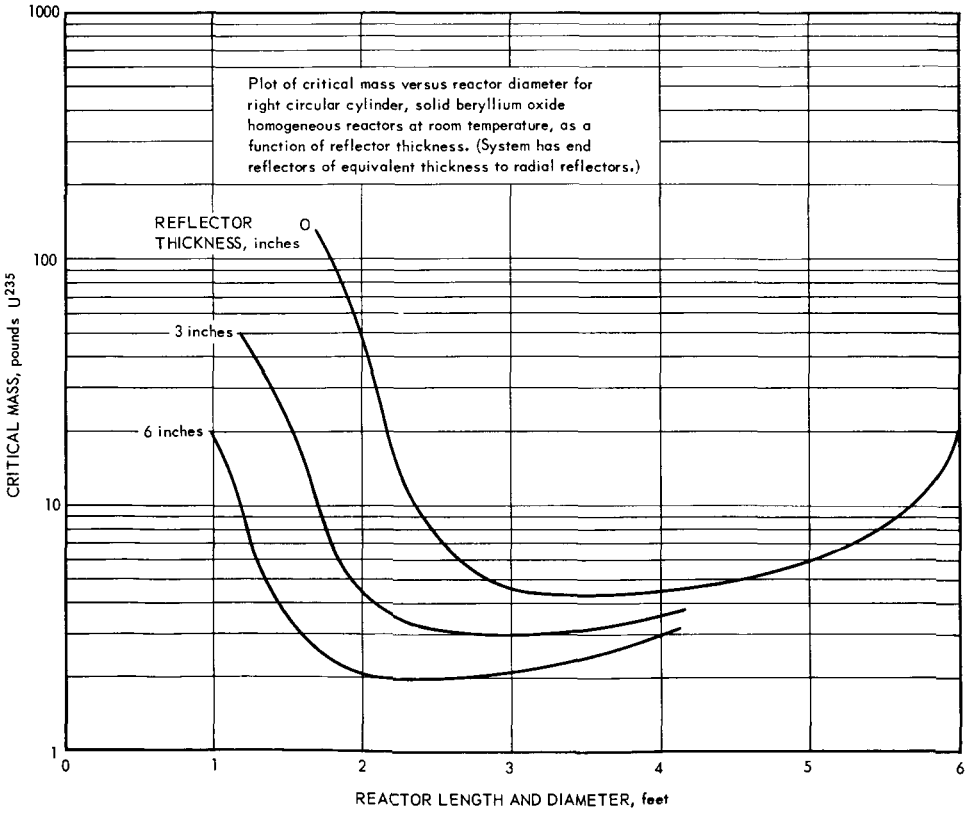

Fig. 12 – Plot of critical mass versus reactor diameter

which might be available in initial design stages. The data shown are critical mass requirements for solid, right circular cylinder cores at room temperature. Certain approximations, derived in part from the diffusion equations, can be used to extend the utility of these data. These approximations are: (1) the fuel inventory of a homogeneous system increases more than 3 percent by weight for a 1 percent increase in reactivity, and (2) the fuel requirements of a core containing uniformly distributed, small voids can be estimated by the use of Equations (18) and (19).

$$\text{Reference diameter of solid core} = D(1 - V) \tag{18}$$

This scaling factor applies to all other dimensions.

$$\text{Fuel requirements of actual core} = \frac{U}{(1 - V)^2} \tag{19}$$

where

V = volume fraction of voids in core
D = diameter of core containing voids
U = fuel requirements of reference core

Figure 13 illustrates a preliminary nuclear screening study based on data of Figure 12 plus the adjustments for void as given by Equations (18) and (19). These data are for a homogeneous, clean room-temperature critical system, and represent the lowest possible fuel requirement based upon a just-critical system. As such, they are adequate for exclusion-type calculations, but are of limited utility for subsequent design studies. Figure 13 shows the combinations of void fractions and reflector thicknesses that are above the fuel concentration limit, the rapid increase of critical mass with higher fuel-element volume fractions, and the ability of the reflector to reduce critical mass. Under ordinary circumstances, the primary design restraints may also include some limitation on total fuel and total reactor diameter; the former because of problems of economics and safety, and the latter because of economics and/or fabrication limitations that affect reactor pressure-shell structural design. Hence, additional limitations may appear on a screening plot such as Figure 13. Also, the use of thicker fuel plates can be considered in order to obviate a fuel concentration limitation.

A basic inadequacy of the data in Figure 13 is the assumption of a homogeneous mixture of the core material whereas the actual system may consist of a discrete separation of fuel and moderator. The homogeneous model also assumed identical neutron flux in both moderator and fuel, although, in the actual system, the flux is depressed in the fuel when compared to the moderator. (These are variously called thermal utilization and cell correction effects.) Figure 14 shows these heterogeneity effects from the standpoint of geometry (number of channels) and composition (increasing fuel concentration in the fuel channel). Indications of typical nuclear considerations that affect the choice of the number of fuel channels are shown in this figure. Also indicated is the necessity to re-estimate the fuel concentration limitations shown in Figure 13. (For example, with 61 channels, 31.5 pounds of U^{235}, the limiting concentration value, is equivalent to 19.5 pounds on a homogeneous scale.)

Further nuclear limitations can be identified from other items that define the required fuel inventory. Fuel burnup can be established from reactor power requirements, operating life, and the following factors for heat liberation per pound of U^{235}: 3.6×10^{10} Btu or 1.0×10^4 mw-hr.

* Assuming that the fuel is 93.2 percent enriched UO_2, with a density of 10.86 grams per cm^3.

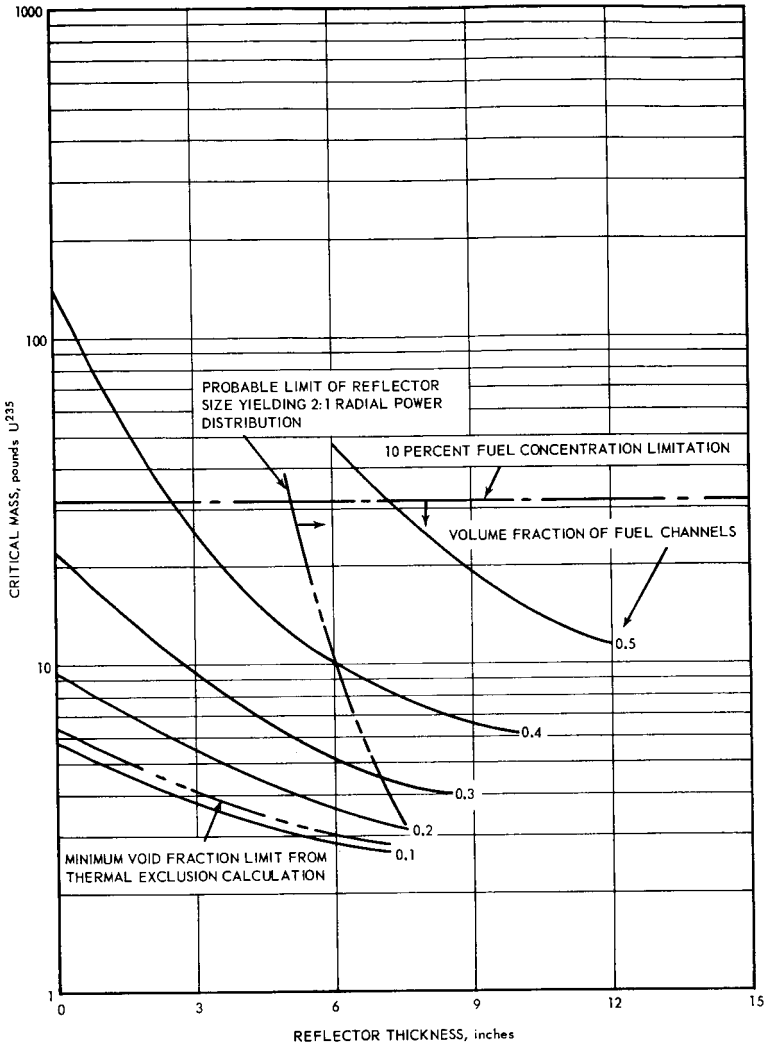

Fig. 13 – Plot of critical mass screening study (based on data from Figure 12)

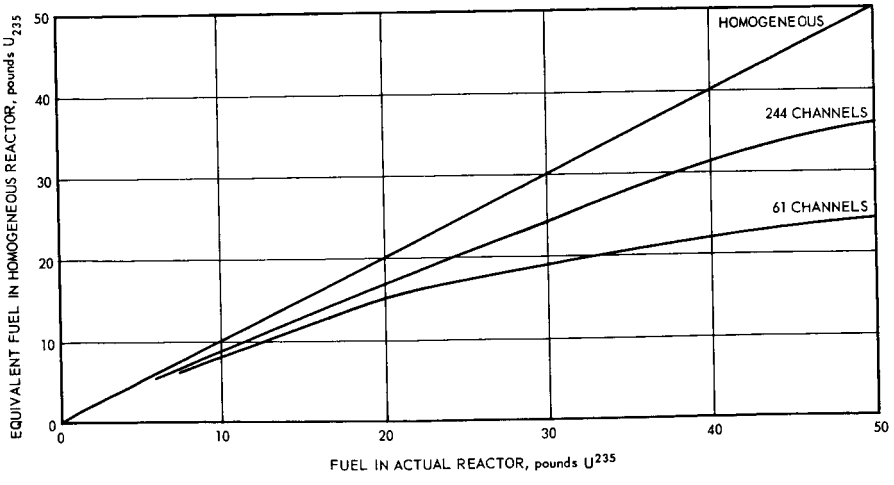

Fig. 14 – Fuel loading versus heterogeneity effects

The fuel required for fission product poison can be initially estimated solely by an assessment of xenon concentrations, since xenon is the most significant poison source in a reactor, except in very long-lifetime systems. A precise evaluation of xenon poisoning requires examination of the energy at which fission occurs (i.e., in fast-spectrum reactors, xenon poisoning is of no concern) and the distribution of power within the reactor. However, an initial estimate of the xenon problem can be made for moderated, fully enriched fuel systems by assuming that a neutron flux calculated from:

$$\phi\left(\frac{\text{neutrons}}{\text{cm}^2\ \text{sec}}\right) = \frac{Q'''\ (\text{mw/ft}^3) \times 3.1 \times 10^{16}\ \text{fissions/mw sec}}{N_{235}\left(\frac{\text{atoms U}^{235}}{\text{ft}^3}\right) \times \sigma_f\left(\frac{\text{fissions}}{\text{neutron-atom U}^{235}\ \text{pair}}\right)} \qquad (20)$$

using thermal cross sections, defines the highest possible magnitude of reactivity required to overcome xenon buildup during operation since the equilibrium values of reactivity versus flux for fully enriched systems are as follows:

Thermal Flux (ϕ)	Equilibrium $\left(\frac{\Delta k}{k}\right)$
10^{12}	0.007
10^{13}	0.03
10^{14}	0.046
10^{15}	0.048
∞	0.050

In most nuclear rocket applications, xenon poisoning will not be of concern because of the time dependence of the decay scheme leading to xenon and because the xenon isotope produced is, itself, unstable: The decay process and half-lives are shown below:

$$\text{Te}^{135} \xrightarrow[2\ \text{min}]{} \text{I}^{135} \xrightarrow[6.7\ \text{min}]{} \text{Xe}^{135} \xrightarrow[9.2\ \text{hr}]{} \text{Cs}^{135} \xrightarrow[2 \times 10^4\ \text{yr}]{} \text{Ba}^{135}$$

Hence, xenon would be a problem only if the reactor were required to restart during the first 5 to 40 hours after the power application and then only if the reactor were a high flux thermal type.

Another significant contributor to the fuel inventory requirement may be the effect of temperature on the nuclear properties of the system. Because of the variety of possible temperature effects, simplified evaluations of appreciable accuracy are not easily accomplished. The problems are temperature-induced density changes that affect both the macroscopic cross sections and the overall reactor size, and changes in microscopic cross section with variations of temperature. Usually the density effects are small in solid systems having built-in expansion clearances, although exceptions may arise in small reactors. On the other hand, variation of absorption cross section with temperature is usually a very significant effect. In high-temperature reactors the effect of temperature on xenon poison value must be considered especially because the absorption cross section of xenon decreases appreciably with temperature increases above 1100°F. The value of xenon poison decreases sufficiently to affect the required worth of the poison control system.

To illustrate, assume that suitable approximations of the overall temperature effects are as follows:

Fuel Inventory	Temperature Coefficient of Reactivity
4 lb U^{235}	$-11 \times 10^{-5} \frac{\Delta k}{k} {}^{o}F$
25 lb U^{235}	$-4 \times 10^{-5} \frac{\Delta k}{k} {}^{o}F$

Such values are typical for solid systems. The marked decrease of the temperature coefficient with increased fuel inventory reflects the fact that the major contribution to temperature coefficient is the increased leakage of thermalized neutrons. As fuel inventory is increased, the fraction of thermal fissions decreases, so that the leakage effect is of decreasing significance.

A summary of total fuel inventory for a typical, very well moderated thermal reactor, activity is as follows:

	$\frac{\Delta k}{k}$
Critical mass at room temperature	1.0
Equilibrium xenon	0.045
Other poisons, control	0.020
Temperature coefficient to 1200°F	0.072
Burnup	-
	1.137 plus burnup

Initial nuclear studies normally include evaluations of fuel inventory versus reactivity, which would permit directly relating reactivity to fuel-inventory. Assume that such a relation were established and showed that a 5 percent increase of fuel yields a 1 percent reactivity increase in a homogeneous system. Then, if the base critical system from Figure 13 is taken to be one with 7-inch reflectors that yields a critical mass of 4.5 pounds, the required homogeneous base critical mass is $4.5 + 5 \times 0.137 \times 4.5 = 7.58$ pounds in the homogeneous system or, from Figure 14, about 9.5 pounds in a system with 61 channels. **If 2.83 pounds of fuel happened to be burned, that amount must be added, so the total inventory is 12.3 pounds of fuel. The corresponding multiplication constant is $1.137 + 2.83/7.58 \times 5 = 1.212$. The loading of 12.3 pounds is consistent with the fuel concentration limits shown in Figure 13 for the basepoint calculation. No design alteration appears to be required in the example.**

The preceding discussion and Figure 14 serve to identify a new interrelation affecting both the thermal design and/or fuel concentration limitations. The particular problem, called a fine power distribution effect, is discussed in terms of Figure 15.

The preceding data suggests that the average flux in the fuel channel is about 80 percent of the average in the moderator (7.58/9.5). The outermost fuel plate senses a flux comparable to that in the moderator. A fuel plate half way into the center of the channel will have a flux of about 80 percent of this value; a central plate will have a flux of 60 percent of the outer plate value. The rate of power generation and heat flux for uniform fuel loadings for these plates will also be in the ratio of 1:0.80:0.60, and a problem with fine flow distribution and temperature variation can result. This problem can be alleviated by varying the plate spacing to match the flow distribution to the fine power distribution, or by varying the fuel loading to make the product of the number of fuel atoms times the flux equal to a constant. In particular, the fuel loading of plate 1 would be about 80 percent of average and the ratio of the innermost plate would be 80:60 percent, or about 1.33 times

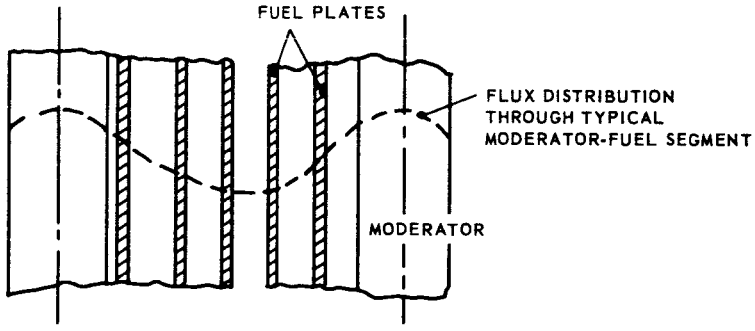

Fig. 15 – Typical flux distribution, plate-type fuel elements

average. Since the average fuel concentration in the example is less than half the postulated limit, such an increase is still within indicated allowances. However, such variation can easily "snowball" fuel concentration problems or dictate channel size.

3.2 Component Power Fractions

The second area of nuclear consideration is the fraction of power deposited in various reactor components. Usually this analysis will incorporate two distinct phases: (1) determination of heat sources among reactor components; and (2) variation of power deposition with time, temperature, control, etc. Typical evaluations and interpretations of these various areas are discussed in the following paragraphs.

3.2.1 Heat Sources Among Reactor Components

The fraction of power generated within the fueled region or active core of a reactor is generally in the range of 93 to 97 percent of the total power generated in the reactor-shield assembly. The fuel element itself may account for 90 to 100 percent of heat generation within the active core. The exact value is dependent upon the type of fuel element, the coolant, and the core materials. In some cases, knowledge of the precise power split-up within the active core can be of critical design importance. Specific examples are illustrated in terms of the following study of energy sources within the reactor core:

1. Fuel: U^{235} pure
2. Neutron Economy:

	Number of Neutrons	Percent
Fission capture	1.00	40.0
Nonfission capture in fuel	0.19	7.6
Nonfuel capture	0.66	26.4
Leakage	0.65	26.0
	2.50	100.0

3. Energy Sources in Core:

Instantaneous	Mev Per Fission
a. Kinetic energy of fission fragments	168
b. Instantaneous gamma rays from fission	7.5
c. Kinetic energy of fission and capture neutrons	3.7
d. Nonfission capture gammas from fuel	1.3
e. Nonfuel capture gammas	4.5

Delayed	Mev Per Fission
f. Fission-product betas	7
g. Fission-product gammas	6
h. Capture-product radiation	2
	200
4. Extra-Core Heat Sources:	
Leakage gammas (20% of gammas from item 3)	4.3
Gammas from leakage neutron capture	4.5
Kinetic energy of leakage neutrons	1.3
	10.1
5. Active Core Heat Sources:	
Fuel (items 3a, 3f, and 5 percent of nonleaking gammas)	175.8
Moderator and structure (item 3c and 95 percent of non-leaking gammas)	19.8
	194.8

6. Power Distribution

	Percent of Power		
Locale	Total	Mev Per Fission	Active Core
Extra-core (shield and reflector)	4.9	10.1	5.30
Active core	95.1	194.8	100.
Fuel	85.5		90.30
Structure and moderator	9.6		9.70
		205.8	

The following significant points can be developed from these data:

1. The magnitude of secondary heating (moderator and extra-core) is sensitive to both leakage effects and degree of neutron energy degradation. Conversely, the magnitude of primary (fuel) heating is relatively insensitive to these effects.
2. Because of the difference in sources, the distribution of secondary heat may differ markedly from the primary heat distribution.

These considerations may identify significant problem areas in reactors which are not coolant moderated, especially when fuel and moderator are not integral. In such cases, both the magnitude and distribution of secondary heating may be critical to design. Conversely, in coolant-moderated systems or in integral solid systems, the secondary heating problem is of minimal concern.

Interest in secondary heating tends to be accentuated by introduction of incremental design techniques. In previous design studies, it was indicated that radial power flattening was desirable and that the choice of channel size can be affected by the ratio of primary-to-secondary heating. It is improbable that radial flattening of the primary power will also yield flattening of secondary power because of the difference of sources. Hence, some design penalty on power or temperature may result.

A final concern is the effect of shutdown on fuel element design. (This topic is considered in detail in a later section, hence only limited coverage is presented here.) Shortly after shutdown, the energy sources in a reactor are only delayed group items. The fraction of delayed beta particles generate heat within the fuel, while the heat generated from delayed gammas tends to be distributed in proportion to the relative weights of active core

components. A comparison of typical operating and shutdown power distributions is given in the following tabulation.

	Percent of Power and Maximum Power For 100 mw Operation	
	Operation	Shutdown
Fuel Elements	95% - 95 mw	60% - 2.4 mw
Structure and Moderator	5% - 5 mw	40% - 1.6 mw

This tabulation illustrates the typically large decrease of fuel element power and relatively smaller decrease in structure and moderator power. This effect may dictate a high aftercooling flow capacity, which may be further accentuated if the reactor flow system was designed to yield a select distribution based on power operation. In some instances, the aftercooling capacity requirements may prove so excessive as to warrant fuel element design based on aftercooling requirements. This situation can be anticipated in reactors with nonmoderating coolants or nonintegral fuel-moderator combinations.

The previous estimate of relative power generation rates in various reactor components was based upon the following data and approximations:

1. The neutron economy used in the example is typical for enriched U^{235} systems; neutron kinetic energy degradation prior to absorption is 2 Mev per neutron.
2. Gamma energy release resulting from any neutron capture can be assumed to be 7 Mev per neutron for all common reactor materials except hydrogen, where 2.5 Mev per neutron should be used.
3. Gamma leakage can be estimated with the aid of Figure 16, which expresses gamma leakage as a function of core size and effective density for spheres and infinite cylinders.
4. The distribution of gamma heating among active core components can be assumed to be in proportion to the weight fraction of the components, except that certain heavy elements, uranium in particular, should be assigned twice its actual weight for weight fraction determination.
5. Fission-product kinetic energy and beta energy generate heat in fuel because of the short range of the particles. Gamma photons are more penetrating; gamma heating distribution will follow gamma source distribution only in very high density systems. More commonly, the distribution of gamma heating will follow a cosine distribution as described for neutron flux; the assumption of 2:1 axial and radial distribution is usually a good first approximation.
6. Fission product decay energy is assumed to have achieved saturation (near complete saturation is achieved only after about 100 days of operation, but about 85 percent saturation is achieved after two hours).

The distribution of gamma heating has been established for the sample calculation with the use of the preceding guides. More precise calculations would use several energy groupings to represent the gamma spectrum.

Evaluation of gross radial and longitudinal power distributions can usually be accomplished with appreciable accuracy only by multienergy, multiregion reactor criticality studies, which are best solved by machine methods. This fact, plus the possibility of a considerable variation in results from different core compositions and fission energy spectrums, generally limits the ability to estimate distributions simply with any appreciable reliability. The best estimate that can be made assumes that the neutron flux is a

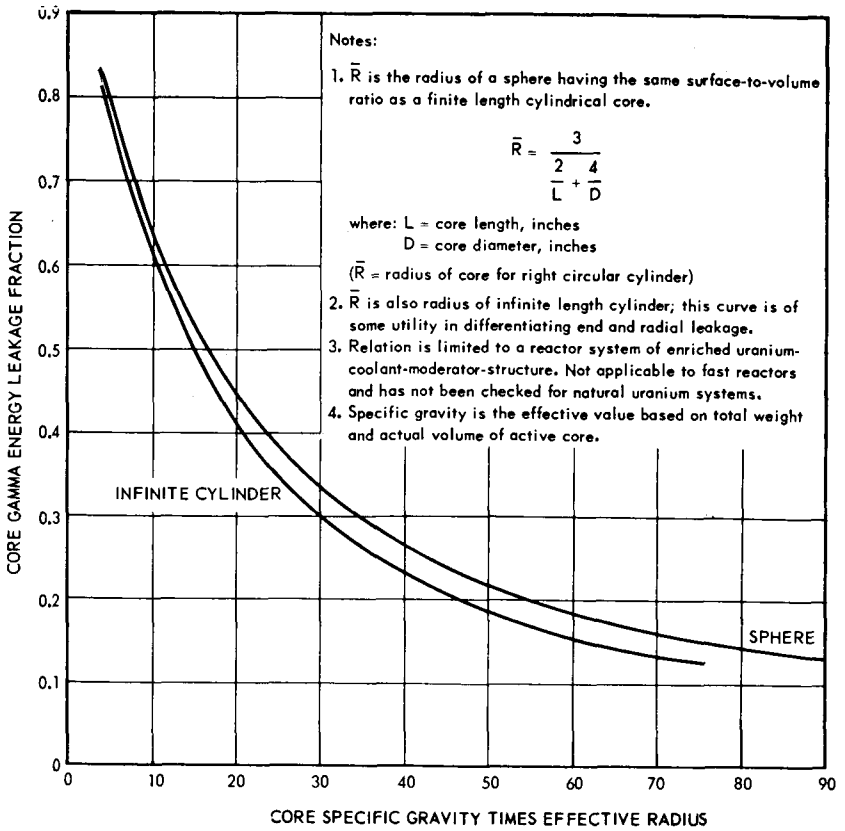

Fig. 16 – Estimating chart for determination of gamma energy leakage in terms of core geometry and density

continuous function through the core and reflector, diminishing to zero at a length outside the core that is equivalent to the reflector savings.

Some additional guides which are often useful are as follows:

1. For a reactor with common moderator and reflector material, and low fuel concentration, reflector savings are approximately:

$$\text{Savings} = \frac{\text{Reflector Thickness}}{\text{Effective Density of Moderator}} \qquad (21)$$

$$\text{Savings} = \frac{\text{Reflector Thickness}}{1 - \text{Core Void Fraction}} \qquad (22)$$

   These equations are limited to savings equal to or less than infinite reflector savings.
2. Reflectors generally will yield flux and power scallops at the core-reflector interface if the ratio of centerline-to-average flux is 1.2:1 or less. The tendency towards scalloping is much more pronounced for a high fuel concentration or a highly absorbing core and a good reflector.

3.2.2 Variation of Power Distribution During Operation

One of the most severe limitations on effective power extraction from nuclear systems is the variation of power distribution during reactor operation. This is also one of the

most difficult design problems to anticipate. The items of concern can be illustrated in terms of the basic relation for nuclear heat generation, previously listed as Equation (5) and repeated below for convenience:

$$Q''' = C\ N\sigma_F\phi \qquad (5)$$

where

C = Constant
N = Number of fissionable nuclei per unit volume
σ_F = Fission cross section
ϕ = Neutron flux-causing fission
Q''' = Volumetric heat-generation rate

General phenomena which may promote power-time dependency effects are:

N variants: Fuel burnup, conversion, or breeding
σ_F variants: Temperature variation affecting cross sections, fuel conversion, and breeding
ϕ variants: Movement of absorber controls; fuel variations; buildup of poisons; moderator temperature and density variation (particularly with coolant moderators which may undergo phase changes); other core composition or density changes

Design considerations of these effects are not aimed toward prevention, since, with few exceptions, all must occur in any power reactor. Instead, the intent is to provide suitable methods of control and compensation in order to minimize power extraction limitations. A general approach to the problem consists of identifying the power-time dependency effect in terms of magnitude and degree of heterogeneity. The method of control or compensation is similarly identified and the most suitable compromise has been determined.

Fuel burnup considerations serve as an illustration of this approach. Burnup results in a decrease of fissionable nuclei concentration and a buildup of fission product poisons, both of which can vary the power distribution. If the power generation is not uniform throughout the reactor, as is normally the case, burnup occurs at different rates within the system and the tendency toward power distribution variation is magnified particularly if the fuel burnup allowance is an appreciable portion of the initial fuel inventory. Since the criterion for steady-state operation of a power reactor is the maintenance of an effective neutron multiplication of unity, some form of control must be considered to override the added reactivity associated with allowance for fuel burnup. In addition, the control must gradually be removed as burnup occurs in order to maintain a neutron multiplication of unity. Both the presence of the control itself and its movement during the operating life of the system introduce variations of power distribution.

A measure of the potential magnitude of variation introduced by burnup considerations is the excess reactivity associated with the fuel burnup requirement (since this is a measure of both the relative composition change and the degree of control movement during operating life). The actual magnitude of power distribution variation depends on an ability to match or to compensate for the burnup variations by use of the control mechanism or by local adjustment of the fuel concentration. The most desirable situation is one in which the variation introduced by the control exactly cancels the variation introduced by burnup. This situation can be approached by the use of a poison which burns out with the fuel (this may be mandatory in some cases). If control rods are used as an alternative, the differences in the locale of the burnup and of the rod-induced variations determines the actual magnitude of the variation in power distribution.

The power-time dependency variables given in the preceding paragraphs can be summarized as follows:

1. The potential magnitude of a power-time dependency variation can be defined by the maximum value of reactivity that must be controlled.
2. The degree to which the potential magnitude of variation actually occurs depends on an ability to compensate for the variation source with respect to time, magnitude, and reactor location.
3. Limitations on the ability to compensate stem from the following sources:
   a. The methods of control and compensation will, in themselves, introduce variation sources.
   b. Several variant sources (differing in magnitude, time dependency, and locale) will normally exist in the operating reactor; ability to compensate decreases with increasing number of variations.
   c. Reactor operating requirements, particularly power level changes, introduce alternate control system restraints which limit compensation ability.

Some specific problems of power distribution variation in relation to time are illustrated in the previous example. The excess reactivity required at startup and the time of operation at which the total reactivity allowance is counterbalanced by the causitive effect are shown in Table 4.

TABLE 4

TIME-DEPENDENT REACTIVITY EFFECTS[a]

Item	Δk/k	Operating Time Required To Counterbalance Reactivity
Temperature coefficient	0.072	Time required to bring system to operating temperature
Equilibrium xenon	0.045	~24 hours
Burnup	0.075[b]	Total life (240 hours)[b]
Miscellaneous control	0.020	Total life

[a]Per example previously assumed; applicable to a low fuel inventory, very well moderated thermal reactor.

[b]This is significantly greater than in a single use of any rocket reactor but is included for illustration.

Of the items listed, burnup is anticipated as the most significant source of variation that will affect power extraction because the total reactivity change is large and occurs gradually throughout the operating lifetime while the reactor is at operating temperature. In contrast, the temperature coefficient, also a large magnitude reactivity effect, is not a significant variable source, since the compensating control is removed from the reactor as soon as operating temperature is achieved.

The total excess reactivity of the system also yields some insight to the problem. For example, if control rods are used, several factors (such as practical size, safety considerations, and power distribution distortion effects) serve to define the maximum reactivity worths of individual rods. Three types of control rods are usually considered: safety rods, shim rods, and regulating rods. Safety rods are high-speed, high-reactivity worth units that normally are removed from the system and used under emergency conditions only. Shim rods are also of relatively high worth but are low in speed. These units are used for coarse control. The regulating rods are high-speed, low-worth units used for fine control.

Practical size limitations generally dictate a maximum shim-rod worth of about 3 percent reactivity, whereas safety considerations dictate regulating rod worths of less than

0.75 percent. In order to minimize power distortions, it is desirable to minimize individual rod worths and use multiple rods to prevent high local-power distortions. However, the use of a large number of rods may adversely alter reactor structure and introduce significant limitations on the fuel element passage design. The total effective worth of multiple rods is usually less than the sum of individual rod worths because of interactions, except in large reactors having widely spaced rods. The total reactivity of the sample design, (about 20 percent) is near the limit that is controllable by a rod system.

In the sample design, the control rods required for the bulk of the temperature coefficient effect can be accommodated by several high-worth shim rods, since power distortion considerations are not of limiting concern. In contrast, the worths and distribution of the remaining control requirements are significantly affected by power distortion limitations.

Control rods affect flux distributions in some local areas to a high degree, even though the overall flux distribution is relatively unchanged. As an example, penetrating-absorber control rods, which normally enter the cold end of a reactor, tend to shift power to the rear of the core. However, the fuel channel in close proximity to the rod is more strongly influenced than the average, and there may, in addition, be a scalloping of distribution at the control rod tip. Some typical effects of control rods, illustrated in Figure 17, show that power distortions can severely limit power extraction. Common techniques for mitigating power distortion effects are illustrated in Figure 18. The distribution of a required total control worth among multiple rods should yield minimum distortion, in contrast to the distortion that results when a single, high-worth rod is used. Similarly, minimizing rod position changes with time yields minimum variation of distribution with time (e.g., if power distribution is distorted but invarient with time, it will generally prove to be a less severe design limitation than a time-dependent distortion effect). Multiple rods afford some flexibility with regard to time-dependent effects since it is possible to choose the grouping to minimize power distortion.

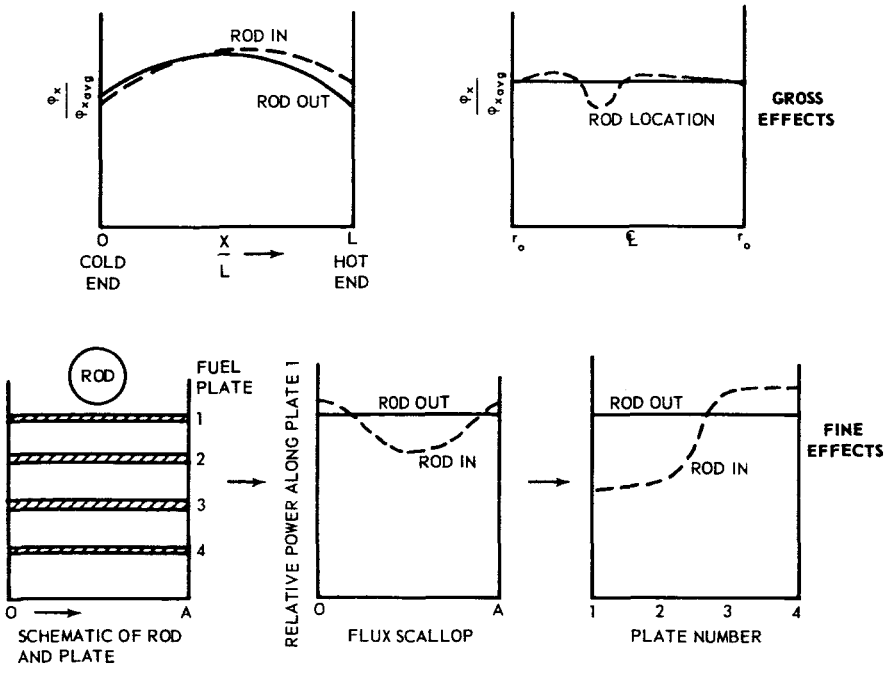

Fig. 17 – Power distortion versus control rod locations

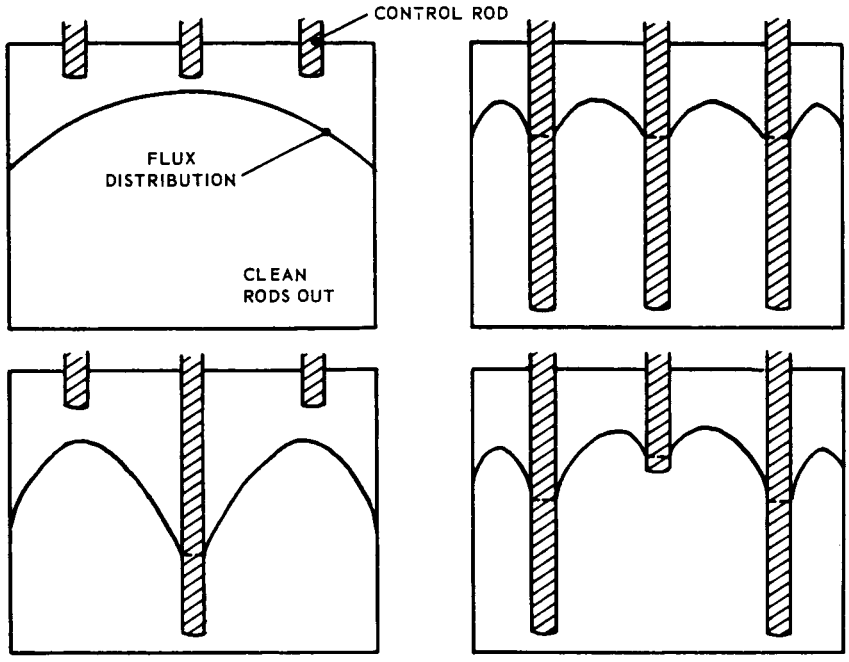

Fig. 18 – Flux control by selective control rod positioning

In the sample design, a burnable poison in the system would compensate for fuel burnup and essentially eliminate time dependency. This corresponds to the use of an infinite number of control rods. For purposes of illustration, assume that this can be accomplished even though considerable design complication may result. The percentage of burnup in a particular fuel plate varies with the radial location of the fuel channel, the longitudinal location of the plate in the fuel channel, and the distance between the fuel plate and moderator. Thus, a power distribution that is truly independent of time may require the use of a variable concentration of burnable poison in the fuel plates.

Control compensation for xenon could be accommodated either by a burnable poison or by control rods. The use of a burnable poison introduces a complication in that the poison must compensate for two variable sources, each of which exhibits a different degree of time dependency (fuel burnup and xenon formation). In such a case, the probability of achieving ideal compensation for both is low.

To complete the example, assume that the reactor control system for the sample design is as follows:

Item	Type of Control
Temperature coefficient	3 to 4 high-worth shim rods
Fuel burnup	Burnable poison in fuel
Equilibrium xenon and miscellaneous control	More than 9 regulating rods

In the preceding summary, the number of regulating rods is indicated simply as being greater than the number defined by safety requirements. The actual number would be defined by the allowable power distortion, a significantly larger number may be necessary. An alternative to using more regulating rods would be to bias the thermal design on the basis of control considerations. If it can be established that the bulk of power distortion

due to a rod is localized,* it might be possible to oversupply coolant to a particular adjacent fuel channel intentionally so that a fairly significant power distortion can be accommodated. This solution to the problem, rather than design alteration would be particularly desirable if less performance penalty were involved in significantly decreasing the discharge temperature from one or several of the 61 fuel channels.

To complete an initial control study in the design sequence, it would also be necessary to appraise additional effects that might necessitate either inclusion of or movement of a control mechanism. These effects include a decrease of xenon absorption with temperature, system power demand changes, and special startup and shutdown requirements. An additional design problem is the limitation on analytical prediction of flux distortions that are attributable to control rods. Analytical interpretations of multiple control rod configurations are of limited accuracy; local effects can generally be established only by measurement in critical experiments.

All of the preceding design discussion has been concerned with absorber controls. The same general problem areas and points of investigation would apply to other possible control methods.

3.3 Afterheat and Aftercooling

3.3.1 General

One of the most significant features that differentiates nuclear power systems from other power generation systems is that the nuclear unit continues to generate heat after shutdown. The after-shutdown heat, called afterheat, generally imposes the need for auxiliary cooling systems. The characteristics of afterheat can be identified with the aid of reference to Figure 19.

Figure 19 also shows emergency scram, in which reactor controls are capable of reducing power by a factor of 3 to 6 within milliseconds. A gradual shutdown considerably alters the time-power relations shown for intervals A and B.

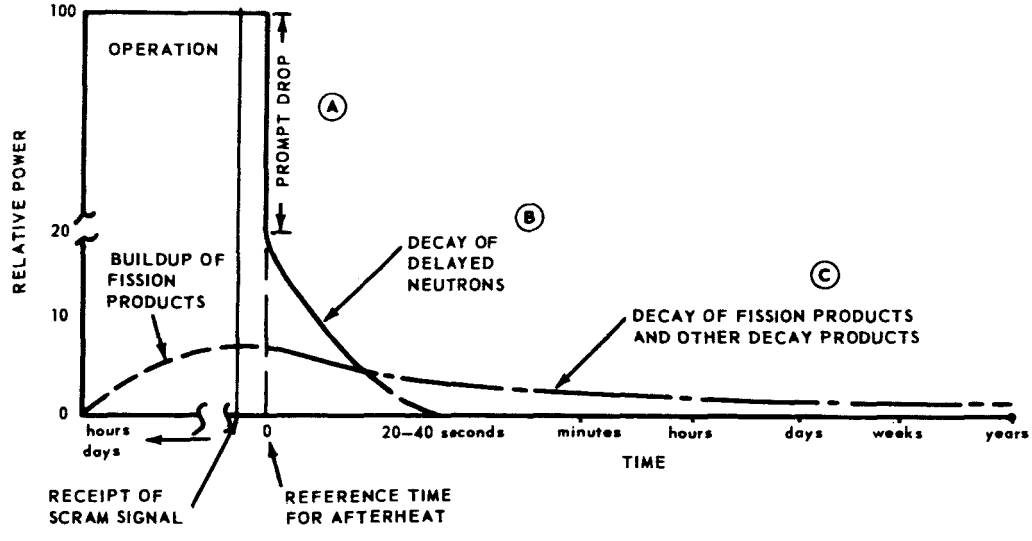

Fig. 19 – Effects on relative power after scram

*Control-rod-induced distortions tend to be localized only in high-fuel-density, nonthermal reactors. Highly thermal reactors (enriched fuel, water-moderated such as the MTR) generally will exhibit both steep local distortions and overall distribution effects.

The afterheat dissipation (aftercooling) system usually is designed for three conditions: (1) emergency; (2) normal operation, during which an aftercooling unit is sized to replace the main coolant system (or to reduce the flow rate of the main coolant) sometime during period C; and (3) reactor disassembly during which the time and cooling requirements necessary for reactor disassembly are specified.

3.3.2 Fraction of Afterheat Power Deposition in Reactor Components

In order to assess aftercooling problems, the distribution of afterheat in the reactor system must be examined. To do this, consider the reactor as consisting of an active core, a reflector, and a surrounding shield. Then compare the distribution of power during operation and after shutdown. The energy per fission during operation can be categorized as either instantaneous (occurring at the same time as, and being a result of a particular neutron reaction) or delayed (caused by a prior fission or neutron birth). After a period of operation (so that the delayed sources approach equilibrium) the approximate sources of energy within the reactor core are as given in Table 5.

TABLE 5

ENERGY SOURCES WITHIN REACTOR CORE

	Mev Per Fission	Percent Of Group	Percent Of Total
Instantaneous Group			
1. Fission fragment kinetic energy	168.0	89.6	83.0
2. Kinetic energy of fission neutron	5.0	2.67	2.46
3. Instantaneous gamma rays	7.5	4.0	3.7
4. Capture gamma rays[a]	7.0	3.73	3.45
Group Total	187.5	100.00	93.61
Delayed Group			
5. Beta and gammas from fission products	13.0	87.0	6.41
6. Radiation from capture products[a]	2.0	13.0	0.98
Group Total	15.0	100.0	7.39
Total	202.5		100.00

[a]Variable with specific materials.

Most of this energy manifests itself as heat within the active core except for a portion of the gammas, usually 15 to 30 percent, and fast neutrons that escape to the shield and reflector. Heat may also be generated outside the core by leakage neutrons that interact with material in the shield and reflector. A typical heat distribution for an operating reactor may be as follows:

	Mev
Total gammas in active core (Table 5, items 3, 4, 6, and part of 5)	23.0
Escape gammas	6.9
Gammas generating heat in core	16.1
Heat in fuel (Table 5, item 1; beta fraction of 5, 50% gammas)	182.5
Heat in moderator (50% gammas, about 60% of item 2)	11.0
Heat generation in shield and reflector from neutrons	7.0

(assuming 1 neutron escape per fission that yields 5 Mev per capture, plus the kinetic energy of escaping neutrons.)

In terms of relative power distribution this becomes:

Locale	Mev	Power, %
Fuel	182.5	88.0
Moderator	11.0	5.3
Shield and reflector	13.9	6.7
Total	207.4	100.0

After the decay of delayed-neutron effects, the sources of heat are confined to the delayed group items. If capture-product radiation is neglected, the afterheat distribution is approximately as follows:

Energy: 50 to 60 percent beta; 50 to 40 percent gamma	Afterheat, %
Gamma leakage to shield and reflector	10
Fuel: All betas, 50 percent nonleaking gammas	70
Moderator	20
Total	100

3.3.3 Power from Decay of Fission Products

In order to evaluate the afterheat from the decay of fission products and that of other radioactive species, understanding of the process of formation and decay of the various species present and an understanding of this relationship with respect to afterheat power level is necessary. Assuming monoenergetic neutrons and constant operating power, a simplified differential equation for the formation of a fission product is:

$$\frac{dA}{dT} = - A (\lambda_A + \sigma_A \phi) + Y_A \Sigma_F \phi \qquad (23)$$

Rate of buildup = rate of formation minus (decay rate and interaction removal rate)

For most substances, except for those of high cross section, and long half-life in high flux (e.g., xenon),

$$(\sigma_A \phi + \lambda_A) \cong \lambda_A \qquad (24)$$

Thus the equation reduces to:

$$\frac{dA}{dT} = - A\lambda_A + Y_A \Sigma_F \phi \qquad (25)$$

which yields, upon integration:

$$A = \frac{Y_A \Sigma_F \phi}{\lambda_A} \left(1 - e^{-\lambda_A T_O}\right) = A_O \qquad (26)$$

where

$\frac{dA}{dT}$ = Rate of formation of A
T = Time (seconds)
T_O = Time, operating (seconds)
T_S = Time, shutdown (seconds)
A = Number of Nuclei of A per cm^3
P_O = Operating power
P_S = Shutdown power
Y_A = Yield, amount of A formed per fission

$\Sigma_F\phi$ = Fission cross section times flux (fissions/cm^3-sec)

λ_A = Decay constant = $\ln\left[\frac{2}{\text{Half-life}}\right]$ (seconds)

After shutdown, A decays as:

$$\frac{dA}{dT} = -\lambda_A A \tag{27}$$

and, if the energy per disintegration is C, the power in afterheat attributable to A is:

$$A = A_o e^{-\lambda_A T_s} \tag{28}$$

$$\text{Power} = C\frac{dA}{dT} = \left(-\lambda_A A_o e^{-\lambda_A T_s}\right) C = P_s \tag{29}$$

$$A_o = \frac{Y_A \Sigma_F \phi}{\lambda_A}\left(1 - e^{-\lambda_A T_o}\right) \tag{30}$$

$$P_s = \frac{\lambda_A Y_A \Sigma_F \phi}{\lambda_A}\left(1 - e^{-\lambda_A T_o}\right)\left(e^{-\lambda_A T_s}\right) C \tag{31}$$

$$= -C Y_A \Sigma_F \phi \left[e^{-\lambda_A T_s} - e^{-\lambda_A (T_o + T_s)}\right] \tag{32}$$

Finally, since $\Sigma_F\phi$ is a measure of the operating power P_o, an equation of the form indicated can be developed:

$$\frac{P_s}{P_o} = \text{Constant times } C Y_A \left[e^{-\lambda_A T_s} - e^{-\lambda_A (T_o + T_s)}\right] \tag{33}$$

Thus, the afterheat power can be expressed as a function of operating power, periods of operation and shutdown, product yields, half-lives, and the decay energies of fission products. Systematic identification of fission products has permitted either analytical or empirical relations to be derived for the overall afterheat power from uranium* fission products. Data from two sources are shown in Figure 21.

The general relationships for afterheat usually takes the form of Equation (33), which indicates that power after shutdown increases with increased operating time and decreases with time after shutdown. In addition, when dealing with a mixture of fission products, such as U^{235}, it is important to consider the implication of the variety of species. The fission product decay releases both beta and gamma radiation. Of interest in aftercooling are the relative quantities of beta and gamma particles, and the gamma energy distribution. Since, at different times after shutdown, different species are primarily responsible for the extant power, it is possible that both the spectrum of gamma energies and the beta-gamma ratio will be time dependent. Actually, considerable information is available for the gamma spectrum because of its importance in shielding calculations; beta information is much more scarce. Figure 3.2-20 shows what is considered to be the most complete evaluation of the beta-gamma energy division. †

*Decay products from U^{235} differ somewhat from those found in natural uranium.

†XDC 60-1-157, "The Activities of Fission Products of U^{235}, M. R. Smith.

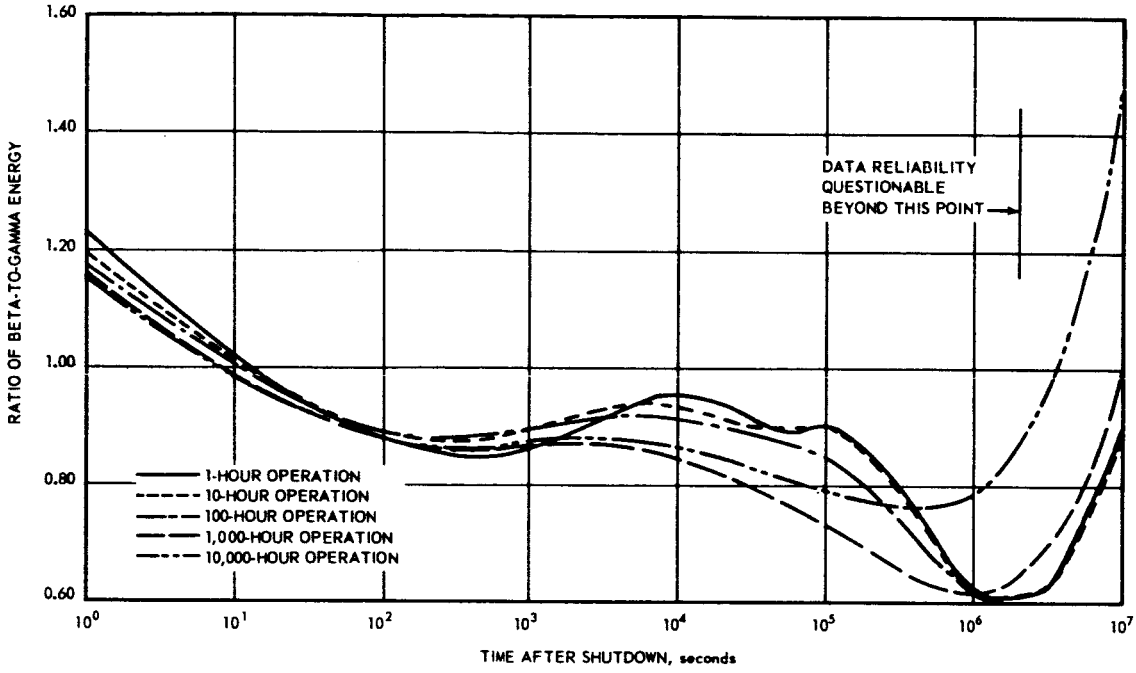

Fig. 20 – Beta-to-gamma energy ratios versus operating and shutdown times

Empirical formulae could be developed from the data on Figure 20 and used to identify the existence of other materials that might yield decay energy in the same time period as the fission products. In that case, in lieu of fission cross sections, the equation for the quantity of species present at the end of operation is given by Equation (34).

$$A'_O = (\text{Absorptions per Fission}) \text{ times } \frac{\text{Fissions}}{\text{sec}} \text{ times } \frac{\left(1 - e^{\lambda_{A'} T_O}\right)}{\lambda_{A'}} \qquad (34)$$

$$A'_O = \frac{\text{Yield A}}{\text{Absorption}}$$

Materials that are present in large quantities, and have high-absorption cross sections, high yields, and high-energy decay particles may be of consequence. From a practical standpoint, it is doubtful that such conditions can exist in most common reactor systems. However, the decay of radioactive, nonfission-product sources may be a principal heat source for long periods after shutdown when fission-product decay is at a low level. Although Equation (34) is identified with neutron reactions, a variety of other possibilities exist. In particular, gammas interact with beryllium to yield neutrons, which in turn react and yield new fission products.

3.3.4 Power from Decay of Delayed Neutrons

The behavior of neutrons during scram is almost exclusively a function of the mechanical design and worth of the safety or scram control system. After receipt of a scram signal there is a definite time delay, usually of about 10 to 100 milliseconds, before the control is actuated. Almost immediately after the control responds, the reactor undergoes a prompt drop. The change in power can be estimated from Equation (35):

$$\frac{P_{pd}}{P_O} = \frac{1}{\left(1 - \frac{\Delta k}{0.0075}\right)} \qquad (35)$$

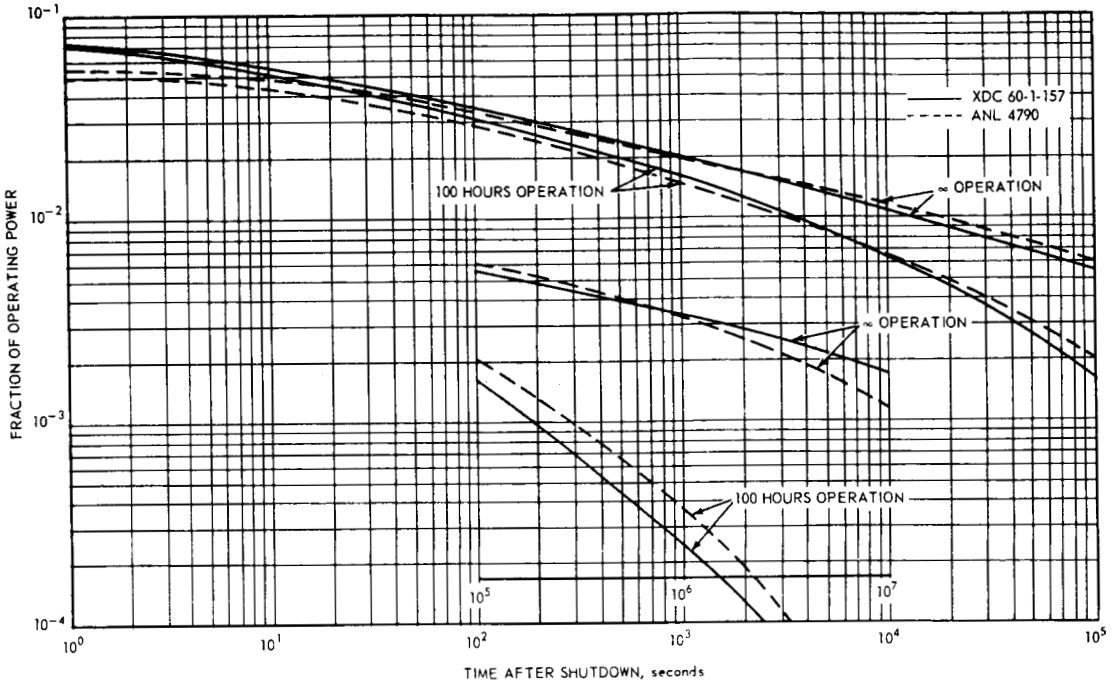

Fig. 21 – Fission product decay energy versus operating and shutdown times

where

0.0075 = Delayed neutron fraction

Δk = Reactivity change (negative for shutdown)

P_{pd} = Power after prompt drop

A comparison between results of Equation **(35)** and rigorous calculations, where all groups of delayed neutrons are considered, is shown in Figure 22. The decay of delayed neutrons after prompt drop is a function of the reactivity change during shutdown and temperature-induced reactivity changes. Table 6 is a decay history for a reactor with negligible temperature-coefficient effect.

TABLE 6

$\frac{P_S}{P_O}$ (FROM DELAYED NEUTRONS ONLY) AS A FUNCTION OF TIME AFTER PROMPT DROP

Time After Prompt Drop, sec	Negative Reactivity (-Δk), %					
	1	1.5	2	3	4	5
0	0.44	0.34	0.28	0.20	0.15	0.12
5	0.29	0.20	0.16	0.12	0.078	0.069
10	0.21	0.145	0.105	0.08	0.051	0.044
15	0.16	0.115	0.082	0.061	0.038	0.034
20	0.135	0.095	0.067	0.050	0.029	0.026
30	0.098	0.068	0.046	0.034	0.0195	0.017
40	0.075	0.050	0.034	0.024	0.0136	0.0115
50	0.058	0.037	0.025	0.0175	-	-
60	0.046	0.028	0.019	0.013	-	-

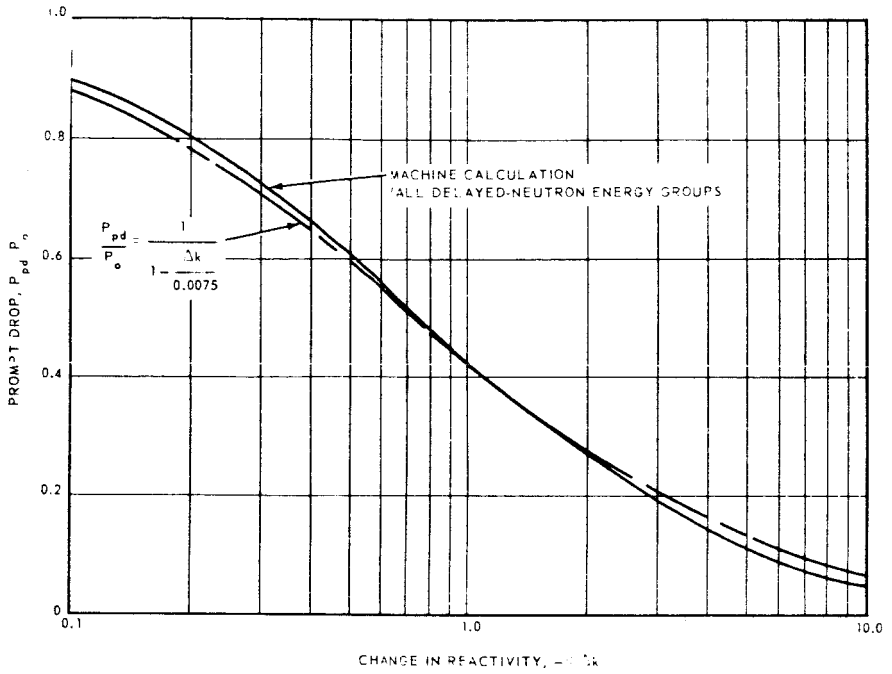

Fig. 22 – Prompt drop as a function of reactivity change

Table 6 illustrates that both the lowest initial power level and the most rapid subsequent decay are associated with the largest reactivity change. The average power in the 20-second period after shutdown is 23 percent of operating power for a 1 percent reactivity decrease and approximately 3.7 percent for a 5-percent reactivity decrease. The decay rate will also vary with the reactor temperature coefficient of reactivity (negative temperature coefficient, decreasing rate of decay; positive temperature coefficient, increasing rate of decay). However, the variation usually is not significant.

3.3.5 Summary of the Sources of Afterheat and Aftercooling Design

Examination of the sources and variation of afterheat can be used to assess the characteristics of system design. General characteristics are as listed below:

1. For design purposes, the afterheat power level should be based on the longest operating time and the highest power of operation. In addition, the emergency condition powers should be based on the minimum change of reactivity scram.
2. A basic problem in design for removal of afterheat is the significant change of power-source distribution between afterheat and operation. For example, 2 minutes after shutdown from long-time operation, the total power is one-thirtieth of the operating value. The fuel elements may be at one-sixtieth of their operational value, but the moderator shield and reflector may be as much as one-fifth of their own operational level. This problem is of particular concern in heterogeneous systems, especially those where it is necessary to maintain discrete coolant passages that are sized to the operational power distribution.
3. The accent on aftercooling problems is largely a function of the source of coolant-pumping power, the thermal capacity of the reactor system, the coolant characteristics, and permissible downtime of the power system. For example, if the reactor powers its own coolant-pumping unit (closed-cycle gas turbine), aftercooling problems become of concern at the instant of reactor shutdown. Low thermal capacity and short permissible downtime generally necessitate designing for the short shutdown times and, hence, higher power levels. Specific coolant characteristics (e.g.,

melting or freezing point, heat capacity, density, and sensitivity to power-induced flow distribution effects) are of obvious consequence in that they can impose special limitations and influence thermal capacity, or pyramid aftercooling-capacity requirements.

In order to determine the required aftercooling capacity, it is necessary to establish the power level and the distribution of power during the shutdown period as functions of time after shutdown. On the basis of these data, the reactor component that dictates the required aftercooling capacity is established, and it is possible to define capacity as a function of time after shutdown. The capacity curves are then examined in order to determine aftercooling requirements. The following is a typical design schedule.

1. Establish the afterheat power level versus shutdown time, assuming maximum operating power and time of operation and minimum shutdown reactivity change for power operation.
2. Establish the distribution of power sources in the afterheat period.
   a. For decay of delayed neutrons, assume that the heat sources are distributed as in operation.
   b. For fission product sources, assume that the ratio of betas to gammas is as indicated in Figure 20. Since the betas have extremely short range, they serve, almost entirely, to generate heat at their point of origin. Thus, beta heat sources will have, essentially, a distribution identical to the operating power distribution.
   c. The distribution of gammas from fission products can only be approximated. Since gammas are relatively penetrating, they tend to be stopped away from their point of origin. Both the distribution and leakage of gammas from the active core are functions of the gamma energy spectrum, which changes significantly during shutdown. A reasonable approximation of gamma heat distribution is usually possible by relatively simple methods. In particular, the distribution of gamma energy for a uniform, but not necessarily homogeneous, system is approximately proportional to the weight fraction of the material in the active core. (The weight assigned to uranium is taken as twice the actual value.) Thus, for a particular component:

$$P_A = \frac{W_A}{(W_T - W_U) + 2W_U} \left[P_\gamma (1 - L_\gamma)\right] \qquad (36)$$

   where

   P_A = Gamma heat generation in material A
   P_γ = Total gamma power from fission products
   W_A = Weight of material A
   W_T = Total weight of active core (fueled region)
   W_U = Weight of uranium
   L_γ = Gamma leakage fraction

   Equation (36) follows from the fact that, over a wide energy range, common to the fission-product gamma range, the gamma-absorption cross section, divided by density, is essentially constant for all materials. Thus, the amount of gammas absorbed is proportional to weight, with uranium, lead, and tantalum being specific exceptions. The leakage fraction of gammas is usually lower than during operation. Serious error is not introduced if L_γ is assumed to be zero for calculation of active core components.
   d. The gamma flux distribution within the core usually resembles the fast neutron flux distribution in operation, and, for cylindrical systems, the distribution is approximately 2:1 cosine functions both radially and longitudinally. Equations (37a) and (37b) define gamma heat-source distributions for this case.

$$(Q_A''')_{x,r} = \frac{P_A}{V_A} \times \left[1.35 \cos\left(\frac{\pi r}{3R}\right)\right] \times \left\{1.21 \sin\left[\frac{\pi\left(\frac{X}{L} + 0.25\right)}{1.5}\right]\right\} \qquad \textbf{(37a)}$$

where R = core radius

$$\begin{pmatrix}\text{Gamma heating per unit volume of A at } x, r\end{pmatrix} = \begin{pmatrix}\text{Average heating rate}\end{pmatrix} \times \begin{pmatrix}\text{Radial correction}\end{pmatrix} \times \begin{pmatrix}\text{Longitudinal correction}\end{pmatrix} \qquad \textbf{(37b)}$$

e. Although, in certain cases, both the quantity and distribution of heat sources in the region outside the active core (shield and reflector) can be defined by simplified approximations, it is more desirable to obtain preliminary estimates from shielding calculations. This is especially true for instances where the distribution of heat sources is of particular concern. During the initial period of afterheat when delayed neutrons exist, the major sources of shield and reflector heat are attributable to gamma and neutron leakage from the core and the subsequent reactions of neutrons with reflector and shield materials. After cessation of delayed-neutron activity, heating is due almost exclusively to leakage of core gammas. In both cases, additional effects are possible. These effects include the decay of activated materials and gamma reactions with beryllium, which yield photoneutrons. Such effects are inclined to be of most significance in the later time periods. As previously mentioned, the mean energy of gammas from decay of fission products is almost always lower than that of operating fission-product gammas. In addition, the gamma energy spectrum tends to decrease with time after shutdown. Hence, it can be anticipated that the gamma-leakage fraction in afterheat will generally be lower than that in operation, and that the leakage and distribution, respectively, should decrease and vary with time after shutdown.

3. When the heating rates in the reactor components are established, the instantaneous coolant-flow-rate requirements can be determined in order to maintain the most temperature-sensitive reactor component at a safe level. This calculation is made for a variety of power levels that exist in the afterheat period. The results define the maximum values of aftercooling capacity required. In order to define the minimum requirements, it is necessary to examine the transient effects associated with the exponential decay of power with time after shutdown. As an example, assume that the maximum allowable temperature to which a reactor material can be taken is $(T)_{max}$ and that the initial temperature of that material at scram is $(T)_0$. In order to define the minimum coolant requirements, a series of coolant flow rates are assumed and the time temperature history of the component is established as shown in Figure 23.

4. The calculation system described in this section is actually applicable to all phases of afterheat evaluations even though the illustration is for the emergency condition only. For normal shutdown, the required coolant curve is a function of shutdown time until the establishment of some value of time and capacity consistent with process limitations. For the reactor disassembly period, a power level is established at which the reactor is self-cooling (has free convection and radiation) or at which the system can be left without coolant for enough time to facilitate partial or complete disassembly. Many variations, such as intermittent cooling (subcooling of the system for a short period, followed by a no-cooling period) are possible for these latter situations.*

*This discussion assumes reactor coolants with freezing points below room temperature. For the case of liquid metals the afterheat problems are more likely concerned with supplying sufficient heat to prevent freezing of the reactor coolant.

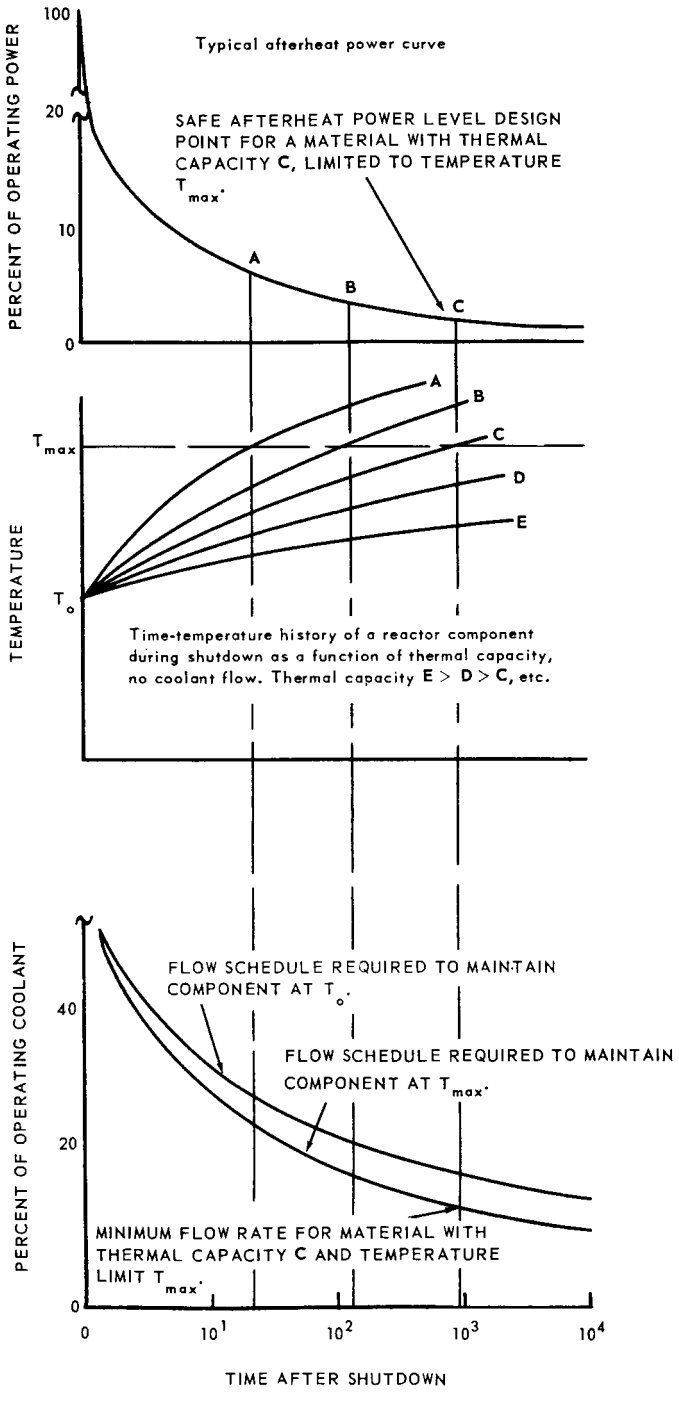

Fig. 23 – Flow and temperature relationships after shutdown

Although it is not possible to consider calculations for a variety of specific reactor types, the following generalizations may be of value:

1. Liquid-cooled systems normally have higher thermal capacities than gas-cooled systems; hence, the afterheat design-point power level is lower for liquid-cooled systems.*
2. The more homogeneous the reactor, the greater the likelihood that relatively low coolant requirements will exist throughout the afterheat period.
3. Liquid-cooled systems are more likely to reach a self-cooling state than are gas-cooled systems because of both the higher thermal capacity and the free convection effects. (Also, as the fuel element becomes more compact, the possibility of free convection becomes increasingly difficult in liquid systems and nonexistent in gas systems.)
4. Particular attention should be paid to the possibility of a change in power distribution during the reactor disassembly period, especially if the coolant is to be drained and if the coolant weight is a significant portion of the total core weight. Examination for possible decay of nonfission-product heat sources is generally of particular concern during this period, also.

Interpolation on the fission-product decay curve, as explained in the following paragraph, is possible because of the construction and the equations that are applicable to the fission-product decay curve. To find P_s/P_o at time t after shutdown following operation for time T_o:

1. Locate the value of P_s/P_o for t seconds after shutdown and $T_o = \infty$.
2. Locate the value of P_s/P_o for $(t + T_o)$ seconds after shutdown and $T_o = \infty$.

The required answer is a - b.

4 MECHANICAL DESIGN CONSIDERATIONS

Mechanical design activities in the initial design sequence are largely devoted to identification of feasible configuration concepts and relationships to the total system configuration. During the final design sequence the mechanical design function becomes quite significant because it is generally the function responsible for the statement of fabrication specifications.

During the initial design sequence, the mechanical designer must establish configurations that are consistent with nuclear and thermal design restraints and must, simultaneously, identify the mechanical design features that are restraints on the thermal and nuclear design. The former will include heat transfer surface area and configuration, and the volumes of several reactor components, i. e., fuel, moderator, and control rods. The latter will include component operating temperature capabilities relative to the aerodynamic loads imposed and the amounts and locations of the required structural materials that must be accounted for in the nuclear design.

Initial design considerations must consist of identification of load paths throughout the reactor under all modes of operation and subsequently must identify strains and resulting stresses for essentially all reactor components. Interrelationships with other system components must be isolated. For example, a reactor may be bolted to a shield component and the assembly supported as a cantilevered beam by attaching one end of the shield component to the basic system structure. Control rods may be withdrawn from the reactor into the shield. Significant problems in identifying clearances required for differential thermal expansions and deflections caused by acceleration loads will normally result.

Assembly and disassembly procedures will need to be identified early and basic concepts justified. Remote handling capability must be planned early in the design sequence.

In the final design sequence, mechanical design assessment and component design verification will become significant activities. Gas-cooled high-temperature reactors will, in general, be designed with small margins making analytical studies only, inadequate. Safety of operation and economic considerations place a high priority on experimental evaluation of reactor components prior to a full reactor test. In the final design sequence, the mechanical designer is concerned with identification of capabilities for reactor components to perform safely under environments imposed in an operating reactor.

Strong motivation for experimental investigations is created when analyses cannot provide sufficiently accurate answers, or more importantly when insufficient materials data are available and existing analytical capabilities are insufficient for the required calculation model.

A dominate part of the experimental program will consist of proving endurance capability of high-temperature fuel elements. Significant effort will be expended to simulate reactor-imposed conditions in laboratory tests in order to minimize the amount of more expensive, but necessary, tests in irradiation test facilities. Tests in irradiation test facilities normally permit close simulation of reactor component operating conditions. Design of components and procurement of specimens becomes a major activity. Proof of certain characteristics may require significantly modified configurations, e. g., thicker walls to compensate for lower heating rates when simulating strains required for internal temperature gradients associated with conduction of heat to the convective heat transfer surface.

Additionally, the experimental program will include configuration mockups for evaluation of tolerance effects and determination of behavior under acceleration conditions.

Tests may include control rod movement at high temperatures to identify wear and force characteristics.

Finally, the mechanical design function will evaluate fabrication processes and verify the adequacy of existing processes or their extensions. Achievability of close tolerances will be evaluated relative to fabrication costs. After tolerance questions are resolved, acceptable criteria including inspection requirements will be identified.

5 ASSESSMENT OF UNCERTAINTY FACTORS IN THE INITIAL DESIGN SEQUENCE

The final study involves an evaluation of remaining design uncertainties. Specifically, the preceding studies have served to establish the merits of particular development possibilities. Some design possibilities have been eliminated by primary design restraints; others have been eliminated by requirements, not immediately obvious, that were dictated by these restraints. At some point in the sequence, further differentiation requires a design decision that will based largely on allowances for the various remaining uncertainties. These uncertainties may include allowances for analytical and developmental investigations not completed within the design study period.

Table 7 is a summary of the variation of estimated system-pressure loss through basepoint evaluations as the method described in Section 2.1 is applied. Preparation of a table such as this serves both to summarize preceding work and to introduce typical uncertainty allowances.

A review of the final estimate of pressure loss suggests the following major unqualified assumptions:

1. The friction factor assigned to geometry is 1.5 times that of a comparable smooth, uninterrupted configuration.
2. The negligible flow maldistribution attributable to either basic flow system or power-induced variations are not considered in the calculations.
3. The entrance and exit pressure-loss allowances are consistent with mechanical requirements for the fuel element support.

Qualification of these assumptions is primarily dependent on experimental evaluation, particularly since items 1 and 3 are sensitive to specific configurations. If the experimental determinations that confirmed the estimates were available, the final design study

TABLE 7

ESTIMATED VARIATION OF SYSTEM PRESSURE LOSS

Calculation Model	ΔP, psi	Comments
1. Ideal power distribution, zero plate thickness	3. 19	Screening calculation only
2. Cosine longitudinal distribution, zero plate thickness	4. 1	Reflects decision to eliminate power shaping in design
3. Cosine longitudinal and radial power distribution, zero plate thickness	7. 58	Reflects decisions to power flatten with reflector alone; achieve uniform fluid discharge temperature by flow compensation
4. Cosine longitudinal and radial power distribution, 20-mil plate thickness	10	Reflects determination of mechanical, fabrication limitations; nuclear studies defining fuel concentration effects
5. Cosine longitudinal and radial power distribution, 20-mill plate thickness plus choice of number of channels	10. 9	Allowance for frictional surface of channel
6. Final estimate	13. 3	Allowance for entrance and exit effects in channel

would consist largely of a finalized uncertainty study considering tolerances and similar problems as shown in Table 8.

In the absence of experimental data, the adequacy of the design would rest on a decision as to whether the difference in the design estimate (13. 3 + 2. 2 psi) and an allowance of 20 psi imparts an adequate margin of flexibility.

The same general approach would be considered for other items that are limited by primary design restraints. Two particular restraints are fuel concentration and temperature considerations. Generally, these items are categorized as either those that affect coolant temperature or those that affect surface-to-fluid temperature difference. A summary of typical items, often called hot channel factors, is presented in Table 9.

Although the magnitude of uncertainties varies significantly with a variety of items (type of fuel element, coolant, etc.) Table 10 shows some typical numerical values. The values are expressed as an uncertainty factor, F, where (F-1) is a measure of the uncertainty.

TABLE 8

UNCERTAINTY EFFECTS ON PRESSURE LOSS

Item	Uncertainty, %	Potential Increase Of ΔP, psi
Tolerance on fuel channel	±2	0. 40
Tolerance on fuel plate	±2	0. 20
Accuracy of friction data	±6	0. 65
Distortion of channel in operation	±5	0. 55
Uncertainty of flow distribution	±2	0. 40
Total		2. 20

TABLE 9

CAUSES OF HOT CHANNEL FACTORS

Source Of Variation	Design Considerations Affected
Gross radial power distribution uncertainties	Power-to-coolant in channel; average heat flux in channel; power-induced flow maldistributions
Gross longitudinal power distribution uncertainties	Variation of heat flux distribution in channel
Fine power distribution, flux scallops	Heat flux of particular fuel plates or at axial locations in channel
Gross flow distribution uncertainties (among channels)	Coolant temperature rise in channel; heat-transfer coefficient
Channel and fuel element dimensional tolerances and/or variation during operation	Coolant flow to channel; coolant distribution within channel; geometry factors affecting coefficient
Heat-transfer data uncertainty	Heat-transfer coefficient
Fuel loading tolerance	Channel power and heat flux; local heat flux in fuel plate
Fine flow distribution and variation of fluid mixing within a channel	Local fluid temperatures in channel

The factors in Table 10 are used in the proper convective heat-transfer and heat-balance equations in order to interpret uncertainty in terms of temperature. Many of the items are simple linear relations; however, items such as power-induced flow maldistributions, geometry tolerance influence on coefficients, and localized variations are more complex relationships. A summary of the minimums of the preceding table, expressed as either a multiplier to fluid temperature, F_T, or surface-to-fluid ΔT, $F_{\Delta T}$, is as follows:

Product of items 1, 4, 7, and 8	1.105	
Flow variations deduced from 1, 5, and 6	1.03	
Product	1.14	$= F_T$
Product of items 1, 2, 3, 6, and 7	1.21	
Flow variations affecting coefficient	1.06	
Others	1.02	
Product	1.31	$= F_{\Delta T}$

These two combined factors are used as corrections to a final evaluation. The safest approach of design application would be the use in such a manner as to assure that the maximum design-temperature limitation is not achieved except with the most pessimistic combination of uncertainties. A comparison of features of this design alteration and the basepoint design given previously is as given in Table 11.

The final uncertainty allowance can introduce significant design alteration or a conflict with an initial design restraint (in this case, for example, the system pressure loss would be near marginal with design alteration for the temperature uncertainties indicated). In such a situation, the philosophy of assuming that all uncertainties exert maximum deleterious effect in a common locale is often questioned on the basis of statistical improbability. The uncertainty effect sometimes can be lessened by limiting case studies. Typical examples for the sample design include studies of the mitigating effects of thermal radiation, and selective location of high-side and low-side measurable tolerance

TABLE 10

HOT CHANNEL FACTORS

Item	F-Factor[a]	Usual Source Of Uncertainty
1. Gross radial power	1.05 - 1.30	Limited representation of operating reactor by critical experiment (e.g., mocking up a system whose distribution varies significantly with time, power, or temperature)
2. Gross longitudinal power	1.03 - 1.20	Limited representation of operating reactor by critical experiment (e.g., mocking up a system whose distribution varies significantly with time, power, or temperature)
3. Fine power distribution flux scallops	1.05 - 2.0	Inability to analyze or measure localized control effects, core-reflector interface scallops
4. Gross flow distribution	1.02 - 1.10	Shielding or mechanical restraints forcing plenum chamber design inconsistent with good flow distribution, orifice, and channel tolerance
5. Fuel element tolerances and/or operational warpage	1.02 - 1.08	Lack of manufacturing knowledge prior to design. Limited knowledge of operational damage
6. Heat-transfer data	1.06 - 1.3	Fuel element geometry not amenable to analysis or experimental definition
7. Fuel loading	1.01 - 1.05	Fabrication and quality control
8. Fine flow distribution	1.02 - 1.20	Fuel element geometry not amenable to analysis or experimental definition

[a]The lower value is a probable limit of measurement accuracy. (F-1) is actually a plus or minus number, but the worst case is generally considered in design.

TABLE 11

ALLOWANCES FOR UNCERTAINTIES

Design Assumption	ΔP^a	$\frac{A_H}{V_f}$	V_S	D_H	$(T_{max})^b$
Uncertainties neglected	10	156	1.135	0.268	1900°F
Uncertainties considered	16	207	1.505	0.192	1600°F

[a]Fuel element section only.
[b]Assuming most pessimistic combination of uncertainties.

items. In addition, a statistical weighting factor for uncertainties can be established from operating experience with a closely analogous system.

In a situation where the safe philosophy yields an undesirable configuration alteration, it may prove preferable to accept the uncertainty as inferring a decrease in the guaranteed power of the system or as implying that the system will achieve design power only if maximum uncertainty stackup is not achieved. This artifice actually represents a tacit recognition of the possibility that uncertainties may stackup in an advantageous fashion. Also indicated is an inability to realize such potential if the system is designed safe. If the uncertainties were such as to actually permit increase of reactor power over the de-

sign requirement, this could be realized in the system whose design infers a guarantee below actual desired power. Conversely, the additional pressure loss resulting from the safe design would serve to eliminate such realization. It is not uncommon to encounter a set of primary design restraints that merit an assessment of uncertainty during reactor operation. The sample design studies discussed in this section are representative of a complete initial design cycle, except for concern regarding the quantity of work and the details of investigations. An actual design usually requires several cycles of the nature indicated to establish a final design. The number of initial designs needed is dependent on an ability to estimate the component design requirements in any one iteration. Also, the final design phase should include a highly intensive uncertainty analysis of greater magnitude than indicated in the sample studies.

Appendix A
FUEL ELEMENT GEOMETRY CHARACTERISTICS

GEOMETRY CLASSIFICATIONS

Fuel element geometries are best discussed in terms of the following classifications:

1. Unit surface fuel elements
2. Compound surface elements
   a. Defined geometry
   b. Statistical geometry
3. Reactor matrix elements

BASIC CONSIDERATIONS

The basic considerations usually applicable to all fuel elements are as follows:

Geometry Variables

1. High surface-to-volume ratio is desired.
2. Coolant has access to entire fuel element surface.
3. Minimum selective channeling of coolant through structure
4. High ratio of heat transfer to pressure loss
5. Minimum surface and volume required for structural support
6. Compatible with removal and replacement operations
7. Permits uniform distribution of fuel and/or places no restrictions on fuel quantity and distribution

Fabrication and Mechanical

1. Minimum distortion caused by structural load, vibration, changes of power level, pressure difference, and thermal stress
2. Configuration simplicity consistent with ease of fabrication
3. Minimum tolerance sensitivity
4. Amenable to multiple production
5. Compatible with inspection techniques
6. Compatible with operating instrumentation

General Considerations

1. Configuration consistent with accurate nuclear and thermal analysis (tends towards symmetrical systems and simple geometries), or alternately amenable to experimental evaluation
2. Minimum cost (a function of all preceding items)

It is apparent that additions to the basic desirable characteristics are possible and that few systems will exhibit all of the desired characteristics. Possibly the least understood characteristic is that of economics; it is possible that a significant fuel element limit could evolve from compatibility with reprocessing methods as an example. The following

paragraphs present information primarily concerned with geometry variables for the indicated classifications.

Simple Fuel Elements

Simple surface fuel elements such as single plates, rods, and spheres are useful in low power density reactors. Typical geometry characteristics of these fuel elements are presented in Table **A-1.**

Since it is desired to have both maximum surface-to-volume and minimum values of ΔT_i, minimum characteristic dimensions are indicated. However, with dimension decrease, it is progressively more difficult to obtain mechanical integrity, thus, compound surfaces are required. Table **A-2** gives some indication of the limitations on unit surface fuel elements.

TABLE **A-1**

GEOMETRY CHARACTERISTICS OF SIMPLE SURFACE FUEL ELEMENTS

Surface	Characteristic Dimension	Surface-To-Volume[a] Ratio	Internal Temperature Difference,[b] ΔT_i
Plate	Thickness t	2/t	$(Q'''/k)^c$ $(t^2/8)$
Rod	Diameter D	4/D	(Q'''/k) $(D^2/16)$
Sphere	Diameter D	6/D	(Q'''/k) $(D^2/24)$

[a]Volume of fuel element.
[b]ΔT_i = Temperature difference (maximum minus surface) within element.
[c]Q''' = Volumentric heating rate.
k = Material thermal conductivity.

Thus, it appears that simple fuel elements (assuming that a 1-inch rod represents a typical structural integrity limit for this type) must be limited either to low-power enriched or natural uranium reactors.

The natural uranium-fueled reactor is worth additional discussion since in this case nuclear considerations dictate the desirability of having a rod diameter of 1 inch or more. With a 1-inch rod, the maximum heat flux at the rod surface would be of the order of 100,000 Btu/hr-ft^2. With water as the coolant, heat transfer coefficients of the order of

TABLE **A-2**

LIMITATIONS ON UNIT SURFACE FUEL ELEMENTS

Reactor Type	Fuel Weight	Fuel Volume, ft^3	Reactor Power ($\bar{Q}$), mw
Natural uranium - graphite	50 tons	45	70
Natural uranium - heavy water	6 tons	6	10
Enriched uranium	3-300 pounds	0.003-0.3 (0.015-1)[a]	0.005-1.6

[a]Assuming fuel concentrations of the order of 20 percent in a matrix material where $\bar{Q}$ = total reactor power based on 1-inch diameter rod, $\Delta T_i = 300^oF$.

500 to 1000 Btu/hr-ft^2-^{o}F appear reasonable. A typical coefficient range for gases is 20 to 150. Maximum fuel element temperatures for two typical cases are as follows:

	Water	Gas[a]
Fluid temperature	100^{o}F	100^{o}F
Surface-to-fluid ΔT	100^{o}F (h = 1000)	2000^{o}F (h = 50)
ΔT_i	300^{o}F	300^{o}F
T Maximum	500^{o}F	2400^{o}F

[a]Typical of natural-uranium fueled reactor having a fuel rod of 1 inch diameter or more.

As shown, the gas system would probably be unsatisfactory due to material overtemperature. A reduction of temperature can be achieved by adjusting factors which influence surface-to-fluid ΔT ($\Delta T = Q/A_H h$). In natural fuel reactors cooled by gas, e.g., Brookhaven, Calder Hall, extended surface fuel elements are considered in lieu of increasing h. Typical extended surface fuel elements are shown in Figure A-1.

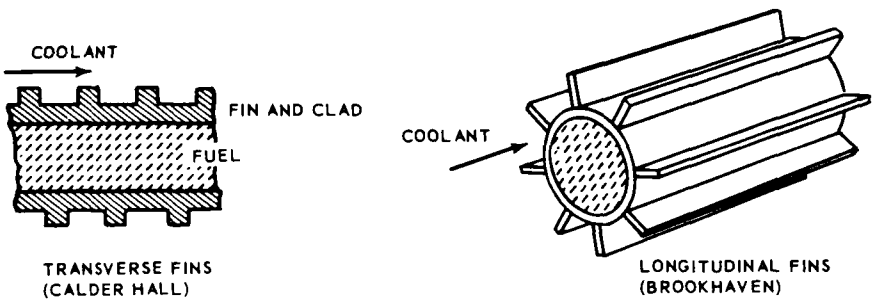

Fig. A-1 – Typical extended surface fuel elements

A significant point relative to extended surfaces is that the fin area is not as efficient in transferring heat as the surface of the rod itself. Thus, reduction of heat flux (Q/A_H) is not a simple function of ratio of fin surface area to bare tube area. The effective heat flux for an extended surface is, in simplified form:

$$\frac{Q}{A_H} = \frac{Q}{(A_t + \eta A_{fin})} \qquad \text{(A1)}$$

where

A_t = exposed area of tube
A_{fin} = fin area
η = effectiveness of fin

The fin effectiveness is a function of fin geometry, heat transfer coefficient, and thermal conductivity of fin material; high heat transfer coefficients and low conductivity yield poor efficiencies. Thus, extended surfaces generally are not considered where high coefficients prevail. There are only a limited number of materials which combine satisfactory nuclear characteristics with high conductivity and ease of fabrication, e.g., aluminum, magnesium. These latter characteristics are increasingly difficult to obtain with higher temperature requirements. This suggests considerable restriction on extended surface fuel element types.

The simple surface type of fuel element will be used to discuss considerations of coolant channeling and heat transfer parameter requirements. Figure A-2 illustrates typical problems.

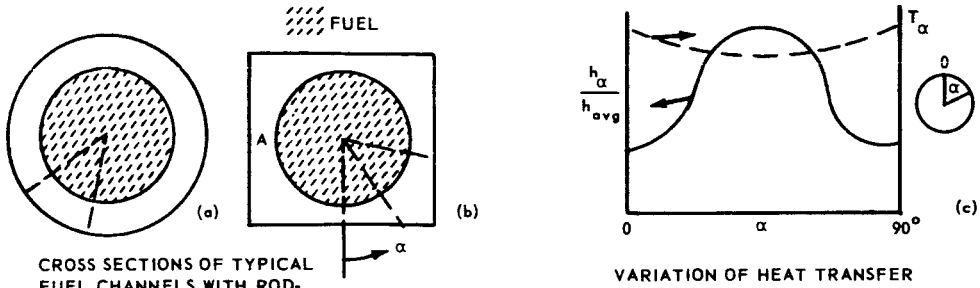

Fig. A-2 – Coolant channels – rod-type fuel elements

Part a of Figure **A-2** shows a fuel element which would not be expected to exhibit surface access or channeling effects. Alternately, part b illustrates an element with significant problems in these respects. Specifically, there will be a high tendency for conditions illustrated in part c to occur because of asymmetric characteristics of the rod-square channel configuration. This is perhaps better illustrated by construction of constant central-angle sectors from rod center to channel wall. In part a, the ratios of fuel element volume to surface and coolant flow area to fuel element surface are constant for a given central angle at all peripheral locations; in part b, the ratios of coolant flow area to surface and fuel element volume vary with peripheral location, the tendency towards variable ratios being responsible for part c characteristics.

An added significance of Figure **A-2**, part c is that it indicates some of the special considerations for heat transfer data. At point A in part b of the figure, the heat transfer coefficient is below average, indicating a higher than average surface-to-fluid ΔT and hence higher actual temperatures than indicated by average calculations. Since such variations often impose severe design restrictions, fuel element heat transfer data may often include local effect variation (as contrasted to more common process heat transfer work wherein average considerations usually suffice). In Figure **A-2**, coefficient variation reflects lack of similarity between fuel element and channel cross sections. However, many fuel elements will exhibit surface coefficient variation; spheres and rods in cross flow are typical examples. Note also that many simple cross sections such as polygons result in asymmetric internal temperature gradients.

Compound surface fuel element systems have evolved with the utilization of enriched uranium and the necessity of providing continuous support of the thin structural members required to achieve high surface-to-volume ratios. Compound surface systems can be considered as an array of single fuel elements.

The characteristics of compound surface fuel elements are best discussed in terms of the following outline of characteristics:

1. Heat transfer coefficient relation
2. Friction factor relations
3. General geometry characteristics
4. Special effects and limitations

Usually the heat transfer coefficient can be expressed by some relation of the form:

$$\frac{h\bar{D}}{k} = a\left(\frac{\bar{D}G}{\mu}\right)^m \left(\frac{C_p\mu}{k}\right)^n \qquad \textbf{(A2)}$$

where

a, m, n are constants
C_p = specific heat
μ = viscosity
k = thermal conductivity
$\bar{D}$ = dimensional characteristics
h = heat transfer coefficient
G = mass velocity

Equations of this nature are usually a satisfactory means of defining coefficients for all coolant-geometry systems except liquid metals and fluids that undergo a change of phase during heating. Although it is not intended to provide a complete survey of heat transfer phenomena, sufficient information is included to permit interpretation of data available in more comprehensive texts. Simple tubes (Figure A-3) will be used as a basis for the discussion that follows.

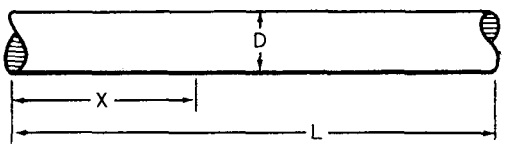

Fig. A-3 – Typical simple-tube fuel element

The heat-transfer coefficient is nominally defined by the relation:

$$h = \left(\frac{Q}{A_H}\right)_x \left(\frac{1}{T_s - T_b}\right)_x \qquad \text{(A3)}$$

where

$\frac{Q}{A_H}$ = heat flux
T_s = surface temperature
T_b = average fluid temperature

A more general definition of the heat-transfer coefficient, expressed in terms of Figure A-4, is:

$$h = \frac{-k\left(\frac{dT}{dY}\right)_0}{(T_s - T_b)} \qquad \text{(A4)}$$

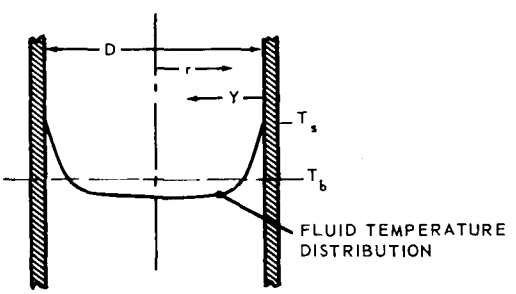

Fig. A-4 – Typical temperature distribution for turbulent flow of a heated fluid

where

k = conductivity

$\left(\frac{dT}{dY}\right)_0$ = slope of temperature profile at tube wall, Y=0

The differential $(dT/dY)_0$ is a function of all items which define the complete temperature profile. These include the velocity distribution and a grouping of physical property terms, the Prandtl number ($C_p\mu/k$) which represents the ratio of heat-to-momentum transfer within the fluid. The variation of form of correlation in Figure A-5 represents differences in velocity profiles for the different flow regimes. Most fuel element work is concerned with turbulent flow, although specific exceptions occur.

Additional considerations pertinent to Figure A-4 through A-6 can be best illustrated in terms of a specific equation for turbulent flow in smooth tubes:

$$\frac{hD}{k} = 0.023 \left(\frac{DG}{\mu}\right)^{0.8} \left(\frac{C_p\mu}{k}\right)^{0.33} \qquad \textbf{(A5)}$$

Significant points of interest are:

1. Equation (5) is a simplification of a more precise relation which, being complicated, is of limited engineering utility. The specific values 0.023 and the Prandtl number exponent of 0.33 are usually applicable to all liquids, except liquid metals. For gases, corresponding values are 0.021 and an exponent of 0.4.

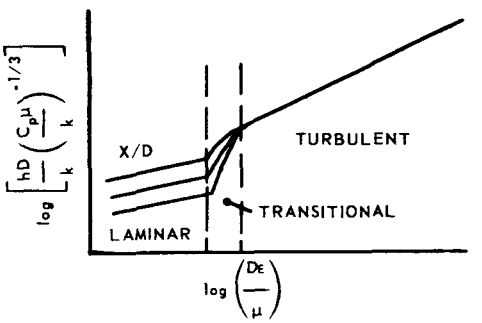

Fig. A-5 – Typical correlation plot for smooth tube heat transfer coefficients

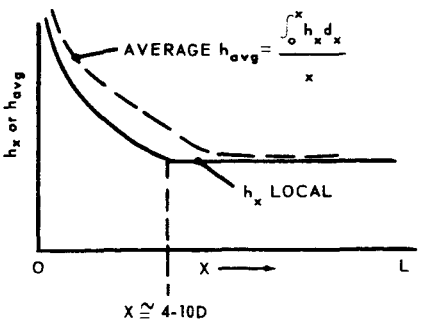

Fig. A-6 – Typical variation of heat transfer coefficient in entrance region of smooth tubes

2. When the difference between surface and fluid temperatures is large or when significant variation of physical properties occur in this range, some question arises as to the temperature at which properties are evaluated. For most fluids, the exceptions include supercritical water and certain organics, it is satisfactory to evaluate properties at the average of fluid and surface temperature. However, many empirical relations exist.
3. With most fluids, the differential $(dT/dY)_0$ at a point x is independent of events occurring prior to x, except in the entrance region as shown in Figure A-6. The entrance region corresponds to the length required for development of the velocity profile and temperature distribution. For fluids with Prandtl numbers below unity (chiefly liquid metals) $(dT/dY)_0$ may also be influenced by mode of heat input prior to x.
4. Many reported data concern average coefficients for finite lengths of tubes. Usually, the tube considered is of sufficient length that the average coefficient thus determined corresponds to the local coefficient required. However, particular care should be exercised if the data used are average coefficients for tubes with small length-to-diameter ratios.

Although the simple tube is not always used as a fuel element shape, the relationships established for it are useful for making estimates for a variety of systems and results are usually satisfactory when more reliable data are not available.

The average coefficient in any conduit can be obtained with the following substitutions:

1. In lieu of tube diameter use D_H, the hydraulic diameter defined by:

$$D_H = \frac{4 \text{ (free flow area)}}{\text{heated perimeter}} = \frac{4 \text{ (free volume)}}{\text{heat transfer area}} \tag{A6}$$

2. The mass velocity G is defined by:

$$G = \frac{\dot{W}}{A_{ff}} \tag{A7}$$

$\dot{W}$ = mass flow rate
A_{ff} = free flow area

With these substitutions, the simple tube formulae are approximately correct for any duct cross section, parallel flat plates, concentric rings, or any duct where the flow is essentially unidirectional, uninterrupted, and turbulent. It is difficult to estimate the effect of roughness on the heat-transfer coefficient. Roughness consists of surface differences, e.g., a granular ceramic surface as contrasted to a smooth drawn metal surface or the effect of minor flow disturbances, such as spacers in the fuel element passages, which produce eddies in the flow. The coefficient increase is usually less than the friction increase in rough tubes for all systems except liquid metals.

The temperature differential concept expressed in Equation (4) also serves to identify situations in which the average coefficient has limited meaning as a design parameter. For example, in a round tube the velocity and temperature profile exhibit radial symmetry; no peripheral coefficient variation exists. Conversely, in a polygon cross-section duct considerable variation does exist because of asymmetric velocity effects that yield marked variation of dT/dY at the wall. In this case, average considerations must be implemented by local peripheral effect considerations. In certain systems, local coefficients approaching zero are possible, particularly where acute-angle corners exist.

Many compound surface geometries will exhibit characteristics similar to those of smooth tubes; it will often be necessary to consider length and peripheral variation effects

in order to develop element design data. Usually, it will be found that only limited data of this nature are available (since the averaged value is usually satisfactory for other than nuclear heat transfer situations, and in addition, is much more easily attained experimentally). This absence may be sufficient to exclude the particular system from contention or necessitate inclusion of a high uncertainty factor. It will also become apparent that many systems can only be designed, even for preliminary assessment purposes, by a multistep process; i.e., in cases where peripheral coefficient variation exists, it is common to first establish the average geometry so that mitigating effects of conduction or radiation can be estimated, and then proceed to the actual geometry iteratively.

The general behavior of friction factors required for pressure loss calculations parallels those indicated for heat transfer coefficients in that the basic form of correlation varies with flow regime. Entrance effects and peripheral variations occur. However, except in unique circumstances, only the averaged friction factor is of concern, since the design consideration is overall pressure loss as opposed to local considerations. The friction factor for round tubes can generally be used for other type cross sections by using the relations given in Equations (6) and (7). Considerable uncertainty exists concerning the evaluation of friction factors for heated fluids. However, it is often adequate to define friction factors on the basis of bulk fluid temperatures.

The general geometry characteristics and special considerations stem from many of the items previously considered. In particular, certain geometries do not lend themselves to dimensional variation required for idealized temperature utilization, others present inherent problems of surface and flow area effectiveness, special support limitations, etc. In the following paragraphs, an attempt is made to summarize these general problems for particular fuel elements. It will be observed that the major point of differentiation among the various types of fuel elements is related to the degree of support required to achieve desired surface-to-volume, e.g., an array of round rods can be increased in surface-to-volume ratio by decreasing the rod diameter and spacing between rods; at some point the dimensions become so small that simple end supporting of fuel elements is not possible and the array of rods becomes synonymous with a screen type.

The following paragraphs present summaries of fuel element data in accordance with the outline mentioned previously. Heat transfer data are given for common fluids (all but liquid metals) for a known Reynolds number range, usually that corresponding to turbulent flow.

Continuous Flat Plate, or Equivalent Fuel Elements (Figure A-7)

1. Fuel element type - continuous flat plates
   Equivalent geometry - continuous concentric tubes
   Characteristic dimensions - plate thickness (t); plate spacing (Δ)
   Surface-to-volume (solid plus channel) ratio - $2/(\Delta + t)$
   Characteristic thermal dimension - $D_H \cong 2\Delta$

2. Heat transfer characteristics - data applicable are the same as those for round tubes, with D_H replacing tube diameter, G based on free flow area.

   a. For turbulent flow

$$\frac{hD_H}{k} = 0.023\left(\frac{D_H G}{\mu}\right)^{0.8}\left(\frac{C_p \mu}{k}\right)^{0.33} \qquad \text{(A8)}$$

$$\frac{D_H G}{\mu} > 10,000$$

For gases use coefficient of 0.021 and Prandtl exponent of 0.4.

Notes:

1. Ratio of flow to heated surface may differ from average in channel defined by outermost plate and channel wall in all systems. Probability of flow-surface mismatch in this location increased in curved and corrugated plate system.
2. Local heat transfer coefficient variations may occur within corrugations, especially if angle within corrugation is small.
3. In the concentric tube system channel flow-heated surface mismatch may often occur at the innermost tube due to inability to fabricate innermost tube to same hydraulic diameter as the average in the array. The heat transfer coefficient in an individual passage of a concentric tube array is actually a function of the ratio of diameters of the tubes forming that passage. Usually, this ratio is sufficiently close to unity so that variation may be neglected. Exceptions may occur at innermost tubes where plate spacing is large with respect to tube diameter.

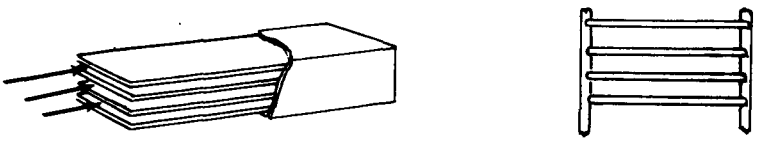

PLAIN FLAT PLATES

CONCENTRIC CYLINDERS

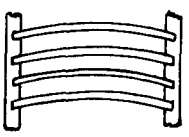

CURVED PLATES

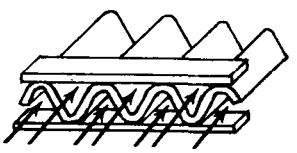

CORRUGATED PLATES

Fig. A-7 – Continuous plate-type fuel elements

b. For laminar flow use data for annuli or approximate with data for flat ducts, noting that both laminar and transitional regime information have high intrinsic uncertainties in application.

3. Pressure loss characteristics

a. Friction factor behavior for turbulent flow parallels that for round tubes. Incompressible (Fanning) relation of the following form may be used for most fluids including gases with low pressure loss.

$$\Delta P = \frac{4fG^2L}{2g_c D_H \rho} \qquad \text{(A9)}$$

b. For smooth surfaces

$$5000 < \left(\frac{D_H G}{\mu}\right) < 100,000 \qquad \text{(A10)}$$

$$f = \frac{0.046}{\left(\frac{D_H G}{\mu}\right) 0.2}$$

4. Geometry characteristics

   a. The coolant has access to the entire surface with no inherent problems of flow-surface mismatch except at outermost or innermost plate and outermost tube of a concentric-tube system.

   b. The heat transfer coefficient is applicable to all surface locations except as indicated in Figure A-7.

   c. Surface area variation with length, to permit incremental design for maximum utilization of materials temperature, is not possible without change of characteristics.

   d. Affords high flexibility with respect to fuel loading and displacement (e.g. considerable variation of permissible fuel loading is possible without change of characteristics)

   e. Local overheating or flow maldistribution within one channel of the array is not mitigated by internal mixing.

Discontinuous Flat Plates or Concentric-Tube Fuel Elements

The discontinuous flat plate or concentric-tube fuel elements are considered where local surface area variation is desired as part of an incremental design technique. The characteristics of these fuel elements are in part defined by the degree of subdivision. Usually, if the length between discontinuities is of the order of 20 or more times the plate spacing, all characteristics, except friction factor, may be considered as being identical with those described for the continuous system. The effective friction factor for these arrays can be represented by an equation of the form:

$$f' = f + c\left(\frac{A_f - A_b}{A_f}\right)^{-2} \qquad \text{(A11)}$$

f' = effective friction factor
f = friction loss due to element surface drag
c = constant
A_f = element frontal area
A_b = area blocked by fuel plates

The second term of the preceding equation accounts for the expansion and contractions occurring at the discontinuities. As an initial estimate, these losses may be approximated by standard expansion and contraction loss data. The actual effective friction factor will probably be somewhat higher than this because of the necessity of structure required for support at each discontinuity. With reasonable design, the effective friction factor can be taken as 1.5 to 2 times that of the continuous system.

The space between increments in the longitudinal direction cannot usually be made large enough to insure significant mixing of flow.

As the ratio of incremental length-to-plate spacing decreases, the system loses semblance with the long continuous system and system characteristics vary markedly with method of support. Approximate data for the many variants possible can usually be developed from compilations of compact heat exchanger data for strip fins and other radiator types. When the degree of subdivision is increased sufficiently, the edges of the plates may begin to represent a significant portion of the total surface area.

Parallel Flow to Unsupported Rods

1. Fuel element types - rods on triangular or square pitch
   Characteristic dimensions - rod diameter (D) center-to-center spacing of rods (S)

   Surface-to-volume ratio:
   Triangular pitch - $3.63D/S^2$
   Square pitch - $3.14D/S^2$

   Characteristic thermal dimension (D_H):
   Triangular pitch - $\left(1.102\,\frac{S^2}{D} - D\right)$

   Square pitch - $\left(1.274\,\frac{S^2}{D} - D\right)$

2. Heat transfer data - the recommendation is for use of D_H, as defined, and G based on flow area with smooth tube relation and the following correction factors:

		Multiplier for tube relation		
	S/D =	1	1.1	2.0
Triangular		0.6	1.0	1 to 1.2
Square		0.7	1.0	1 to 1.25

   These data are for average coefficients.

3. Pressure loss characteristics - friction factor behavior can be assumed to be the same as for round tubes with the following correction factors:

		Tube relation multiplier		
	S/D =	1	1.1	2.0
Triangular		0.55	1.0	1.05
Square		0.6	0.8	1.05

4. Geometry characteristics

   a. The coolant does not have access to the entire rod surface for S/D = 1 and preferential flow distribution effects exist in the complete range of $2 \geq S/D \geq 1$. However, at S/D > 1.2 or more, all surface may be considered as being effectively exposed to fluid.
   b. Heat transfer coefficient behavior essentially parallels flow distribution. Significant peripheral coefficient variation occurs for the S/D range of 1 to 1.2 (Figure **A-8**).
   c. Complete transverse mixing of heated fluid does not appear to occur without introduction of a turbulence promoter. Hence, the system tends to behave as a series of separated flow channels, and the fluid in close proximity to rod surface may be at higher-than-average temperature.
   d. The configuration usually exhibits slight to significant problems of flow-surface unbalance in proximity to the channel wall (e.g., a series of concentric tubes within

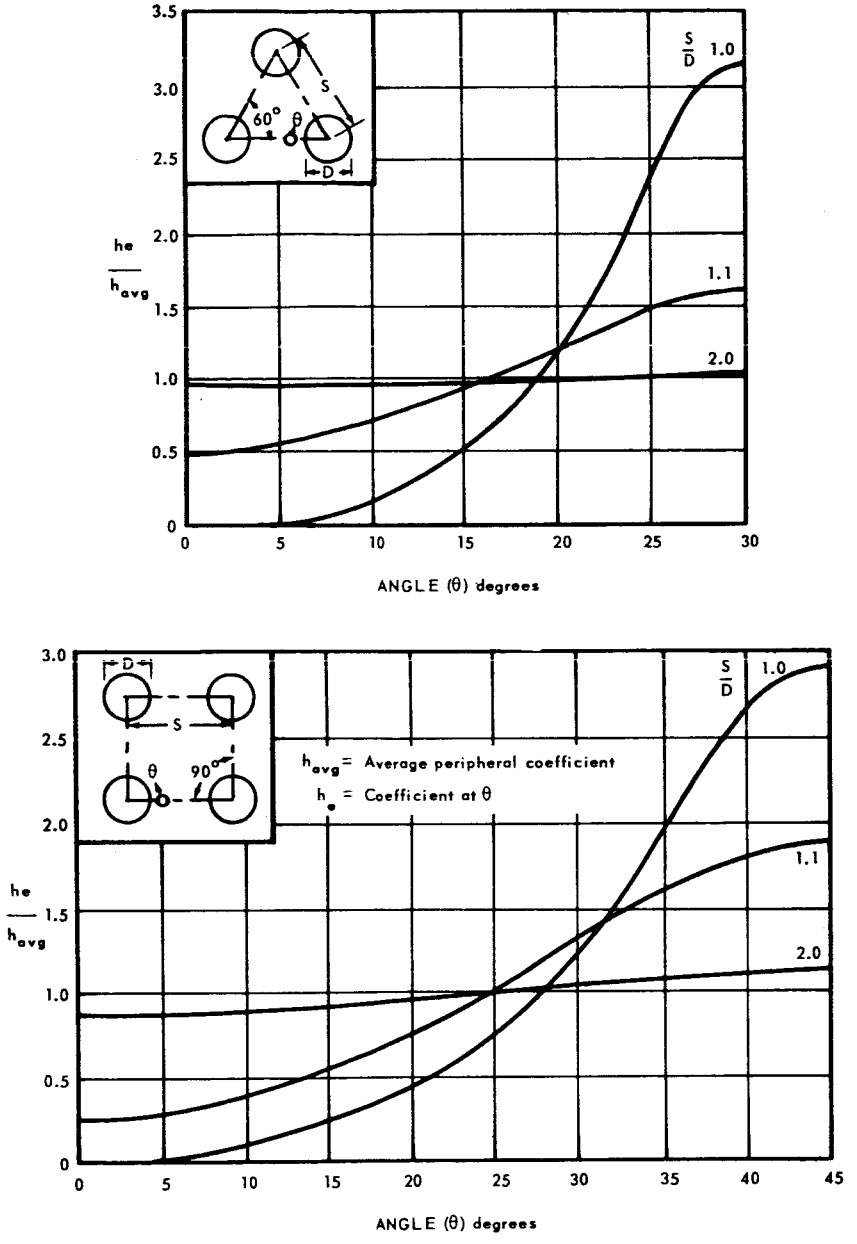

Fig. A-8 – Predicted peripheral variation of heat-transfer coefficient for parallel flow to rods as a function of array type and spacing

a circular channel has essentially the same characteristics as an infinite array of concentric tubes; conversely, the outermost units in a rod array may exhibit characteristics defined by the channel shape, rather than those of the infinite rod array).

e. The configuration is limited by minimum diameter of the rod which can be maintained with end support only. The probable minimum (strongly dependent on particular material and reactor) is approximately 1/4 inch.

Parallel Flow to Supported Rods

This configuration stems from either mechanical limitations of end-supported rods or desirability of insuring spacing between rods in array. A common spacer considered is a

helical wire wound around each tube in the array. The effects of the spacers are as follows:

1. Increase of pressure loss
2. Decrease of peripheral coefficient variation
3. Increase of transverse mixing

Fuel elements for the Sodium Reactor Experiment (SRE) consist of seven 0.709-inch rods in a 2.805-inch tube with S/D = 1.12 in a triangular array. The friction factor for this system with a 10-inch pitch helical wire spacer is approximately twice that of a smooth tube equivalent.

Rods in Crossflow

1. Fuel element type - in-line or staggered banks of rods
   Characteristic dimensions - rod diameter (D_o), longitudinal spacing (S_L), transverse spacing (S_T)

   Surface-to-volume ratio - $\frac{\pi D}{S_L S_T}$

   Characteristic thermal dimension - D

2. Heat transfer characteristics - most available correlations are based on experimental evaluations of length-averaged coefficients for airflow through the tube banks. Many evaluations of individual configuration behavior are available. A good overall correlation is given below:

$$\frac{h_{avg}D}{k} = 0.405\, F_a \left(\frac{DG_{max}}{\mu}\right)^{0.6} \left(\frac{C_p\mu}{k}\right)^{0.33} \qquad \textbf{(A12)}$$

G_{max} = mass velocity based on minimum free flow area (either perpendicular or transverse to flow direction)

h_{avg} = average coefficient for N banks of tubes

F_a = arrangement factor, a function of N and type of arrangement shown below:

Limitations: $S_T D > 1.25$, $S_L/D < 3.0$

$$\left(\frac{DG_{max}}{\mu}\right) > 2000$$

No. of rows (N)	1	2	3	4	5	6	7	8	9	10	∞
In-line	0.6	0.66	0.71	0.75	0.78	0.81	0.83	0.85	0.86	0.87	0.91
Staggered	0.6	0.67	0.74	0.79	0.84	0.88	0.89	0.91	0.92	0.93	1.0

Of more concern to fuel element work is the average peripheral coefficient h_N of an individual rod as a function of row position. Approximate values of the ratio h_N/h_∞ are as follows:

No. of rows (N)	1	2	3	4	5	>6
In-line	0.61	0.92	0.97	1.0	1.0	1.0
Staggered	0.63	0.76	0.93	0.98	0.99	1.0

h_∞ = average coefficient for infinite number of rows

The variation of the heat transfer coefficient around the rod periphery is of interest. Although few data are available, it is apparent that variation of peripheral coefficient behavior should be effected by row position and configuration, e.g., a wide spaced

in-line tube bank should exhibit peripheral variation comparable to that observed for cross flow over a single cylinder; as spacing decreases, configuration effects occur. A rough approximation is that the minimum peripheral coefficient is 0.6 h_p and 0.75 h_p for in-line and staggered systems respectively. Detailed surveys of tube bank characteristics are presented in reference 2.

3. Pressure loss - the pressure loss through an array of rods in cross flow can be expressed in the form of the Fanning equation:

$$\Delta P = \frac{4f(G_{max})^2 N_i}{2g_c \rho} \qquad \text{(A13)}$$

where N and f are defined by array characteristics, as shown in Figure 3B-9.

4. Geometry characteristics

   a. The coolant has access to the complete surface area; no inherent overall problems of flow-surface area mismatch exist except possibly at the channel wall.
   b. The heat-transfer coefficient is not applicable to all surface locations and significant variation may exist around the rod periphery.
   c. Local overheating or flow maldistribution is almost completely mitigated by internal mixing in staggered arrays, and to a lesser degree in the in-line systems.
   d. Spacing may be varied with length to permit utilization of incremental design techniques.
   e. The configuration utility is limited by both the minimum diameter of the rod which can be supported and the ability to fabricate side supports.

Screen-Type Fuel Elements

1. This type of fuel element has been proposed in order to permit attainment of high surface-to-volume ratios achievable with small diameter rods or wires. Support of these wires is achieved almost entirely within the element structure by interweaving or overlapping wire layers. This section presents typical data for close-packed square mesh screens. Many screen-type fuel elements will not exactly resemble this configuration **(Figure A-10)** but reasonable data for other than the true screen case can generally be obtained from information presented.

   a. Characteristic dimensions - wire diameter (D), mesh (M) bed
   b. Porosity (P) - volume fraction of voids
   c. Surface-to-volume ratio - 4(1-P)/D
   d. Porosity - the surface-to-volume ratio and porosity of screens can be defined by assuming that the standard screen thickness is 2D and assigning a characteristic value to the wire curvature introduced by interweaving. These idealizations become progressively poorer approximations as wire spacing decreases. A comparison of ideal and actual porosities is shown in graphic data in Figure **A-11.**

2. Heat transfer characteristics - the average heat-transfer coefficient for a close-packed bed of square mesh screens is illustrated graphically in Figure **A-12.** A simplified approximation of the best curve through early data is:

$$\frac{h_{avg}D}{k} = 0.55\left(\frac{DG}{\mu P}\right)^{0.56}\left(\frac{C_p\mu}{k}\right)^{0.33} \qquad \text{(A14)}$$

$$1 < \frac{DG}{\mu P} < 30,000$$

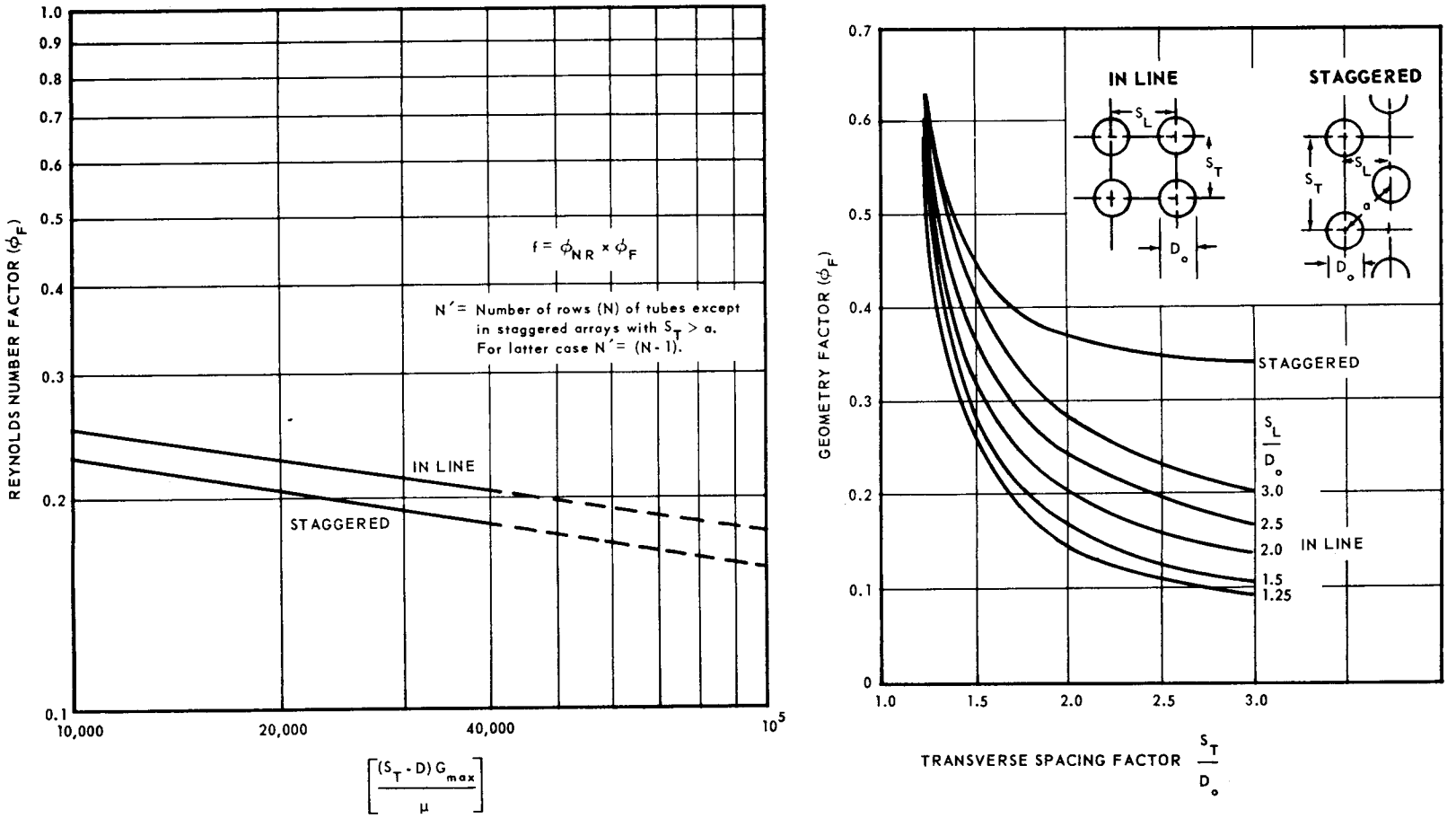

Fig. A-9 – Friction factors for flow across rod banks

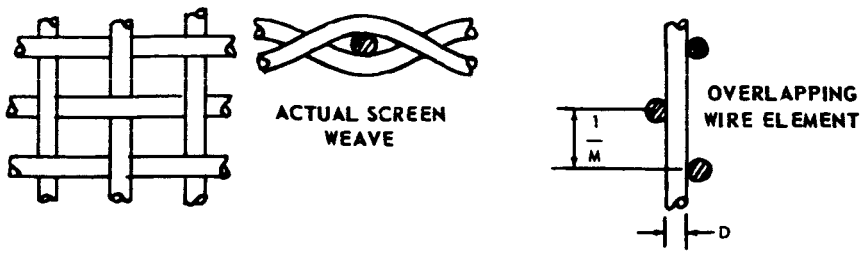

Fig. A-10 – Screen-type fuel element configuration

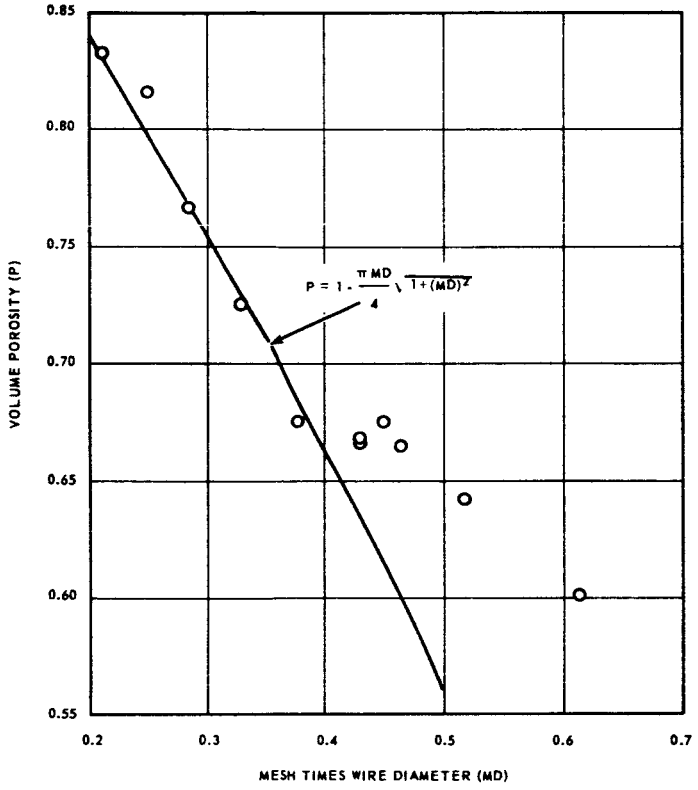

Fig. A-11 – Plot of calculated and actual porosities of square mesh screens (Tong, Stanford University Report No. 28)

D = screen wire diameter

G = mass velocity based on frontal area of bed

P = bed porosity

h_{avg} = average coefficient for screen bed

Because of the complexity of the fuel element structure, only limited data are available for other than average cases. The best interpretations appear to be as follows:

1. **The average peripheral coefficient of a particular screen varies with screen position in about the same fashion as indicated for flow across tube banks. Namely, the first**

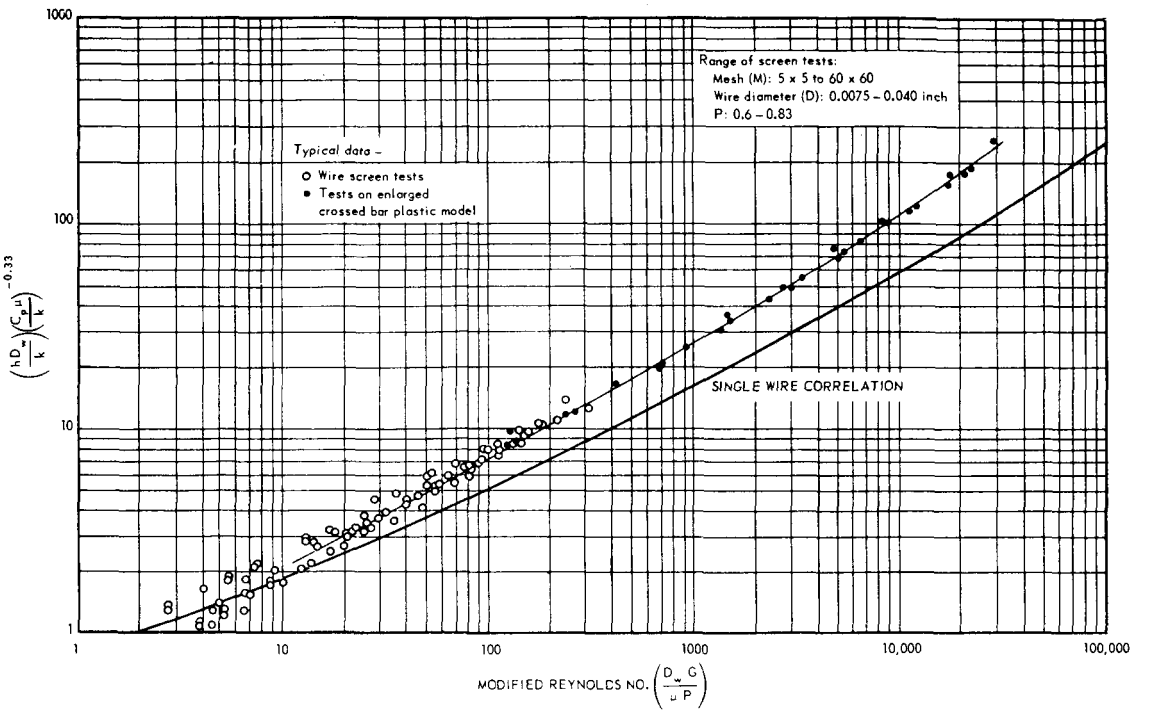

Fig. A-12 – Plot of heat transfer data for close-packed square mesh screens as a function of modified Reynolds number

four to six screens yield lower coefficients than those observed in a deep bed. The magnitude is about the same as indicated for staggered rod banks.

2. Peripheral variation of coefficient around the individual wire appears to be somewhat less than that observed in staggered tube banks. A somewhat conservative estimate of overlap effect suggests that the overlapped area be treated as being completely devoid of convective cooling.

3. Pressure loss characteristics - considerable experimental data are available for pressure loss through screens because of their utility in aerodynamic tests, etc. Although more precise correlations are available, the following relation is useful because of its relative simplicity:

$$\Delta P = 0.17 \frac{G^2}{2g_c\rho}\left(\frac{N}{F^{2.15}}\right)\beta \qquad \textbf{(A15)}$$

G = mass velocity based on frontal area of bed
F = free flow area ratio of screen
β = correction factor for Reynolds number (Figure A-13)
N = number of screens in bed

Limited to close-packed screen beds, $0.6 > F > 0.2$

4. Geometry characteristics

   a. The coolant does not have complete access to all surface area, and the amount of area voided may be unknown.
   b. A high degree of internal fluid mixing

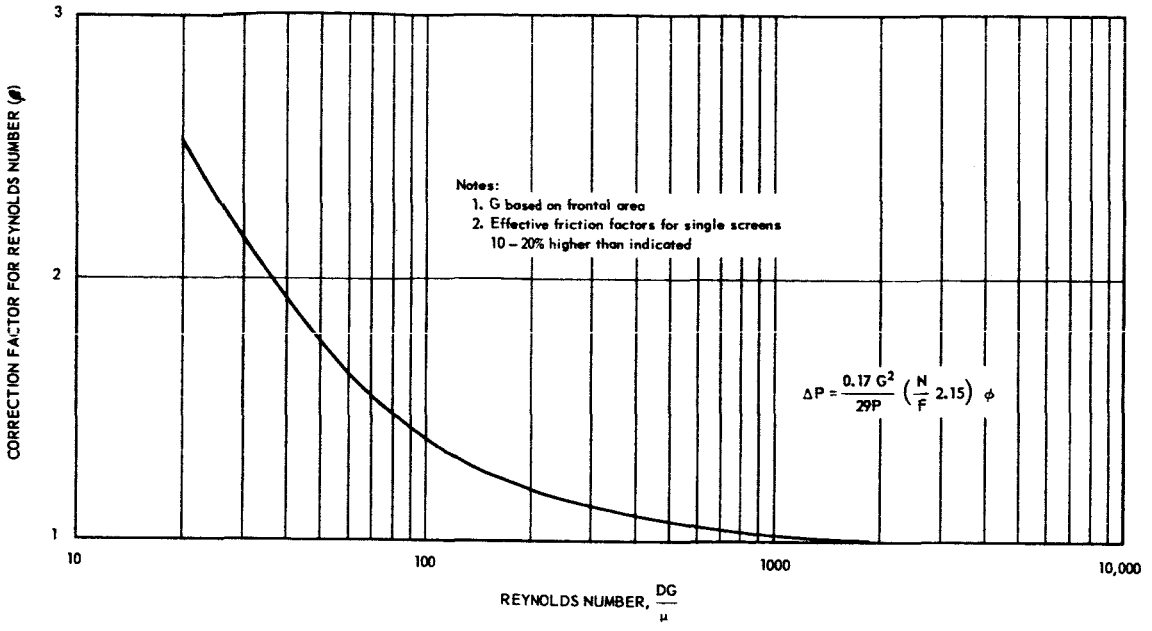

Fig. A-13 – Plot of friction factor relation for close-packed square mesh screens

c. The system thermal characteristics are difficult to define with accuracy, either analytically or experimentally.
d. The geometry may be varied with length to permit incremental design in some cases.
e. Local temperature characteristics may be strongly affected by tolerance considerations since the tolerance value will usually be significant with respect to wire size and spacing.

5. Miscellaneous - Figure **A-12** suggests that the screen data may be estimated from single wire data by correcting the velocity to the average value within the screen bed. Actual screen bed coefficients are higher than this estimate because of turbulence and eddies introduced by crossed wires, expansion and contraction effects, etc., particularly at higher Reynolds numbers. If the screen bed had random wire spacing, this conservative estimate might be used in design since there would be a high probability of certain wires not being affected by the added turbulence.

Packed Bed Fuel Elements

1. This category of fuel element types represents a method of attaining self-supporting fuel elements and permits use of small size units with associated high surface-to-volume ratios. The general configuration is a container channel filled with packing of the desired shape. In contrast to other types, the surface-to-volume ratio of packed beds is defined by individual characteristics of the packing. For example, the surface-to-volume ratio of an infinite bed of packing is:

$$\frac{A_H}{V} \cong \frac{6(1-P)}{D} \qquad \textbf{(A16)}$$

P = bed porosity
D = diameter of sphere equivalent to packing

In most cases, the porosity of the infinite bed is defined by the packing diameter or equivalent dimension; hence, the surface-to-volume characteristics can usually be determined solely in terms of a nominal diameter. Basic geometry problems of packed beds can be illustrated with spherical packing as an example. The porosity of a sphere bed depends on relative alignment of the spheres. By systematic sphere stacking, a variety of arrangements with porosities in the range of 0.26 to 0.48 are possible. In practice, particularly with small diameter spheres, it is not usually possible to arrange for systematic stacking and the porosity is a random characteristic. The actual porosity value is determined by the manner of bed formation, roughness, uniformity of particle size, and boundary effects; the latter being defined by ratios of sphere diameter to container diameter and bed height. With careful preparation, beds with particle sizes less than 0.1 of the bed diameter should exhibit porosities in the range of 0.35 to 0.4. In addition, the porosity of the bed is not constant at all locations since the container wall influences alignment and, hence, local porosity of spheres in its vicinity. Typical data pertinent to these elements are shown in Figure **A-14.**

It is apparent, in terms of these data, that it is not immediately possible to identify even average characteristics of packed beds and that problems of reproducibility of bed geometry may be a significant design consideration. These characteristics constitute a portion of the random nature of such geometries.

In the following paragraphs, two types of packing are considered; namely, spheres and Berl saddles. Both of these systems are of interest because they lend themselves to relatively simple fabrication techniques. The Berl saddle or equivalent may be of particular interest in that it is designed to yield relatively constant porosity at all bed locations and high reproducibility. Geometrical characteristics of Berl saddles are shown in Figure **A-15.** These two types also represent approximate extremes of porosities available in typical packings.

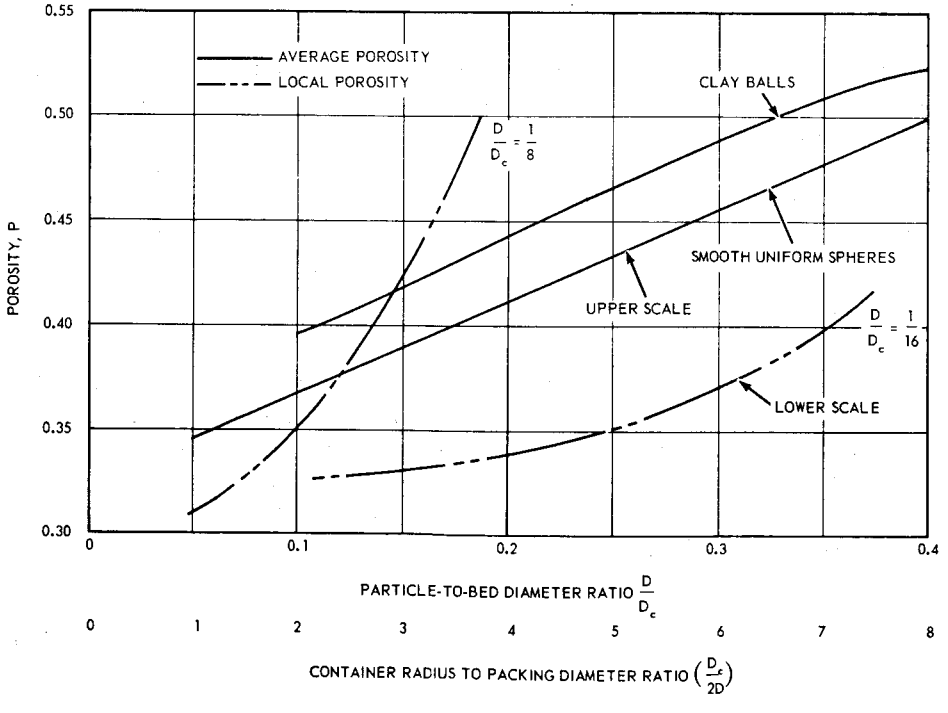

Fig. A-14 – Plot of average bed porosity and radial variation of porosity in packed sphere beds as a function of sphere to bed diameter ratio (D/D_c)

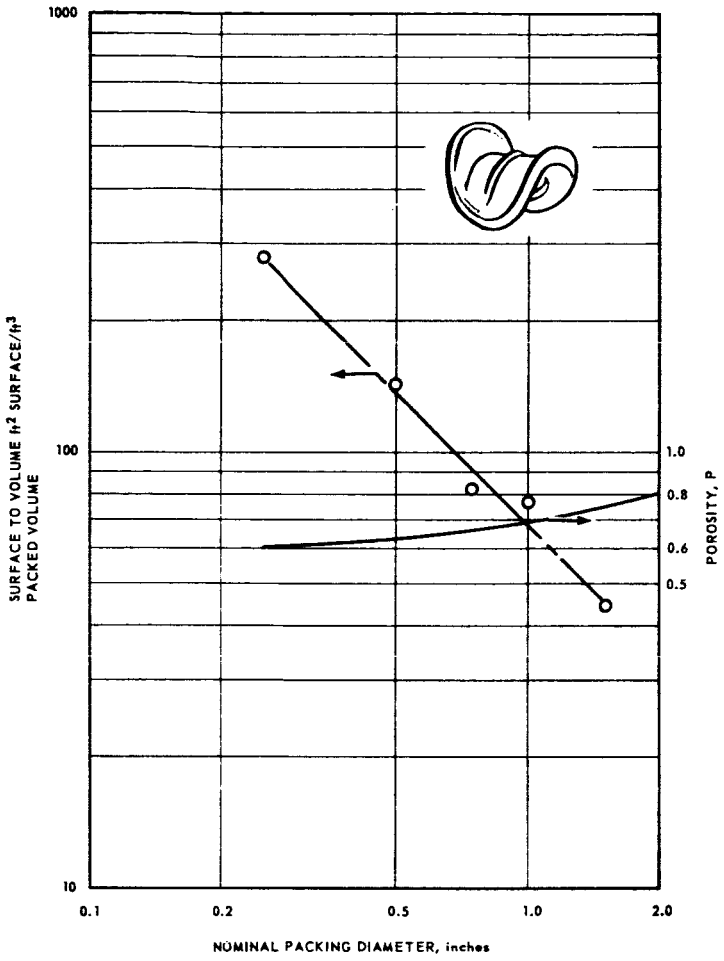

Fig. A-15 – Plot of typical geometrical characteristics of berl saddles as a function of nominal packing diameter (Commercial Packing)

2. Heat transfer characteristic - essentially, all data available are applicable to average coefficients for large beds. For packed beds of spheres, the following correlation can be used:

$$\left(\frac{h}{C_p G}\right)\left(\frac{C_p \mu}{k}\right)^{\frac{2}{3}} = 1.77\left[\frac{DG}{\mu(1-P)}\right]^{-0.44} \qquad 30 \leq \left[\frac{DG}{\mu(1-P)}\right] \leq 50,000 \qquad \textbf{(A17)}$$

Considerable variation of coefficient around the sphere surface has been observed in limited testing of packed bed models, but data adequate for generalizations is not available.

Approximate data for commercial Berl saddles suggests utilization of the preceding equation with the following substitutions:

a. Use D/(1-P) equal to $6/\gamma$ where γ is the surface-to-volume ratio of the packing.
b. Introduce an empirical correction factor of 1/0.65 (a measure of the fraction of

total surface of saddle effective in heat transfer) in both the Reynolds number and the left-hand side of the equation. Thus,

$$\left(\frac{h}{C_p G}\right)\left(\frac{C_p \mu}{k}\right)^{\frac{2}{3}} = 0.95\left(\frac{6G}{\gamma \mu}\right)^{-0.44} \qquad \textbf{(A18)}$$

3. Pressure loss characteristics - the pressure loss in a packed bed can be expressed by the following relation:

$$\frac{\Delta P}{L} = \frac{2fG^2}{g_c D \rho}\left(\frac{1-P}{P^3}\right) \qquad \textbf{(A19)}$$

G = mass velocity based on frontal area of bed
P = porosity of bed
f = friction factor as shown in Table **A-3**

TABLE **A-3**

PACKED BED FRICTION FACTORS

Type Of Surface	Range Of Modified Reynolds Number, $N_{Re'}$	Friction Factor, f
All roughnesses	1 - 200	$(75/N_{Re'})^a + 0.875$
Glass, smooth metal	200 - 50,000	$2.14\,(N_{Re'})^{-0.1}$
Clay	200 - 50,000	$2.14\,(N_{Re'})^{-0.1}$
Jagged granules	200 - 50,000	$4.9\ \ (N_{Re'})^{-0.1}$

[a] $N_{Re'} = DG/\mu(1-P)$

For Berl saddles substitute: $\gamma/6$ for $(1-P)/D$

4. Geometry characteristics

   a. The coolant does not have access to complete surface area. Both amount and type of surface area blockage is a random quantity which may vary significantly within a single bed.
   b. Significant variation of internal geometry (porosity) always occurs at the channel wall, particularly if the packing is large with respect to channel dimensions.
   c. Precise geometry characteristics usually cannot be defined except by experimental evaluation of channel-packing system. Problems of reproducibility of bed characteristics may be significant, particularly with spheres.
   d. Because of random nature, the system appears applicable only where a high safety factor can be included, or where mockup tests of system behavior are possible.
   e. Limitations of allowable variation in surface-to-volume (inability to vary porosity significantly without change of packing shape) may eliminate element type in various systems or necessitate special reactor flow passage arrangement.
   f. The flow mixing within the bed is high except at the channel wall.
   g. Wide range of sizes and shapes of packing can be considered.

Reactor Matrix Fuel Elements

1. Reactor matrix fuel elements are primarily of interest for use with solid moderator systems wherein the moderator can be impregnated with fuel. The fuel element consists essentially of a moderator-fuel block penetrated by cooling channels. A variety of coolant channel cross sections can be used, but only the circular cross section

will be considered here. The matrices may be classified as either homogeneous or heterogeneous. In the former case, each coolant channel is associated with a constant volume of fuel-bearing matrix. In the latter case, the fuel is selectively located within the matrix. Typical matrix characteristics are shown in Figure **A-16.**

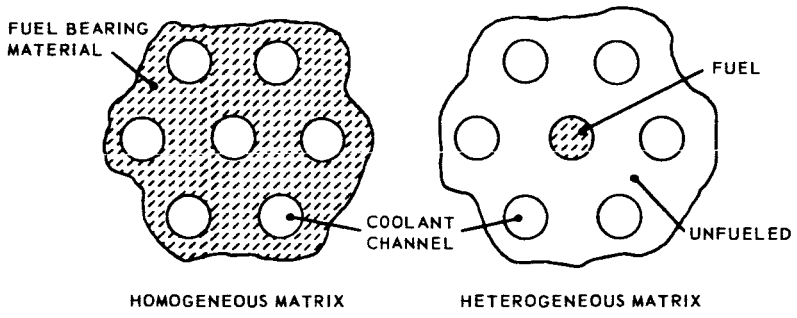

Fig. A-16 – Matrix fuel elements

The thermal design characteristics of the coolant passages can be found by the design relations for smooth tubes. Of equal interest is the effect of matrix geometry on distribution of temperature and heat flow within the matrix. The general problems of matrix fuel elements can be discussed in terms of the typical geometry shown in Figure **A-17.** The system is an array of coolant holes on an equilateral triangle pitch. The shaded hexagonal area represents the volume of heat-generating matrix associated with an individual cooling channel. Since the typical section does not exhibit radial symmetry, variation from average temperature conditions can be expected. The particular problems of the matrix are determination of variation of heat flux around the coolant passage periphery to permit calculation of maximum passage surface temperature and calculation of maximum temperature and temperature differences within the solid material. The latter calculations are of particular interest in thermal stress considerations. Solutions to these problems are tedious because of the necessity of iteration in numerical computations. The following information indicates maximum limitations and, in addition, yields actual values for many cases.

a. The difference between maximum and average coolant channel surface temperature at a given point in the reactor can be approximated by:

$$T_{s_{max}} - T_{s_{avg}} = K_c(T_{s_{avg}} - T_b)$$

$T_{s_{avg}}$ = average coolant passage surface temperature

$T_{s_{max}}$ = maximum coolant passage surface temperature

T_b = average fluid temperature

K_c = function of matrix geometry (Figure **A-17**)

K_c is defined by considering radial variation of heat-generating matrix-volume to channel-surface area in a typical segment and by assuming that heat flows only in the radial direction.

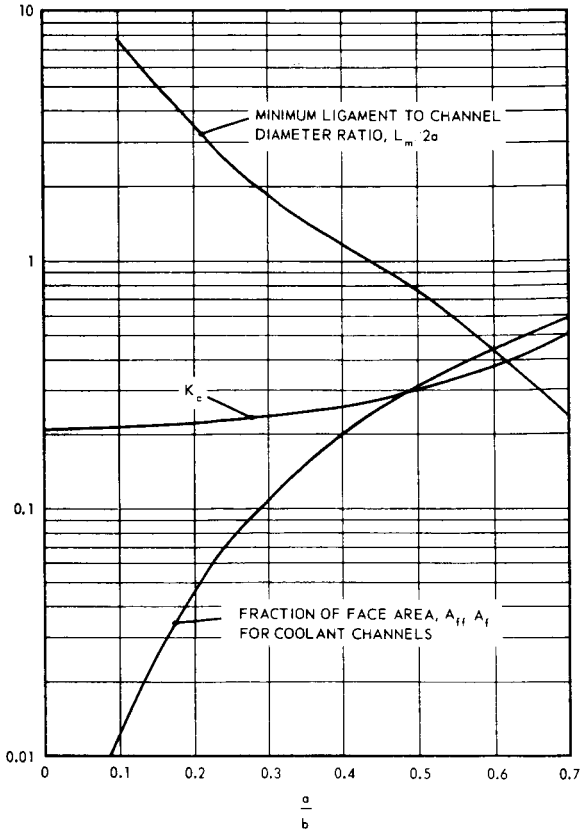

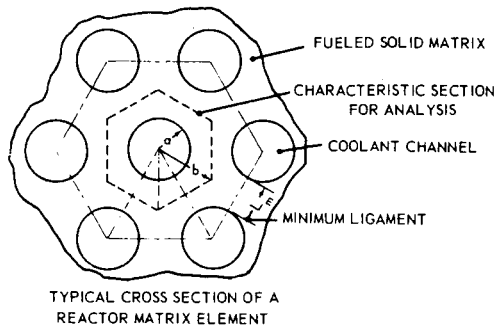

TYPICAL CROSS SECTION OF A REACTOR MATRIX ELEMENT

$$\frac{L_m}{2a} = \frac{\cos\frac{\pi}{6}}{\left(\frac{a}{b}\right)} - 1$$

$$\frac{A_{ff}}{A_f} = \frac{\frac{\pi}{6}}{\sin\frac{\pi}{6}\cos\frac{\pi}{6}}\left(\frac{a}{b}\right)^2 = 1.209\left(\frac{a}{b}\right)^2$$

$$K_c = \frac{1-\left(\frac{a}{b}\right)^2}{\frac{6}{\pi}\sin\frac{\pi}{6}\cos\frac{\pi}{6}-\left(\frac{a}{b}\right)^2} - 1 = \frac{0.173}{0.827-\left(\frac{a}{b}\right)^2}$$

Fig. A-17 – Geometrical characteristics of equilateral triangle centered circular coolant channel matrix

b. The maximum temperature difference within the solid material can be approximated by several methods if it is assumed that the temperature at all points along radius r are constant. Figure **A-18** illustrates two such approximations. The cylindrical approximation is based on a conduction model where the typical hexagon is replaced by a circle having the same area. The circular harmonics calculation is a more realistic approximation although it too becomes questionable at r-to-b ratios in excess of 0.7.

2. Limitations - the general problem with reactor matrix elements in choosing a geometry which results in the desired heat-transfer area while satisfying moderator volume requirements, temperature distribution limitations, thermal stress considerations, and fabrication limitations. Considerable compromising may be required because of these competing effects. It will generally be found that power density and surface-to-volume characteristics of the element may be more limited than other types. Actual limitations are a strong function of the particular materials considered. Some useful materials such as graphite, beryllium, and beryllia all have relatively high thermal conductivities which may result in minimization of thermal stress problems. The heterogeneous matrix shown in Figure **A-16** offers the possibility of isolation of fuel and, hence, ease of fuel addition and fission fragment retention at the expense of temperature increase for a particular power density. Alternately, lower

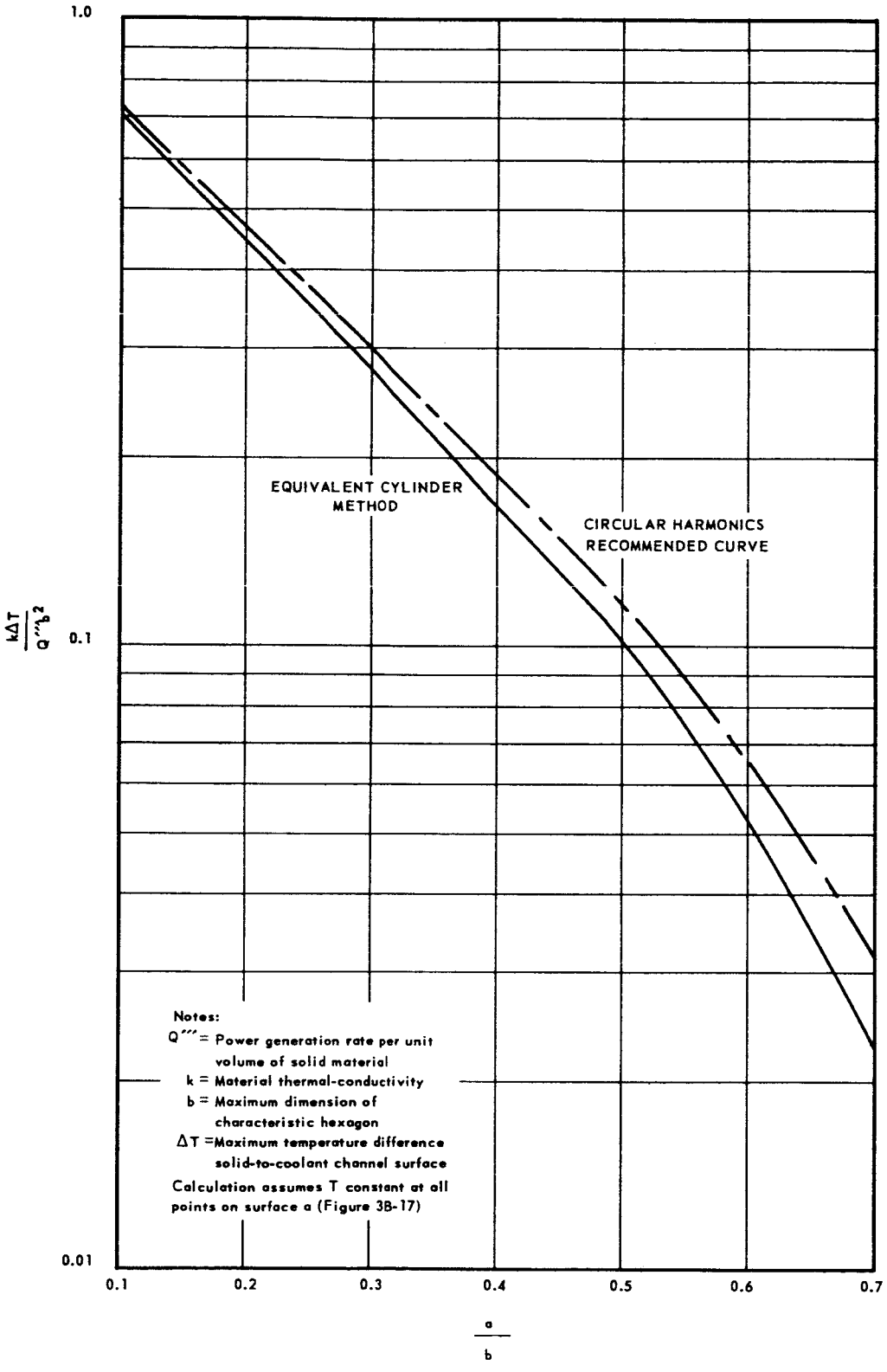

Fig. A-18 – Calculation plot for determining maximum internal temperature difference in matrix

internal temperatures are possible by concentrating fuel in thin cylinders around each coolant channel, but with complications of fabrication and design for retention of fission products.

3. Geometry characteristics

   a. Significantly limited by specific material characteristics and probably not applicable to other than solid moderators, low-absorption high-thermal-conductivity materials, or low-power-density systems
   b. The characteristics of the flow passage are identical with those tabulated for continuous flat plates, except for peripheral temperature considerations.
   c. Their integral nature offers potential structural and support simplification, and eliminates the problems associated with selective cooling of solid moderator.
   d. They are applicable to incremental design techniques basically by fuel concentration variation, or gross matrix changes for radial power variation or compensation.
   e. They are subject to some problems equivalent to matching fuel element to channel wall if whole reactor core must be made from a large number of matrix units. The number of units is probably defined by differential temperature consideration.
   f. The most significant tolerance considerations appear to be related to fuel concentration variations and the effect of allowed tolerances for differential thermal expansion effects.

Variants of Reactor Matrix

A variation of the reactor matrix or possibly of rods in parallel flow is the close-packed stacked-tube arrangement, i.e., internally cooled tubes on equilateral triangle center (Figure **A-19**). This system eliminated the internal temperature and heat flow variation of the solid matrix, and mitigates thermal stress limitations.

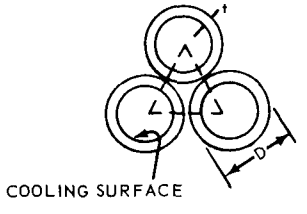

$$\frac{A_H}{V} = 3.63 \frac{(D - 2t)}{D^2}$$

Fig. A-19 – Close-packed, stacked-tube-matrix fuel element arrangement